

**Field Performance of  
Subbases Constructed  
with Industrial Byproducts**

**SPR# 0092-45-18**

---

**Tuncer B. Edil and Craig H. Benson  
Department of Civil and Environmental Engineering  
University of Wisconsin-Madison**

September 2005

**WISCONSIN HIGHWAY RESEARCH PROGRAM #0092-45-18**

**FIELD PERFORMANCE OF SUB-BASES CONSTRUCTED  
WITH INDUSTRIAL BYPRODUCTS AND GEOSYNTHETIC  
REINFORCEMENT**

**A FINAL REPORT on the WHRP Project**

**“Field Performance of Sub-Bases Constructed with Industrial By-Products”**

Principal Investigators: Tuncer B. Edil and Craig H. Benson,  
Post-doctoral Research Associate: Aykut Şenol  
Graduate Research Assistants: Md Sazzad Bin-Shafique,  
Burak F. Tanyu,  
Woon-Hyung Kim

Geo Engineering Program  
Department of Civil and Environmental Engineering  
University of Wisconsin-Madison

**SUBMITTED TO THE WISCONSIN DEPARTMENT OF  
TRANSPORTATION**

October 31, 2005

## ACKNOWLEDGEMENT

Financial support for the study described in this paper was provided by the Wisconsin Department of Transportation. However, the conclusions and recommendations are those of the authors and do not reflect the opinions or policies of WisDOT. Additional financial support for the fly ash research was provided by the U.S. Department of Energy through the Combustion Byproducts Recycling Consortium and the University of Wisconsin-Madison Consortium For Fly Ash Use In Geotechnical Applications. Appreciation is expressed to Grede Foundries, Alliant Energy, Mineral Solutions, Inc., Presto Products Co., Amoco Fabrics and Fibers Co., and Tenax Corporation for supplying the industrial by-products and geosynthetics and assisting with placement of these materials. Messrs. A. Sawangsuriya and R. Allbright collected the SSG and the DCP data, respectively. Drs. B. Albrecht and T. Abichou assisted with the instrumentation and the fly ash construction, respectively. Finally we acknowledge the cooperation of the contractor of the project, H. James and Sons, Inc. and the WisDOT personnel.

## **DISCLAIMER**

This research was funded through the Wisconsin Highway Research Program by the Wisconsin Department of Transportation and the Federal Highway Administration under Project # 0092-45-18. The contents of this report reflect the views of the authors who are responsible for the facts and accuracy of the data resented herein. The contents do no necessarily reflect the official views of the Wisconsin Department of Transportation or the Federal Highway Administration at the time of publication.

This document is disseminated under the sponsorship of the Department of Transportation in the interest of information exchange. The United State Government assumes no liability for its contents or use thereof. This report does not constitute a standard, specification or regulation.

The United States Government does not endorse products or manufacturers. Trade and manufacturers' names appear in this report only because they are considered essential to the object of the document.

## Technical Report Documentation Page

1. Report No. 00-45-18	2. Government Accession No	3. Recipient's Catalog No	
4. Title and Subtitle Field Evaluation Performance of Sub-bases Constructed with Industrial Byproducts		5. Report Date	
		6. Performing Organization Code	
7. Authors Tuncer, B. Edil, Craig H. Benson, Aykut Şenol, Md Sazzad Bin-Shafique, Burak F. Tanyu, and Woon-Hyung Kim		8. Performing Organization Report No.	
9. Performing Organization Name and Address Department of Civil and Environmental Engineering University of Wisconsin-Madison 1415 Engineering Drive Madison, WI 53706		10. Work Unit No. (TRAIS)	
		11. Contract or Grant No.	
12. Sponsoring Agency Name and Address Wisconsin Department of Transportation 4802 Sheboygan Avenue Madison, WI 73707-7965		13. Type of Report and Period Covered	
		14. Sponsoring Agency Code	
15. Supplementary Notes			
<p>16. Abstract</p> <p>Alternative methods for providing a stable platform over soft subgrades were evaluated using a 1.4-km section along a Wisconsin state highway that incorporated twelve test sections to evaluate nine different stabilization alternatives. A variety of industrial by-products and geosynthetics were evaluated for stabilization. The industrial by-products included foundry slag, foundry sand, bottom ash, and fly ash as subbase layer materials. The geosynthetics included geocells, a non-woven geotextile, a woven geotextile, a drainage geocomposite, and a geogrid. The same pavement structure was used for all test sections except for the subbase layer, which varied depending on the properties of the alternative material being used. All test sections were designed to have approximately the same structural number as the conventional pavement structure used for the highway, which included a subbase of granular excavated rock. Observations made during and after construction indicate that all sections provided adequate support for the construction equipment and that no distress is evident in any part of the highway. Each of the alternative stabilization methods, except a subbase prepared with foundry sand, appear to provide equivalent or greater stiffness than that provided by the control section constructed with excavated rock. However, the foundry sand subbase is also providing adequate support. Analysis of leachate collected from the base of the test sections shows that the by-products discharge contaminants of concern at very low concentrations.</p>			
17. Key Words Soft subgrade, by-products, geosynthetics, stabilization, flexible pavement		18. Distribution Statement No restriction. This document is available to the public through the National Technical Information Service 5285 Port Royal Road Springfield VA 22161	
19. Security Classif.(of this report) Unclassified	19. Security Classif. (of this page) Unclassified	20. No. of Pages	21. Price

## EXECUTIVE SUMMARY

Alternative methods for providing a stable platform over soft subgrades were evaluated using a 1.4-km section along a Wisconsin state highway that incorporated twelve test sections to evaluate nine different stabilization alternatives. A variety of industrial by-products were evaluated for stabilization. The industrial by-products included foundry slag, foundry sand, bottom ash, and fly ash as subbase layer materials. Additionally, several types of geosynthetics sections were incorporated as alternative platforms including geocells, a non-woven geotextile, a woven geotextile, a drainage geocomposite, and a geogrid and presented in this report. The same pavement structure was used for all test sections except for the subbase layer, which varied depending on the properties of the alternative material being used. All test sections were designed to have approximately the same structural number as the conventional pavement structure used for the highway, which included a subbase of granular excavated rock. Observations made during and after construction indicate that all sections provided adequate support for the construction equipment and that no distress is evident in any part of the highway. Each of the alternative stabilization methods, except a subbase prepared with the specific high clay-content foundry sand used in this project, appeared to provide equivalent working platform like the control section constructed with excavated rock. However, the foundry sand subbase is also providing adequate support and other foundry sands with lower clay content are expected to provide even better support.

The longer-term performance (i.e., after 5 years) and contribution to pavement structure strength as evidenced from maximum deflections and back-calculated moduli from the FWD surveys indicate that the alternative platforms have varying median moduli although comparable structural contributions due to their varying thicknesses (i.e., comparable maximum deflections). At the end of 5 years, back-calculated median moduli could be grouped into 4 categories. The first category includes foundry sand, foundry slag, and geocell sections and had the lowest mean moduli. The second category includes breaker run in control sections and reinforced geotextile and drain geocomposite sections and had somewhat higher mean moduli than the first category but comparable to each other (except one of the control sections). The third category includes bottom ash and geogrid-reinforced sections and had mean moduli higher than the second category. Fly ash section had the highest mean modulus at the end of 5 years, which was markedly higher than even the third category. Grouping the back-calculated moduli in this way indicates that these materials have varying stiffness; however, if the stiffness of breaker run is taken as the reference, the stiffness of most alternative materials is equal or higher than breaker run except foundry sand, foundry slag, and geocell. Modulus of the fly section increased considerably with time. The fly ash stabilized subgrade layer, like the geosynthetic-reinforced layers, is a thin platform (i.e., 0.3-m thick); however, it provides a similar structural contribution to the pavement structure when measured in terms of the maximum FWD deflections. Analysis of leachate

collected from the base of the test sections shows that the by-products discharge contaminants of concern at very low concentrations.

A series of subsequent reports analyze the field performance of the sections built with granular alternative materials (i.e., foundry sand, foundry slag, bottom ash, Grade 2 granular backfill, and breaker run) and geosynthetic-reinforced test sections (i.e., using geogrid, geotextiles, and drainage geocomposite) in greater detail. The analysis is supplemented with proto-type large-scale laboratory experiments on the same materials. An evaluation of the stabilization alternatives as working platforms and in terms of their strength contribution to the pavement structure is undertaken (WHRP Project SPR #0092-00-12 and SPR #0092-03-12). The field performance of the fly ash section (i.e., a chemically stabilized alternative) and its design implications are given separately in Appendix C of this report. The monitoring of field performance was extended after the completion of the project and the data available to date are included in this report. Environmental monitoring was also extended under another contract and will be published as a separate report (Recycled Materials Research Center subcontract to the University of Wisconsin-Madison through WisDOT #0663-43-10).



## TABLE OF CONTENTS

ACKNOWLEDGEMENTS .....	i
DISCLAIMER.....	ii
TECHNICAL REPORT DOCUMENTATION PAGE.....	iii
EXECUTIVE SUMMARY.....	iv
TABLE OF CONTENTS .....	v
TABLE OF TABLES .....	vii
TABLE OF FIGURES.....	viii
1. INTRODUCTION .....	1
2. DESCRIPTION OF TEST SITE AND TEST SECTIONS .....	3
2.1 Subgrade Properties .....	4
2.2 Control Sections .....	5
2.3 Alternative Subbase Materials .....	6
2.4 Geosynthetics .....	7
3. INSTRUMENTATION .....	8
3.1 Meteorological Conditions .....	9
3.2 Soil Temperature, Water Content, and Lateral Flows .....	10
3.3 Geosynthetic Strain Gages .....	11
3.4 Earth Pressure Cells .....	14
3.5 Lateral Flow .....	14
3.6 Subbase Leachate .....	15
4. CONSTRUCTION .....	16
4.1 Fly Ash Section .....	16

4.2	Bottom Ash, Foundry Sand, and Foundry Slag Sections .....	17
4.3	Geosynthetics Sections .....	18
4.4	Control Section .....	19
4.5	DCP and SSG Surveys .....	19
4.6	Rolling Weight Deflectometer Surveys.....	21
5.	DATA COLLECTED AND PERFORMANCE TO DATE .....	22
5.1	Meteorological Data .....	22
5.2	Subsurface Data .....	22
5.3	RWD Data .....	23
5.4	FWD Data.....	24
5.5	Lysimeter Data .....	28
6.	SUMMARY .....	29
	REFERENCES .....	34
	APPENDIX A- Boring Logs	
	APPENDIX B- RWD & FWD Data and Back-Calculated Modulus	
	APPENDIX C- Paper on Incorporating A Fly Ash Stabilized Layer Into Pavement Design – Case Study	

## TABLE OF TABLES

TABLE 1. Properties of subbase materials .....	36
TABLE 2. Properties of geosynthetics .....	37
TABLE 3. Total Deflections Obtained from RWD (12) ... ..	38

## TABLE OF FIGURES

FIGURE 1. Layout of test sections at STH 60 site. ....	39
FIGURE 2. $\omega$ , LL, PL, $\gamma_{dmax}$ , $q_u$ , DPI and soil stiffness results of the subgrade in STH 60 .....	40
FIGURE 3. Vertical sections of pavement structures for the by-products and the control sections .....	41
FIGURE 4. Vertical sections of pavement structures for the geosynthetics sections .....	42
FIGURE 5. Layout of field monitoring equipments at STH 60 .....	43
FIGURE 6. Strain gage installation of geotextile .....	44
FIGURE 7. Schematic of earth pressure cell .....	45
FIGURE 8. Location of drainage collection pipe .....	46
FIGURE 9. Drainage collection system in geocomposite reinforced section...	47
FIGURE 10. Flowmeter installation and data collection.....	48
FIGURE 11. Typical layout of lysimeters and construction.....	49
FIGURE 12. Laydown equipment to spread fly ash on subgrade .....	50
FIGURE 13. Placement of foundry slag as subbase.....	51
FIGURE 14. Placement of foundry sand as subbase .....	52
FIGURE 15. Installation of geocell sections infilled with foundry slag .....	53
FIGURE 16. Installation of geocomposite section .....	54
FIGURE 17. Installation of geogrid section .....	55
FIGURE 18. Installation of control section .....	56
FIGURE 19. DPI and soil stiffness results of the subbase in STH 60 .....	57
FIGURE 20. Air temperature and relative humidity data: (a) from site instrumentation and (b) from the NOAA station .....	58

FIGURE 21.	Temperature at the surface of the subbase and subgrade at various locations .....	59
FIGURE 22	Cumulative precipitation data from the NOAA Weather Station	60
FIGURE 23.	Variation of volumetric water content at the surface of subgrade at different test sections .....	61
FIGURE 24.	Maximum deflection from falling weight deflectometer tests after construction, following spring, and a year later .....	62
FIGURE 25	Modulus of Working Platforms (a) October, 2000 to May, 2005 and (b) May, 2005.....	63
FIGURE 26.	Leachate flux at the bottom of the subbase layer .....	64
FIGURE 27.	Concentrations of select elements in leachate on September 14, 2000.....	65

## 1. INTRODUCTION

A common problem in many parts of Wisconsin, as well as other states, is soft subgrade. Nearly 60% of Wisconsin has “poor soils” for highway construction, two-thirds of which are soft silts and one-third of which is soft clay. Problematic organic soils also exist over approximately 10% of Wisconsin. Traditionally these soft materials have been undercut and replaced with a crushed rock having large particles (300 mm or larger) that is referred to as “breaker run.” Breaker run layers are made sufficiently thick to provide a sturdy platform for truck traffic during construction. The thickness of breaker run typically is 0.3 to 0.9 m, but thicker layers are used when necessary. Because breaker run is a select material, it is more expensive than ordinary fill materials and sometimes has to be hauled over considerable distance, further increasing costs. Also, undercutting requires removal of large quantities of soft soil that must be moved to a new location, a process that also is costly.

A taskforce established by the Wisconsin Dept. of Transportation (WisDOT) recently undertook an intensive study to evaluate problems and concerns regarding subgrade design and construction. The task force found that problems associated with subgrade stability during construction often resulted in time delays, additional costs, and contract administration problems (1). The taskforce recommended that alternative methods of subgrade stabilization or methods to reduce the thickness of breaker run layer that provides equivalent subgrade support be evaluated (1). Consequently, WisDOT is developing a strategy for using alternative subbase materials (granular backfill

material, pit run sand and gravel, granular industrial by-products, crushed concrete), geosynthetics, or chemical stabilization techniques (e.g., fly ash, lime, or cement) that will be incorporated in the WisDOT Facilities Development Manual (FDM). The intent is that all alternative methods of subgrade improvement in the FDM should provide equivalent performance. A necessary step in defining how alternative stabilization methods can be used is to assess their effectiveness in a field setting. The primary objective of the field study described in this paper is to evaluate representative types of the proposed alternative methods (e.g., granular materials, chemical stabilization, geosynthetic reinforcement) in a systematic manner and to determine if they provide equivalent performance. A secondary objective is to collect field data that can be used to determine whether the behavior predicted based on laboratory test methods and analytical design techniques is realized at field scale. This report describes properties of the subgrade at the test location, the materials that were used for construction, the test sections that were constructed, the instrumentation that was installed, and the field data collected. A series of subsequent reports analyze the field performance of the test sections in greater detail supplemented with proto-type large-scale laboratory experiments on the same materials and provide an evaluation of the stabilization alternatives as working platforms and in terms of their strength contribution to the pavement structure (WHRP Project SPR #0092-00-12 and SPR #0092-03-12). The monitoring of field performance was extended after the completion of the project and the data available to date are included in this report. The field performance of the fly ash section and its

design implications are given separately in Appendix C of this report. The monitoring of field performance was extended after the completion of the project and the data available to date are included in this report. Environmental monitoring was also extended under another contract and will be published as a separate report (Recycled Materials Research Center subcontract to the University of Wisconsin-Madison through WisDOT #0663-43-10).

## **2. DESCRIPTION OF TEST SITE AND TEST SECTIONS**

The field study is being conducted along a 1.4 km segment of Wisconsin State Highway 60 (herein referred to as “S.T.H 60”) between Lodi and Prairie du Sac, Wisconsin. This location is approximately 40 km north of Madison, Wisconsin. Twelve test sections were designed and constructed. A plan view of the test sections is shown in Fig. 1. Three test sections are control sections (at the two ends and in the central area) that were constructed with granular excavated rock that is being used in adjacent sections of S.T.H 60 as part of a 16-km re-construction project. Four test sections were constructed with industrial by-products. Five test sections were constructed using geosynthetics. The sections using industrial by-products were constructed with foundry slag, foundry sand, bottom ash, and fly ash-stabilized subgrade soil as subbase layer materials. The geosynthetics consisted of geocells, a non-woven geotextile, a woven geotextile, a drainage geocomposite, and a geogrid.



## 2.1 Subgrade Properties

The boring logs obtained by the WisDOT prior to construction along the project route are given in Appendix A. Undisturbed samples of the subgrade were collected along the length of the test section at a depth of 1m below ground surface using thin-wall sampling tubes having a diameter of 75-mm. Index properties and unconfined compressive strengths were measured on test specimens prepared from the tube samples. In addition, dynamic penetration index (DPI) of the subgrade was measured with a dynamic cone penetrometer (DCP) and the subgrade stiffness was measured with a soil stiffness gage (SSG) along the length of the test section. The SSG determines the stiffness of soil in a zone lying deeper than 125 mm below the surface (2). The DCP measures the depth of penetration of a cone having a 60° apex and base diameter of 20 mm that is driven with an 8 kg hammer dropped from a height of 522 mm. The DPI is calculated as the average penetration per blow of the hammer.

Atterberg limits, water contents, and dry unit weights for these samples are shown in Fig. 2a along with the soil classifications determined using the Unified Soil Classification System (USCS) and the ASSHTO Classification System. The subgrade generally is a lean silt (ML) or a lean clay (CL) with water content near the plastic limit, with the material towards the east end being slightly leaner. There is also a pocket of more plastic clay (CH) at the eastern end of the bottom ash section.

The unconfined compressive strengths ( $q_u$ ) are higher in the western end of the test section, particularly in the test section constructed with foundry slag

(Fig. 2b). In this region,  $q_u$  is typically between 150-250 kPa, whereas in the remaining areas  $q_u$  is typically between 100-150 kPa. The DPI and subgrade stiffness follow a similar trend. The DPI (average over the top 0.6 m of the subgrade) fall between 25-50 mm/blow in the foundry slag section and 30-90 mm/blow elsewhere (Fig. 2b). The subgrade stiffness generally falls between 4-10 MN/m in the foundry slag and foundry sand sections, 4-7 MN/m in the central test sections (bottom ash – through geocells), and 2-6 in the remaining sections (Fig. 2c).

## **2.2 Control Sections**

Pavement structure for the control sections is shown in Fig. 3. The pavement system consisted of three layers over the subgrade: asphalt concrete, base course, and subbase course. The centrally located control section was constructed with an 840-mm-thick subbase constructed with excavated rock overlain by 140-mm-thick base course layer consisting of a salvaged crushed asphaltic concrete and a crushed aggregate base course of 115 mm. The uppermost layer is a 125mm-thick layer of hot-mix asphalt. The control sections at the ends employed a subbase layer of excavated rock that was 840-mm or thicker. Excavated rock included cobbles (75 to 350 mm in diameter) and a soil fraction. It was retrieved from the cuts in parts of the project route. Its soil fraction consisted of approximately 30% gravel, 65% sand, and 5% fines.

### **2.3 Alternative Subbase Materials**

Properties of the industrial by-products that were used are summarized in Table 1 along with Grade 2 gravel (crushed dolomitic rock) that was used as base course. All of the materials are granular except for the fly ash-stabilized subbase. Bottom ash and foundry slag are coarse-grained gravel-like materials and thus are insensitive to moisture content during compaction. Foundry sand is primarily a mixture of fine sand and sodium bentonite (~ 10%) that also contains small percentages of other additives. The foundry sand is sensitive to water content when compacted, and exhibits a conventional compaction curve.

The fly ash-stabilized subbase was prepared by mixing Class C fly ash from the Columbia Power Station in Portage, Wisconsin with subgrade soil at its natural water content. A series of mix designs were evaluated in the laboratory by preparing specimens in a Harvard miniature compactor following ASTM D 4609, allowing them to cure in a 100% relative humidity room for 7 or 28 days, and then measuring their unconfined compressive strength. Analysis of the results of these tests showed that a fly ash content of 10% on the basis of dry weight provided sufficient strength and therefore, adopted for field construction.

Thickness of each alternative subbase was determined using the California Bearing Ratio (CBR) of the subbase material and the estimated structural number of the central control section (SN = 4.2) based on a design ESALs of 435,080. The design procedure described in AASHTO (3) was followed. Thickness of each subbase layer is shown in Fig. 3. The required thickness for the subbase layer comprised of foundry sand was determined to be

the same as that used for the excavated rock in the control section (840 mm). A thinner layer would be adequate for the foundry slag subbase but construction sequencing resulted in a 840-mm thick subbase. Thinner layers were adequate when the subbase was bottom ash (610 mm) or fly ash stabilized subgrade (300 mm).

## **2.4 Geosynthetics**

Five different types of geosynthetics were used: geocells (two sizes), a nonwoven geotextile, a woven geotextile, a geocomposite drainage layer, and a geogrid. Pertinent properties of the geosynthetics are summarized in Table 2. All geosynthetics were placed directly on top of the subgrade (Fig. 4). The geotextiles, geogrid, and geocomposite drainage layer were overlain by a 300-mm-thick layer of excavated rock.

Presto Geoweb<sup>®</sup> GW20V and GW30V were used as the geocells. These geocells are constructed from 1.3 mm-thick strips of textured high density polyethylene that are welded to form cells with an opening of 260 mm (GW20V) or 320 mm (GW30V) and height of 150 mm. The geocells were underlain by a non-woven needle-punched (NWNP) Linq 150EX geotextile with a weight of 203 g/m<sup>2</sup> and thickness of 1.8 mm, and filled with foundry slag. An additional layer of foundry slag 100-mm-thick was placed on top of the filled geocells. In this application, the geocells act as a reinforcing layer and the NWNP geotextile acts as a separator for the geocell infill and the subgrade.

Two geotextiles Amoco 4553, a NWNP geotextile with a weight of 316 g/m<sup>2</sup> and a wide-strip tensile strength of 13.1 kN/m, and Amoco 2006, a high-strength slit film woven geotextile with a wide-strip tensile strength of 35.4 kN/m were used in the geotextile sections. The geotextiles function as a separator for the subbase and subgrade and reinforcement for enhancing stiffness of the subgrade.

Tenax Tendrain was used for the geocomposite drainage layer. This drainage layer consists of a tri-planar geonet with NWNP geotextiles heat bonded to each side. Separation is provided by the geotextiles and reinforcement and drainage are provided by the geonet, which consists of a high profile triangular-shaped mesh structure with three sets of overlaid intersecting strands. The inner strands are thicker and heavier to provide higher resistance to compression and reinforcing capability. The wide-strip tensile strength of the geocomposite drainage layer is 25.9 kN/m.

The geogrid was Tenax MS 724, a high strength polypropylene biaxial geogrid with a variable aperture size (about 30 to 45 mm) and wide strip tensile strength of 17.2 kN/m. Reinforcement is the primary function of the geogrid.

### **3. INSTRUMENTATION**

Conditions above, within, and below the test sections are monitored. Strain level at the surface of each geosynthetic material in the geosynthetic-reinforced sections is measured. The data being collected include air temperature and relative humidity; subsurface temperature, water content, strain,

stress, and lateral flows; and quantity and quality of water percolating from the subbase layers. This information will be used to describe the operating weather conditions and estimate depth of frost or thaw. Water content information is needed because of its great influence on the mechanical behavior of subbase and subgrade materials.

Three Campbell Scientific Inc. (CSI) CR10 dataloggers are used to control and interrogate the sensors. The CR10 datalogger controls and records readings from each of the sensors to which it is connected and has the ability to power on and off all the other instruments. Also, the datalogger allows users to specify the execution interval and convert the digital electronic signals it receives into physical quantities. The dataloggers are powered by 12V deep cycle batteries that are recharged during the day by solar panels.

There is several other equipment used in the field monitoring system in this project (Fig. 5). Multiplexers are connected to the thermocouple probes, strain gages, and water content reflectometers (WCRs) so that multiple measurements can be made through a single connection with the datalogger. Data are downloaded from the dataloggers twice per week via a landline wired to each datalogger.

### **3.1 Meteorological Conditions**

Air temperature and relative humidity were measured with a thermistor and a capacitive relative humidity sensor. The CSI HMP35C temperature/RH probe is housed in a radiation shield to eliminate the effects of solar radiation

(Fig. 5). A single-ended voltage measurement is taken and converted into temperature ( $^{\circ}\text{C}$ ) or relative humidity based on the manufacturer's calibration equations. The data collected compared well to the climatic data obtained from the National Oceanic and Atmospheric Administration (NOAA) collected from a weather station located in Prairie du Sac Power Plant (approximately 16 km from the test site). Therefore, the NOAA data were used thereafter as the instrumentation had to be removed due to malfunction after the initial 2 years.

### **3.2 Soil Temperature, Water Content, and Lateral Flows**

Soil temperature is measured at 41 locations in the subbase and subgrade layers using type-T copper-constantan thermocouples from OMEGA Engineering, Inc. Locations of the duplex insulated thermocouples are shown in Figs. 3 and 4.

Water contents in the subbase and subgrade are measured using CSI CS615 water content reflectometers (WCRs). Locations of the WCRs are shown in Figs. 3 and 4. WCRs employ a time-domain reflectometry (TDR) methodology that relates the round-trip travel time of an electromagnetic pulse along a wave guide (a set of two 300-mm-long stainless steel rods having a diameter of 3.2 mm that are separated by 32 mm) to the volumetric water content of the soil (4). The travel time is function of the dielectric constant of the soil, which is strongly influenced by water content (5, 6). The dielectric constant of free water is 81, whereas the dielectric constant of dry soil is typically between three and eight, depending on the conductivity of the soil and its density. Electromagnetic techniques are effective in measuring the soil free moisture content based on the

large contrast between the dielectric properties of liquid water and those of dry soil.

Unlike conventional TDR methods, all of the electronics in a WCR are housed in a small watertight handle attached to the end of the wave guide. The oscillation frequency of the multivibrator is dependent upon the dielectric constant of the material surrounding the conducting rods. Circuitry within the probe head scales the multivibrator output in terms of a frequency for measurement with a data acquisition system. The period of the square wave from the multivibrator ranges from 0.7 to 1.6 milliseconds. This feature precludes the need for a separate signal generator/analyzer, reduces cost, and facilitates multiplexing in the field. WCRs operate at lower frequency (~40 MHz) than conventional TDR (~1 GHz) and consequently, the calibration of WCRs is more sensitive to the electrical conductivity of the soil (4). Thus, soil-specific calibration curves are required. Calibration curves for the WCRs were developed using the method described in Suwansawat and Benson (7).

### **3.3 Geosynthetic Strain Gages**

Strain level on the surface of each geosynthetic material installed in the geosynthetic-reinforced sections is being measured. According to the geosynthetic types used in this project, two different resistance types of strain gages from Micro-Measurement Division, Measurement Group Inc. were used as the geosynthetic strain gage. EP-08-250BG-120 for geocell, geocomposite, geogrid sections, and EP-08-20CBW-120 for geotextile sections were mounted



on the surface of the geosynthetics. The former gage has a gage length of 6.35 mm and width of 3.18 mm and the latter is 50.8 mm long and 4.78 mm wide.

The strain gages consist of an open-faced cast polyimide backing with a grid foil consisting of annealed constantan. The annealed constantan is very ductile and thus can undergo the high elongation ( $\pm 20.0\%$ ). The gages have a 120-ohm resistance with a gage factor of 2 and can measure up to 1,000 microstrains with an approximate fatigue life of 10,000 cycles under laboratory loading according to the manufacturer. The excitation voltage is 2.5 V.

The procedures for attachment and weatherization of strain gages on geosynthetics are as follows, briefly;

- Geosynthetic preparation: M&M M-Prep Conditioner A and Neutralizer 5A were used to remove any dirt, contaminants, and oxides and to neutralize the surface, respectively.
- Gage preparation: Average strain in non-fibrous geosynthetics can be measured with a small gage using a simple attachment method. However, long strain gages are usually used on geotextiles where steep strain gradients or stress concentration points are not expected. Due to the potential stiffening effect of epoxy on long gages, direct attachment of the strain gage using epoxy is not recommended (8). Attaching the gages externally, where two ends of a thin plastic strip (glued to the strain gage) is connected to the geotextile via two aluminum end plates (Fig. 6a).

- Presoldering and gage soldering: M&M CPF-75C bondable terminals are installed adjacent to the gages (1.6 mm to 3.2 mm) with 2-part Araldite. When strain gages with pre-attached lead wires are used, the lead wires are looped and soldered to the bondable terminals (Fig. 6b). A thin coating of soldering flux (M&M M-Flux AR) was applied to the wire and terminal for gluing the solder iron. After soldering, all soldering flux were removed using M&M M-line Rosin Solvent, immediately, to prevent degradation of protective coatings and corrosion of metals.
- Gage protection and weatherization: Roadway environment is a severe application for strain gages. The gages must be protected from moisture and mechanical damage and the flexibility of the strain gage must be maintained. For this purpose, terminals and all lead strands are coated with polyurethane, a fluid type Teflon, non-corrosive Dow Corning RTV 3145 adhesive/sealant, M-Coat FBT, and M&M M-Coat B. Particular attention should be placed on the wire leads that extend from the coatings.

To attach the strain gage to the geosynthetics properly without altering properties of the geosynthetics, a special adhesive (Armstrong A-12 Epoxy Resin Part A and Part B) was used with a 2:3 ratio.

A total of 24 strain gages were installed on the geosynthetics: 8 on the geocell, 3 on the nonwoven geotextile and 3 on the woven geotextile, 4 on the geocomposite, and 6 on the geogrid. Two strain gages at both sides of the

geotextile were installed at each point of strain measurement. For geogrid, a dog-bone shape of geomembrane specimen was used to mount strain gages since the geogrid ribs were too narrow to mount a strain gage directly on the ribs (9). The dog-bone specimen was connected to geogrid through clamps by two strips of geomembrane bar that were bolted to adjacent ribs. This custom-built piece was designed to have the same stiffness as the geogrid ribs that they replaced so that they would have minimum impact on the load-deformation behavior of the geogrid.

### **3.4 Earth Pressure Cell**

Total stress at the interface between the subbase and the subgrade in each section is monitored using an earth pressure cell. A schematic of the earth pressure cell is shown in Fig. 7. Each cell was constructed from PVC plates. A chamber in the center was fitted with a rubber membrane to form a bladder. A face plate was placed on top of the bladder to transmit stress from the soil to the bladder without puncturing the membrane. Fluid pressure within the bladder was measured by a pressure transducer (Honeywell Corporation 26PCDFA6G). In each test section, the earth pressure cell was buried 25.4 mm below from the top of the subgrade except in the geocomposite section.

### **3.5 Lateral Flow**

In the geocomposite test section, a 5.2 m x 30 m edge drainage collection system tied with a perforated PVC pipe was installed on both lanes of the road

directly beneath the shoulder break to collect water captured in the geocomposite drainage net (Figs. 8 and 9).

Lateral flow in the geocomposite drainage layer is collected in a sub-surface pipe running along the edge of the pavement (Fig. 10). The downstream end of the pipe discharges to a drainage swale. A FP-5300 paddlewheel flow sensor with FPM-5740 digital flow indicator manufactured by OMEGA Engineering Inc. installed in the discharge pipe monitors the flow rate. FP-5300 flow sensor has a flow rate range between 0.3 to 6 m/s.

### **3.6 Subbase Leachate**

Two lysimeters of equal size (3.50 m x 4.75 m) were installed beneath each test section constructed with industrial by-products as well as the centrally located control section. The lysimeters were installed to determine the amount of liquid passing through the stabilized soil and to determine the concentration of select contaminants (cadmium, chromium, selenium, silver, and sulfate) in the leachate. A typical layout and construction of the lysimeters is shown in Fig. 11. One lysimeter in each test section was installed along the centerline; the other was installed along the shoulder.

The lysimeters were constructed with 1.5-mm thick textured linear low density polyethylene geomembrane overlain by a geocomposite drainage layer comprised of a geonet with NWNP geotextiles heat bonded to either side. Each lysimeter contains a no-storage sump similar to that described in Benson et al. (10) that drains to a 120-L polyethylene collection tank buried in the shoulder.

The collection tanks are insulated with extruded polystyrene to prevent freezing. Leachate that accumulates in the collection tanks is removed on a regular basis using a pump.

To prevent damage during mixing of the fly ash-stabilized soil, the soil was not mixed above the lysimeters using the conventional procedure. Instead, the lysimeters were filled with soil that had been mixed *in situ* at an adjacent location. The soil mixed with fly ash was placed over the lysimeter immediately after mixing, and then was compacted following the same procedures used for the remainder of the test section.

## **4. CONSTRUCTION**

### **4.1 Fly Ash Section**

Based on the laboratory mix design, the subgrade was stabilized using a fly ash content of 10% at water content of  $21 \pm 2$  %. Water content of the subgrade was measured prior to construction and average water content of 23% was observed through out the test section. Since the water content was within the specified range, no water was added. The required amount of fly ash was spread uniformly on the subgrade using truck-mounted lay-down equipment (Fig. 12) designed specifically for fly ash application with minimal dust generation. After placing the fly ash over the entire test section, a reclaimer was used to mix the fly ash with the subgrade soil to a depth of 300 mm. Immediately after mixing, three different compactors (tamping foot, steel drum, and rubber tire) were used to compact the mixture in sequence to complete the stabilization

process. Compaction to the required density was verified by the nuclear density gauge survey. Within a week of construction, the subbase was stiff and ready to be covered with base material.

#### **4.2 Bottom Ash, Foundry Sand, and Foundry Slag Sections**

Unlike fly ash, the other by-products (bottom ash, foundry sand, and foundry slag) were used in bulk form (as a layer or fill) in the corresponding sections. By-products were placed in 150-mm-thick lifts and compacted with a tamping foot roller and a smooth-wheel roller (e.g., Figs. 13 and 14). The dry unit weight of each layer was measured periodically with a nuclear density gage to ensure that the specified compaction (95% relative compaction based on the standard Proctor maximum dry unit weight) was achieved. After placing and compacting the last lift, the top of each subbase layer was compacted again with steel drum and rubber tired compactors to provide a smooth and uniform surface for the remaining pavement layers.

In general, the handling, placement, and compaction of the industrial byproducts did not present any special problems and were similar to natural aggregate with the exception of foundry sand. The foundry sand used had a relatively high bentonite content (~10%) and showed sensitivity to moisture during construction. It was delivered somewhat wet and with the precipitation events at the site, it became difficult to compact and develop sufficient stiffness. However, with some drying it was possible to complete the construction of the foundry sand section. Kleven et al. (2000) investigated ferrous foundry sands in

the Midwestern states from 14 different sources and found that the effective size ( $D_{10}$ ) ranged between 0.002 mm and 0.18 mm and the fines content ( $P_{200}$ ) ranges between 1.1% and 16.4%. The 2  $\mu\text{m}$  clay content varied from 0.8% to 10.0%. The active clay content of the clay-bonded excess system sands ranged between 5.1 and 10.2%. The specific foundry sand used in the test section is at the high end of the range reported for clay content of foundry sands.

### **4.3 Geosynthetics Sections**

Placement of the geocells occurred in three steps: (i) placement of the NWNP geotextile over the subgrade to provide separation, (ii) spreading and staking each section of geocells, and stapling it to the next section, and (iii) filling the geocells with foundry slag (Fig. 15). Each section of geocells was approximately 2.5-m wide and 6.0-m long. The foundry slag was placed into and above the geocells with a loader until a total subbase thickness of 250 mm was achieved. The loader operator used the filled sections of geocells as a working platform to continue filling of the remaining geocells. After filling the geocells, an overlay was placed to bring up the subbase to a thickness of 250 mm and compacted.

The other geosynthetics (woven and nonwoven geotextiles, geogrid, and geocomposite drainage layer) were placed using a similar procedure. The geosynthetic layer spread over the prepared subgrade and excavated rock was placed over the layer using a loader in a single lift (Figs. 16 and 17).

Spreading the geocomposite drainage layer, which was delivered to the site as pre-assembled panels wide enough to cover each lane required greater effort than the other geosynthetics, but was accomplished without the use of any heavy equipment. The geotextile attached to the geocomposite drainage layer included a flap that extended beyond the edge of the geocomposite panel. This flap was wrapped around the aforementioned drainage pipe located along the edge of the pavement.

#### **4.4 Control Section**

The subbase layer in the control section consisted of excavated rock placed in 150-mm-thick lifts and compacted with a tamping foot compactor (Fig. 18). The dry unit weight of each lift was measured with a nuclear density gauge to ensure that the required compaction was achieved. The top layer of the subbase was also compacted with smooth wheel and rubber tired rollers to provide a smooth working platform for the next layer.

#### **4.5 DCP and SSG Surveys**

Surveys were conducted with the DCP and SSG along the centerline of the test sections after the subbase layers were placed and their surface was finished with the rubber-tire compactor. Measurements with the SSG were made on the surface of the finished subbase. DCP tests were conducted until the whole depth of the respective subbase was penetrated.



Results of the SSG and DCP surveys on the subbase are shown in Fig.19. The DPI reported is the average DPI within the thickness of each subbase. The lowest DPIs were obtained in the sections with fly ash stabilized base and geosynthetics; these sections have similar DPI, varying between 10 and 20 mm/blow. The low DPI for the geosynthetics sections is probably due to the excavated rock placed on top of the geosynthetics, which impedes penetration of the DCP. Low DPI was obtained with the fly ash-stabilized subbase due to the high strength of this material. The foundry slag and bottom ash have intermediate DPIs, ranging between 20-30 mm/blow, which reflects the intermediate strength of these materials relative to the other materials. The highest DPIs (30 to 50 mm/blow) were obtained from the section constructed with foundry sand, which was the weakest and softest of the subbase materials.

Stiffness is provided by the SSG rather than strength as indicated by DCP. The fly ash section had markedly higher stiffness (10 to 18 MN/m) than the other sections, including the control section constructed with excavated rock (9-12 MN/m). The foundry slag and geosynthetics sections had intermediate stiffness (6 to 9 MN/m) that is comparable to that in the control section. The granular materials used in the foundry slag and geosynthetic sections are probably responsible for the modest stiffness of these sections. In general, granular materials are known to have low stiffness under low confining pressures at their surfaces. Stiffness of all other sections was in the range of 2 to 5 MN/m, which is appreciably lower than that of the control section.

Despite the variations in strength and stiffness indicated by the DCP and SSG, each subbase displayed comparable support for the construction equipment and provided a stable working platform. The foundry sand section had visibly soft areas present and truck traffic caused some rutting. This was particularly true during wetter conditions, when the bentonite in the foundry sand appeared to hydrate and soften the foundry sand.

#### **4.6 Rolling Weight Deflectometer Surveys**

Deflections in each granular working platform material (bottom ash, foundry sand and slag, control sections) were measured soon after the working platform materials were placed and before placement of any overlying layers. The deflections were measured using a rolling wheel deflectometer (RWD), which is a rolling platform for measuring deflections imposed by a single wheel load (12). A test wheel (single G286 truck tire inflated to 760 kPa) mounted to a steel frame is loaded by water filled tanks (load = 53 kN). As the RWD passes over the working platform, total and plastic (non-recoverable) deflections of the working platform are measured using rotational potentiometers. Total deflections are recorded every 0.3 m along the alignment during a RWD test. The RWD tests were conducted by Crovetti and Schabelski (12) using the RWD designed and fabricated at Marquette University.

## **5. DATA COLLECTED AND PERFORMANCE TO DATE**

### **5.1 Meteorological Data**

The air temperature data collected from the field instruments between January 2001 and July 2001 are shown in Fig. 20 (a). The air temperature ranged from  $-20^{\circ}\text{C}$  to  $38^{\circ}\text{C}$  with the change of seasons during the period of data collection. The relative humidity ranged from 30% to 100% during the same period. The average air temperature data obtained from the NOAA station is given in Fig. 20 (b) for the period 2000-2005. The test sections have been through 5 Wisconsin winter freezing and spring thaws. The last two winters the average temperatures appear to be lower than the previous two but overall the seasons are comparable. The cumulative precipitation record is shown in Fig. 21 which shows steady increase with some seasonal fluctuations.

### **5.2 Subsurface Data**

The variation of the soil temperature at the surface of the subgrade and subbase is shown in Fig. 22 for 2000-2003. The data collection equipment failed and could not be replaced after 2003. Subbase temperatures are lower than subgrade temperatures in winter months. The opposite is true during spring and summer. The temperature at the top of the subbase layer also varies within a narrower band than the temperature at the top of the subgrade. This behavior reflects the stronger influence of atmospheric conditions closer to the surface.

Overall, the soil temperatures ranged between  $-5^{\circ}\text{C}$  and  $35^{\circ}\text{C}$ . Subgrades with thinner subbase sections such as fly ash, geotextile,

geocomposite, and geogrid, experienced subfreezing temperatures during the winter months. Sections with thick subbase, in general, did not have frost penetration to the subgrade.

The range of volumetric water contents observed at the top of the subgrade for each section during the period 2000-2003 is shown in Fig. 23. Data are not shown for the foundry sand and control sections due to malfunctions in the instruments. The highest water contents were measured in the foundry slag, geocell, bottom ash, and fly ash sections. The materials in these sections are finer than those used in the other sections, and thus tend to retain more water. The lowest water contents were measured in the section with the geocomposite drainage layer. This layer diverts infiltrating water from above and melt water from below during thawing events. Low water contents were also measured in the sections with geotextiles and the geogrid because the excavated rock placed above these geosynthetics drains well.

The earth cell, geosynthetic strain, and lateral flow data are not available due to instrumentation failure and malfunction.

### **5.3 RWD Data**

Deflections measured in the field with the RWD are shown in Fig. B9 in Appendix B. Arithmetic means of the deflections measured with the RWD in each section are summarized in Table 3. The largest deflections were measured in the foundry sand section (at a relatively high field moisture content of 23%), and the smallest were measured in the breaker run sections. Deflections in the

bottom ash and foundry slag sections were a factor of two to three higher than those in the breaker run sections. Table 3 suggests, even though the materials are not intrinsically equivalent, a comparable working platform can be obtained with an alternative material provided the layer of alternative material has adequate thickness. Even the weakest working platform formed by the foundry sand provided adequate support to support the construction of the pavement structure. Foundry sands vary in fines and clay content and a generalization should not be made on the basis of the particular foundry sand used in this project.

#### **5.4 FWD Data**

A falling weight deflectometer (FWD) was used to evaluate the stiffness of the pavement structures in a comparative manner. To understand the effect of seasonal changes on pavement stiffness, FWD tests were performed in fall (October 23, 2000) immediately after construction was completed, the following spring (May 16, 2001) after the pavement had completely thawed, and bi-annually since then. Four different loads (22, 40, 50, and 90 kN) were applied.

Maximum deflections recorded during the FWD tests for 90-kN falling weight for the first 5 measurement cycles (through 2002) are presented in Fig. 24. The readings have stabilized after this period. Maximum deflection, which is measured at the center of the loading plate, is a gross indicator of the aggregate pavement response to the dynamic load. The deflections in spring are comparable to those after construction for the control, foundry slag, and geocell

test sections. Larger deflections were obtained in the spring for the foundry sand, fly ash, and the geosynthetic test sections (excluding the geocell section). The greatest differences between fall 2000 and spring 2001 are in the fine-textured subbase materials, i.e., the foundry sand and fly ash, which are more susceptible to thaw weakening (11). These sections also exhibit greater variability in maximum deflection after thawing, particularly the foundry sand section. But, smaller deflections were measured through the test sections in fall 2001. The maximum deflection from each control section ranged from 0.92 mm to 0.99 mm (Fall 2000), 0.93 mm to 0.98 mm (Spring 2001), and 0.63 mm to 0.86mm (Fall 2001). Essentially a constant baseline existed along the control sections.

Overall, the test sections were essentially equivalent since all deflections were less than 2 mm thus enabling support of construction equipment during the severest challenge to the soft subgrade in terms of stresses. Spring thaw demonstrated that most of the alternatives continued to retain their support capability for the traffic load with the exception of the foundry sand section where the stiffness was nearly dropped by half, i.e., 2 to 4-mm deflections. Spring thaw-weakening is known to result in large decreases in pavement stiffness, e.g. 35 to 65% compared to the normal conditions (11). The foundry sand section, which resulted in the largest deflections early on, eventually recovered probably as a result of moisture equilibration to a drier state. By October 2002, all sections, including the foundry sand section, provide a similar structural contribution to the pavement structure.

Deflection basins from the FWD survey data collected in fall and spring showed that the basins are deeper and narrower in spring, which reflects the effect of thaw-weakening. It can be expected that pavement stiffness recovers again in summer and this is shown in Fig. 24. Distress surveys were implemented in 2003 and there has been no significant distress evident in any part of the test section at the end of the current observation period of 2005, nearly 5 years after the highway was opened to traffic. Surface crack sealing was undertaken in S.T.H. 60 in 2004, however, there is no evidence of differences between sections in this regard based on a visual inspection.

Elastic modulus of the asphalt layer, base course, working platform (subbase), and subgrade were back-calculated using the program MODULUS for 10 cycles of measurement between 2000 and 2005. The data (including maximum deflections) are averaged for each section over 10 seasons and presented in graphical form in Appendix B.

The longer-term performance (i.e., after 5 years) and contribution to pavement structure strength as evidenced from maximum deflections (Fig. B1 in Appendix B) and back-calculated moduli from the FWD surveys (Fig. 25b) indicate that the alternative platforms have varying median moduli although comparable structural contributions due to their varying thicknesses (i.e., comparable maximum deflections). At the end of 5 years, back-calculated median moduli could be grouped into 4 categories as shown in Fig. 25b, which provides the median, one-standard deviation and the range of modulus data for each of the working platforms in the last survey conducted in May 2005 (i.e.,

spacially averaged in each section). Fig. 25a provides the same information averaged temporally over 10 cycles of the FWD surveys. The first category includes foundry sand, foundry slag, and geocell sections and had the lowest mean moduli. The second category includes breaker run in control sections and reinforced geotextile and drain geocomposite sections and had somewhat higher mean moduli than the first category but comparable to each other (except one of the control sections). The third category includes bottom ash and geogrid-reinforced sections and had mean moduli higher than the second category. Fly ash section had the highest mean modulus at the end of 5 years, which was markedly higher than even the third category. Grouping the back-calculated moduli in this way indicates that these materials have varying stiffness; however, if the stiffness of breaker run is taken as the reference, the stiffness of most alternative materials is equal or higher than breaker run except foundry sand, foundry slag, and geocell. Modulus of the fly section increased considerably with time as evidenced by the large spread of the data shown in Fig. 25a. The fly ash stabilized subgrade layer, like the geosynthetic-reinforced layers, is a thin platform (i.e., 0.3-m thick); however, it provides a similar structural contribution to the pavement structure when measured in terms of the maximum FWD deflections as shown in Fig. B1 in Appendix B. The maximum deflection of the fly ash section is equivalent to those of other thicker granular working platforms due to its superior modulus shown in Fig. 25.



## 5.5 Lysimeter Data

Flux of leachate as collected by the lysimeters is shown in Fig. 26 for the 2000-2002 period. There is a separate on-going environmental monitoring program. The lysimeter data collected since 2003 and the laboratory leaching and column tests on all industrial byproducts will be presented at the completion of that study. Once the highway was paved during the first week of October 2000, the fluxes decreased dramatically. The flux during the winter was very small because of frozen conditions. In spring, the leachate fluxes increased to values comparable to those measured in October 2000 before frost penetrated the pavement.

The lowest fluxes were obtained from the foundry sand section, which was anticipated since foundry sand is a sand-bentonite mixture and thus has low hydraulic conductivity (13). Low fluxes were also obtained from the fly ash section after the asphalt paving was complete, which is consistent with the low hydraulic conductivity that is usually reported for mixtures of fine-grained soil and fly ash. The highest fluxes were measured for the coarse by-products and the control section, all of which should have high hydraulic conductivity.

Concentrations of cadmium, chromium, selenium, and silver in leachate collected during the first sampling event (September 14, 2000) are shown in Fig. 27. The concentration of cadmium is slightly lower for fly ash stabilized soil than that for the control section, which is consistent with the results of water leach tests that were conducted in the laboratory prior to construction. In contrast, the concentration of chromium in leachate from the fly ash stabilized soil is higher

than that for control section. The concentration of chromium for the control section was below the detection limit (2  $\mu\text{g/L}$ ). Selenium and silver concentrations for the control section are lower than those for the fly ash stabilized soil.

Concentrations of all the metals from the leachate collected from the bottom ash section are higher than that from the control section as well as from the fly ash section. Unlike fly ash, bottom ash was used in bulk form and thus dilution, fixation, and adsorption due to mixing with soil are not expected (14). Moreover, the data in Fig. 27 reflects the early flush.

Concentrations of all the metals in leachate from the foundry slag section are quite comparable to that from the control section except for chromium, which was slightly higher in foundry slag. Concentrations of all the metals in all the by-product sections are in ppb ( $\mu\text{g}$  per liter) level and these metals are expected to be adsorbed in the subgrade soil as the leachate moves towards the groundwater.

## **6. SUMMARY**

Soft subgrade is a common problem in many parts of Wisconsin, as well as other states. This study is aimed at evaluating alternative methods for providing a stable platform over soft subgrade to complete construction of pavement structures. The alternative methods may also result in superior long-term performance of highways.

To accomplish the objective, test sections were constructed along a 1.4-km stretch of state highway in Wisconsin. The test sections incorporate nine different alternatives using industrial by-products and geosynthetics. These alternatives do not match the alternatives identified in the original proposal but correspond to those that could be developed within the budget available, constraints of an actual construction project, and the contributions that could be obtained from private suppliers. However, they include one or more alternatives in each group of granular materials, industrial byproducts, chemical stabilization, and geosynthetic reinforcement and as such provide a reasonably broad basis for generalizations. Having all these alternatives at the same site provides a systematic approach for assessing the equivalency of the alternatives and determining the viability of existing design methods. The industrial by-products that were used were foundry slag, foundry sand, bottom ash, and fly ash. The geosynthetics were geocells, a non-woven geotextile, a woven geotextile, a geocomposite drainage layer, and a geogrid. The pavement structure was maintained the same in all test sections, except for the subbase layer. Thickness of the subbase layer was selected based on initial laboratory CBR tests so that the structural number for all test sections would be essentially the same.

During construction, quality control data were systematically collected. The data included dry unit weight, water content, dynamic penetration index, and soil stiffness as measured with a soil stiffness gage. After construction of the working platforms, a rolling weight deflectometer survey was conducted in the sections constructed with byproducts and the control sections. No useful data

was collected during construction from earth cells, geosynthetic strain gages, and lateral flow measurements. The test sections have also been monitored since construction using an automated data acquisition system. Data collected with the monitoring system include air temperature and relative humidity, subsurface temperature, and water contents. Due to instrumentation malfunction subsurface monitoring was terminated after the first 3 years. Air temperature and precipitation data, however, were collected from a weather station in close proximity of the test site. Falling weight deflectometer surveys were conducted bi-annually (October and May) subsequent to the completion of the project. The surveys started in Fall 2000 to the present (10 surveys covering 5 winter and spring seasons). Lysimeters were also installed under the test sections constructed with industrial by-products and a control section to measure the quantity and quality of water percolating from the base of these test sections. Both the observations made during construction and the RWD data obtained after construction of the working platforms, indicate that overall equivalency in minimal performance of the alternative stabilization sections as working platforms is essentially achieved. All sections provided adequate support to the construction equipment and allowed the completion of the pavement structure. Currently, there is no significant distress evident in any part of the roadway or any major differences between various test sections. There is an inherent conservatism in designing pavement cross sections. The alternative methods of soft ground stabilization appear to provide equal or better stiffness as the control sections constructed by the traditional method of using rock aggregate. The only

significant exception to this was observed in the section built using foundry sand. This foundry sand had relatively high bentonite content (10%) and is sensitive to moisture as evidenced during construction and during the spring thaw. Foundry sands with lower bentonite content are expected to provide better performance based on past experience. Use of fly ash-stabilized subgrade and geosynthetics-reinforced subbases provided equivalent support with much thinner subbase layers.

The longer-term performance (i.e., after 5 years), as evidenced from maximum deflections and back-calculated moduli from the FWD surveys, indicate that the alternative platforms have varying median moduli although comparable structural contributions due to their varying thicknesses (i.e., comparable maximum deflections). At the end of 5 years, back-calculated median moduli could be grouped into 4 categories. The first category includes foundry sand, foundry slag, and geocell sections and had the lowest mean moduli. The second category includes breaker run in control sections and reinforced geotextile and drain geocomposite sections and had somewhat higher mean moduli than the first category but comparable to each other (except one of the control sections). The third category includes bottom ash and geogrid-reinforced sections and had mean moduli higher than the second category. Fly ash section had the highest mean modulus at the end of 5 years, which was markedly higher than even the third category. Grouping the back-calculated moduli in this way indicates that these materials have varying stiffness; however, if the stiffness of breaker run is taken as the reference, the stiffness of most

alternative materials is equal or higher than breaker run except foundry sand, foundry slag, and geocell. Modulus of the fly section increased considerably with time. The fly ash stabilized subgrade layer, like the geosynthetic-reinforced layers, is a thin platform (i.e., 0.3-m thick); however, it provides a similar structural contribution to the pavement structure when measured in terms of the maximum FWD deflections.

The leachate quality of the by-products shows that they discharge contaminants of concern at very low concentrations, i.e., in part per billion range.

This report describes the development of field test sections and observations during construction and for 5 years of post-construction. For uniformity of presentation, the geosynthetics-reinforced sections are also included even though they are not part of the original contract. A series of subsequent reports analyze the field performance of the sections built with granular alternative materials (i.e., foundry sand, foundry slag, bottom ash, Grade 2 granular backfill, and breaker run) and geosynthetic-reinforced test sections (i.e., using geogrid, geotextiles, and drainage geocomposite) in greater detail. The analysis is supplemented with proto-type large-scale laboratory experiments on the same materials. An evaluation of the stabilization alternatives as working platforms and in terms of their strength contribution to the pavement structure is undertaken (WHRP Project SPR #0092-00-12 and SPR #0092-03-12). The field performance of the fly ash section (i.e., a chemically stabilized alternative) and its design implications are given separately in Appendix C of this report. The monitoring of field performance was extended after the completion of the project

and the data available to date are included in this report. Environmental monitoring was also extended under another contract and will be published as a separate report (Recycled Materials Research Center subcontract to the University of Wisconsin-Madison through WisDOT #0663-43-10). A review of all of these reports together will reveal that all of the original contract requirements are met even though the results are not presented as proposed in each contract, but presented along technically logical units.

## REFERENCES

1. Wisconsin Department of Transportation Subgrade Design/Construction Process Review Team. *Subgrade Design/Construction Process Review*. Final Report, Madison, Wisconsin, 1997.
2. Sawangsuriya, A. Evaluation of the Soil Stiffness Gauge, M.S. Thesis, Department of Civil and Environmental Engineering, University of Wisconsin-Madison, WI, 2001.
3. AASHTO. *Guide for Design of Pavement Structures*. American Association of State Highway and Transportation Officials, Washington, D.C., 1993.
4. Campbell, G. and R. Anderson. Evaluation of Simple Transmission Line Oscillators for Soil Moisture Measurement. *Computers and Electronics in Agriculture*, 20, 1998, pp. 31-44.
5. Topp, G.C., Davis, J.L. and A.P. Annan, A.P. Electromagnetic Determination of Soil Water Content: Measurements in Coaxial Transmission Lines. *Water Resources Research*, Vol. 16, No. 3, 1980, pp. 574-582.
6. Benson, C., and P.J. Bosscher. *Time-Domain Reflectometry in Geotechnics: A Review, Nondestructive and Automated Testing for Soil and Rock Properties*. STP 1350, ASTM, W. Marr and C. Fairhurst, Eds., 1999, pp. 113-136.

7. Suwansawat, S. and C. Benson. Cell Size for Water Content-Dielectric Constant Calibrations for Time Domain Reflectometry. *Geotechnical Testing Journal.*, ASTM, 22(1), 1998, pp. 3-12.
8. Bergado, D., Long, P., Loke, K., Christopher, B., and P. Delmas. Geotextile Reinforcement in Full Scale Test Embankment on Soft Ground. *Proceedings of the 5<sup>th</sup> International Conference on Geosynthetics*, Singapore, 1994.
9. Hayden, S., Humphrey, D., Christopher, B., Henry, K., and C. Fetten. Effectiveness of Geosynthetics for Roadway Construction in Cold Regions: Results of a Multi-Use Test Section. *Proceedings of Geosynthetics '99, Vol. 2. Boston, Massachusetts*, 1999, pp. 847-862.
10. Benson, C., Abichou, T., Albright, W., Gee, G., and A. Roesler. Field Evaluation of Alternative Earthen Final Covers. *International J. of Phytoremediation*, 3(1), 2001, pp. 1-21.
11. Jong, D., Bosscher, P., and C. Benson. Field Assessment of Changes in Pavement Moduli Caused by Freezing and Thawing. In *Transportation Research Record 1615*, TRB, National Research Council, Washington, D.C., 1998, pp. 41-50.
12. Crovetti, J. A. and Schabelski, J.P. (2001), Comprehensive Subgrade Deflection Acceptance Criteria, Phase III Final Report WI/SPR 02-01, WisDOT Highway Research Study #98-1, SPR # 0092-45-95.
13. Abichou, T., Benson, C., and T. B. Edil. Foundry Green Sands as Hydraulic Barriers: Laboratory Study. *Journal of Geotechnical and Geoenvironmental Engineering*, American Society of Civil Engineers, Vol. 126, No. 12, 2000, pp. 1174-1183.
14. Gustin, F. H. and M. R. Thomes. Environmental Aspects of Class C Fly Ash in Soil Stabilization. *The 12<sup>th</sup> International Symposium On Management & Use of Coal Combustion Byproducts (CCBs)*, Orlando, FL., 1997.
15. Kleven, J.R., Edil, T. B., and Benson, C. H. (2000), "Evaluation of Excess Foundry System Sands for Use as Subbase Material," *Transportation Research Record*, 1714, 40-48.



**TABLE 1 Properties of Subbase Materials**

Subbase	Specific Gravity	D <sub>10</sub> (mm)	D <sub>60</sub> (mm)	C <sub>u</sub>	Max. Dry Unit Weight <sup>a</sup> (kN/m <sup>3</sup> )	Optimum Water Content (%)	Max. Unit Weight <sup>b</sup> (kN/m <sup>3</sup> )	CBR	Max. Unconfined Compressive Strength (kPa)	Resilient Modulus <sup>c</sup> (MN/m <sup>2</sup> )
Grade 2 Gravel	2.65	0.09	6	66.7	22.6	8.2	ND	ND	ND	120-350
Fly Ash Stabilized Subbase	NA	NA	NA	NA	16.1	21	NA	32	540	ND
Bottom Ash	2.65	0.06	1.9	31.7	15.1	NA	13.7	21	NA	200-400
Foundry Slag	2.29	0.13	2	15.4	10	NA	8.4	17	NA	600-700
Foundry Sand	2.55	0.0002	0.25	1250	16.1	16	NA	7	NA	400-900

NA = Not applicable      ND = Not done

<sup>a</sup> Obtained from Standard Proctor Compaction (ASTM D 698) test

<sup>b</sup> Obtained from Vibratory Table (ASTM D 4253-83) test

<sup>c</sup> Obtained from AASHTO T294-94 protocol for resilient modulus test

**TABLE 2 Properties of Geosynthetics**

Geosynthetic Type		Property	Test Method	Values <sup>b</sup>
PRESTO Geoweb®	GW20V <sup>a</sup>	Strip Sheet Thickness	ASTM D 5199	1.27 mm
		Cell Depth x Width x Length	-	150 x 259 x 224 mm
		Density per m <sup>2</sup>	-	34.6
		Short-term Seam Peel Strength	-	2130 N
	GW30V <sup>a</sup>	Strip Sheet Thickness	ASTM D 5199	1.27 mm
		Cell Depth x Width x Length	NA	150 x 320 x 287 mm
		Density per m <sup>2</sup>	NA	21.7
		Short-term Seam Peel Strength	NA	2130 N
AMOCO Style 4553 polypropylene nonwoven needle punched geotextile	Thickness	ASTM D 5199	2.7 mm	
	Mass per Unit Area	ASTM D 5261	315.6 g/m <sup>2</sup>	
	Wide Width Tensile	ASTM D 4595	13.1 kN	
	Wide Width Elongation	ASTM D 4595	72 %	
	AOS	ASTM D 4751	0.15 mm	
	Permittivity	ASTM D 4491	0.77 sec <sup>-1</sup>	
AMOCO Style 2006 polypropylene slit-film woven geotextile	Thickness	ASTM D 5199	0.7 mm	
	Mass per Unit Area	ASTM D 5261	268.2 g/m <sup>2</sup>	
	Wide Width Tensile	ASTM D 4595	35.4 kN/m	
	Wide Width Elongation	ASTM D 4595	26 %	
	AOS	ASTM D 4751	0.43 mm	
	Permittivity	ASTM D 4491	0.18 sec <sup>-1</sup>	
TENAX MS™ 724 biaxial oriented polypropylene geogrid	Thickness	ASTM D 5199	NM	
	Mass per Unit Area	ASTM D 5261	253.1 g/m <sup>2</sup>	
	Aperture Size <sup>a</sup>	NA	32 mm	
	Peak Tensile Strength	GRI-GG1	17.2 kN/m	
	Yield Point Elongation	GRI-GG1	20 %	
	Junction Strength <sup>a</sup>	GRI-GG2	10.0 kN/m	
TENAX Tendrain™ tri-planar Geocomposite	Thickness	ASTM D 5199	12.7 mm	
	Mass per Unit Area	ASTM D 5261	1700.6 g/m <sup>2</sup>	
	Tensile Strength	ASTM D 4595	25.9 kN/m	
	Tensile Elongation	ASTM D 4595	23 %	
	Permeability <sup>a</sup> at i = 1, $\sigma_v = 720$ kPa	NA	25,000 m/day	

NA=No standard method available

NM = Not measured

<sup>a</sup> As reported by the manufacturer.

<sup>b</sup> Machine direction only.

**TABLE 3. Total Deflections Obtained from RWD.**

Materials	Thickness at Field Site (m)	RWD <sup>a</sup> Total Deflection (mm)
Breaker run (West End)	0.84	4.0 ± 4.3 <sup>b</sup> (135 measurements)
Breaker run (East End)		5.1 ± 3.6 (157 measurements)
Bottom Ash	0.60	14.3 ± 5.8 (271 measurements)
Foundry Slag	0.84	11.0 ± 8.2 (333 measurements)
Foundry Sand	0.84	47.1 ± 14.3 (356 measurements)

Notes: <sup>a</sup>Average total deflection from RWD tests, <sup>b</sup>± one standard deviation. Number of RWD measurements noted in parentheses

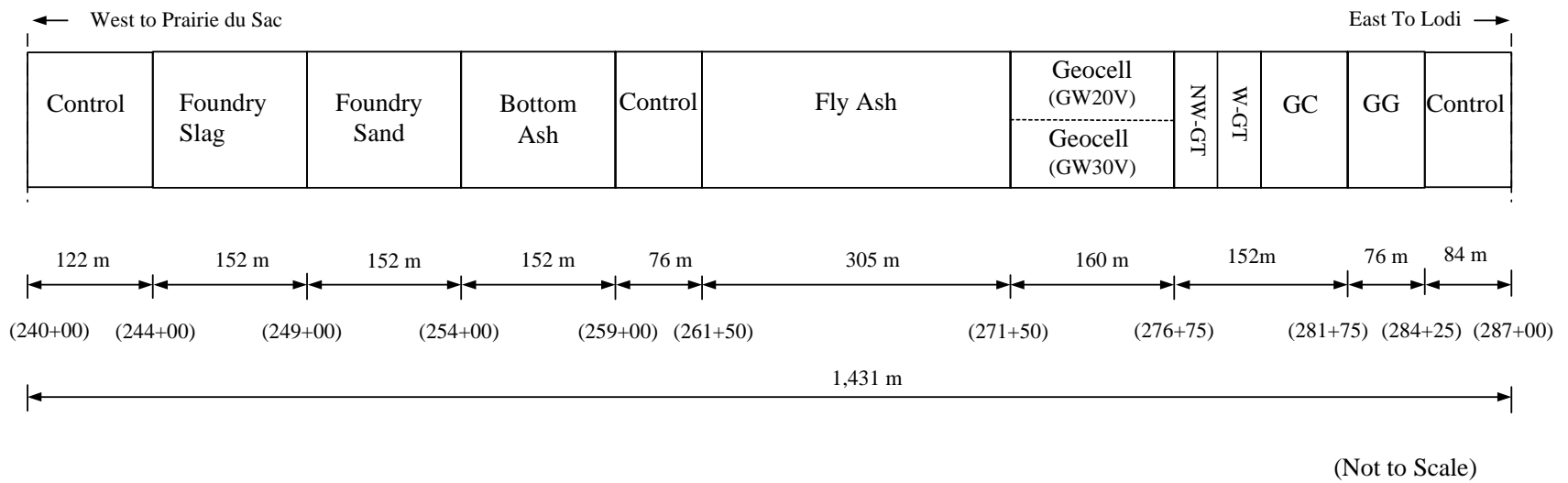


**FIGURE 1** Layout of test sections at STH 60 site.

Foundry slag	Foundry sand	Bottom ash	Control (M)	Fly ash	Geocell	NW-GT	W-GT	GC	GG	Control (E)
--------------	--------------	------------	-------------	---------	---------	-------	------	----	----	-------------

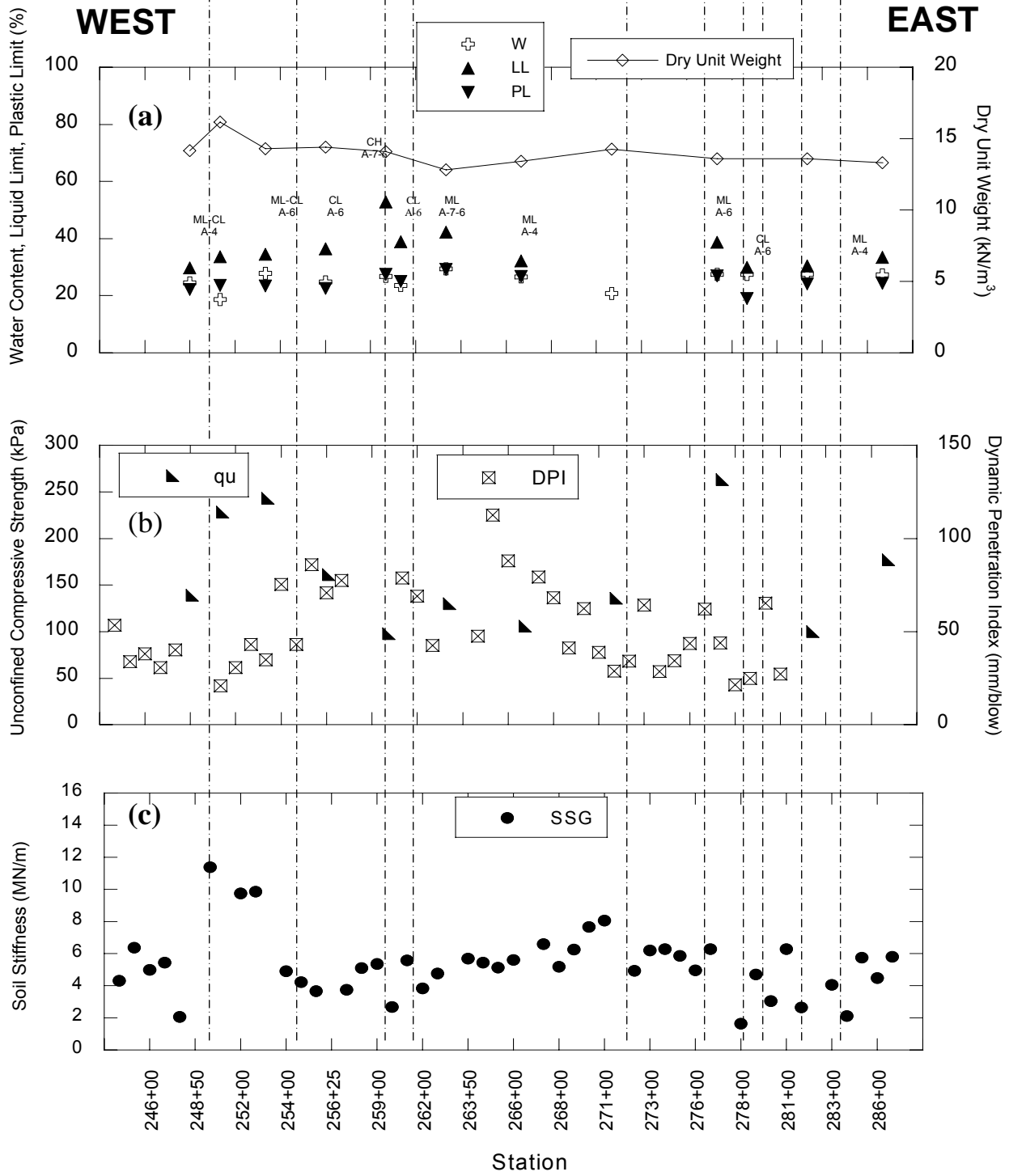


**FIGURE 2**  $\omega$ , LL, PL,  $\gamma_{dmax}$ ,  $q_u$ , DPI and soil stiffness results of subgrade in STH 60.

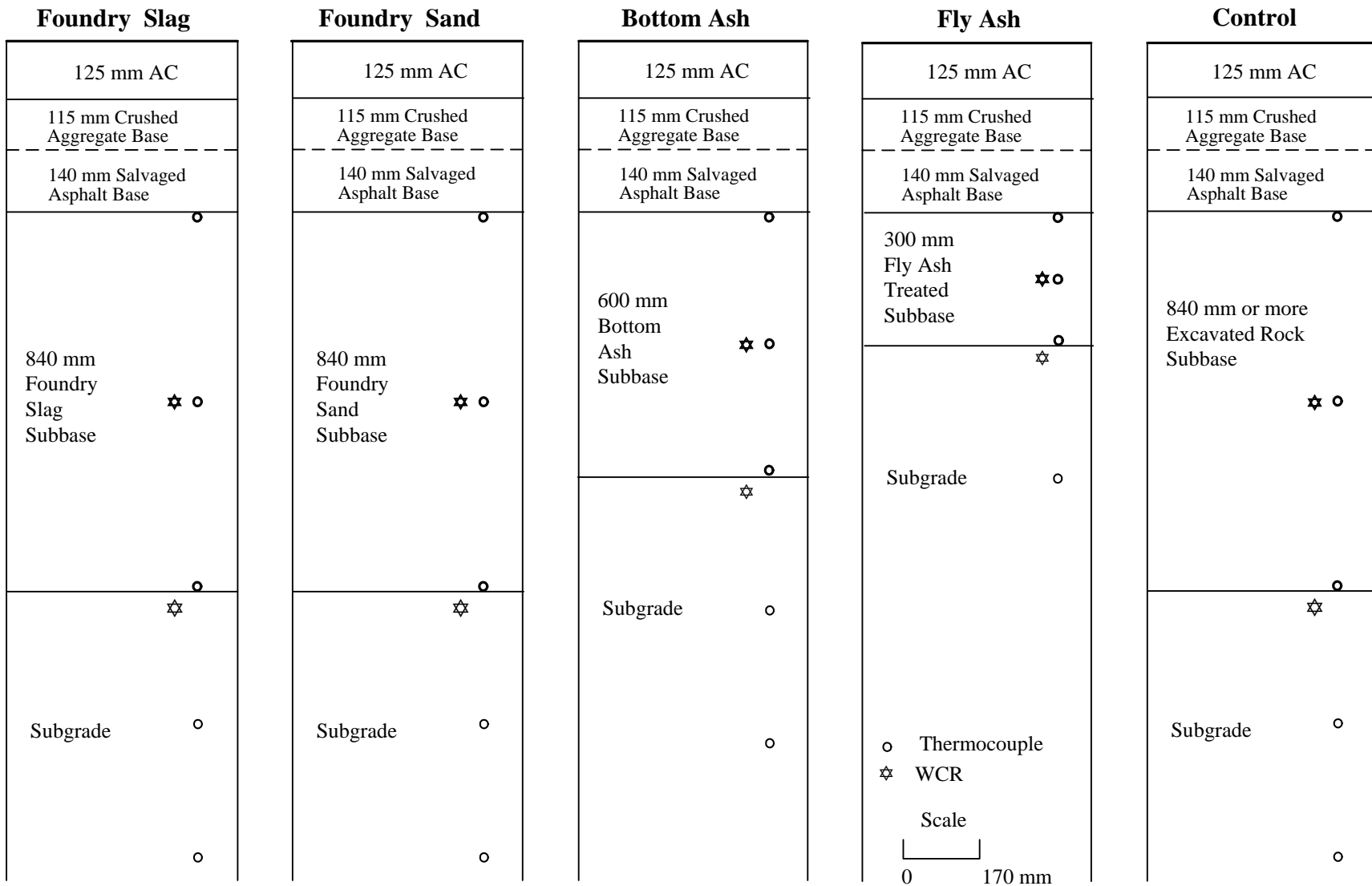


**FIGURE 3 Vertical sections of pavement structures for the by-products and the control sections.**

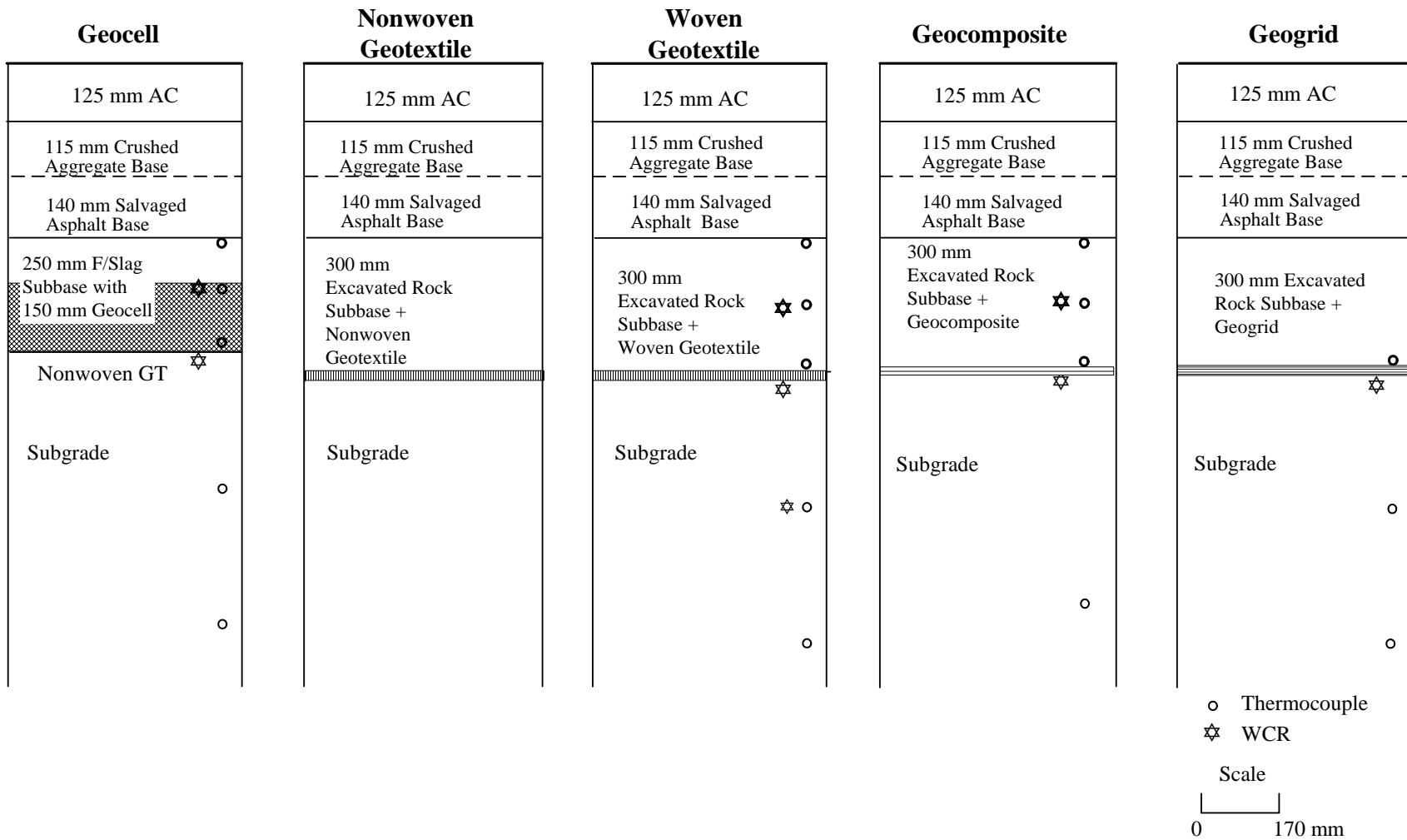


**FIGURE 4 Vertical sections of pavement structures for the geosynthetics sections.**

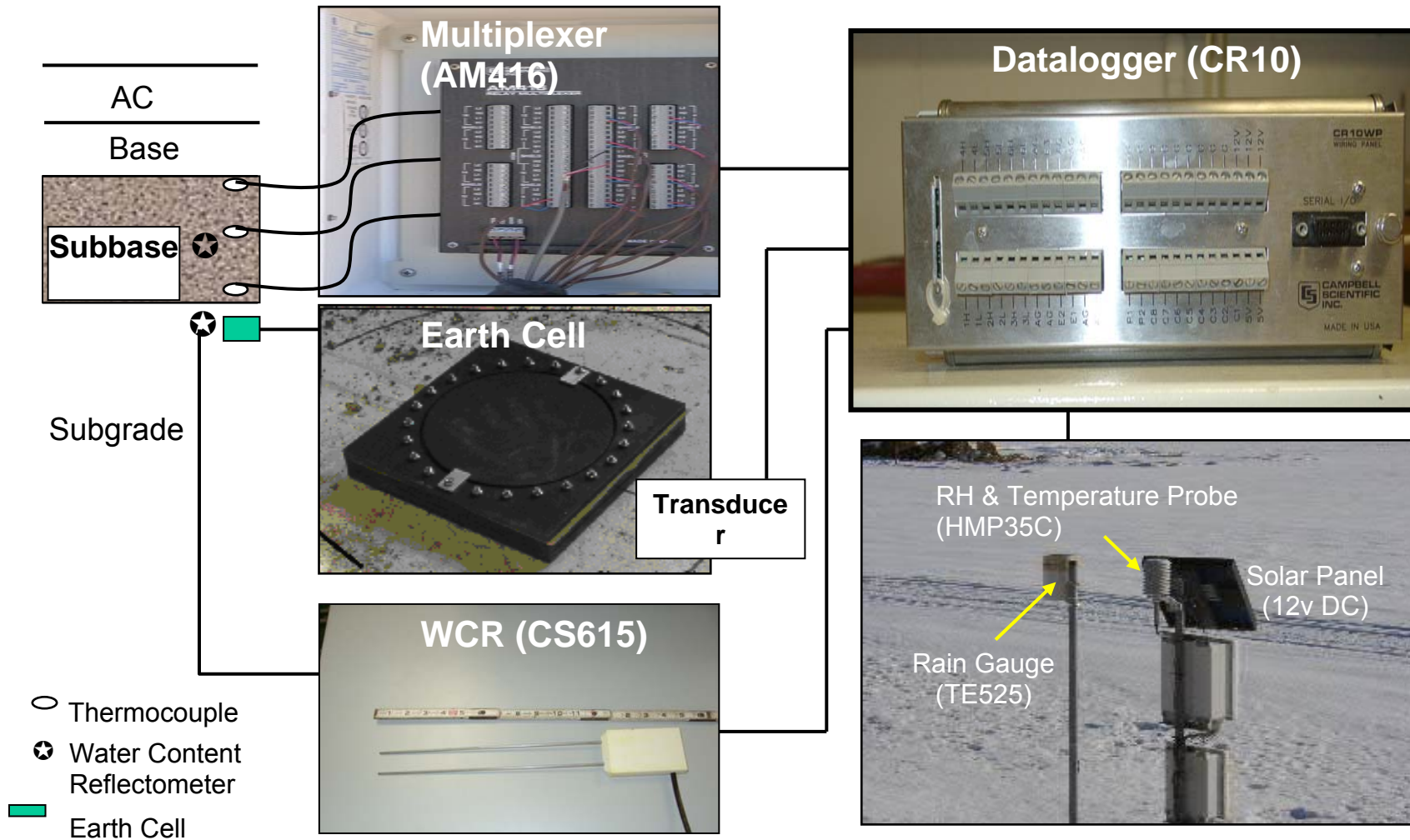
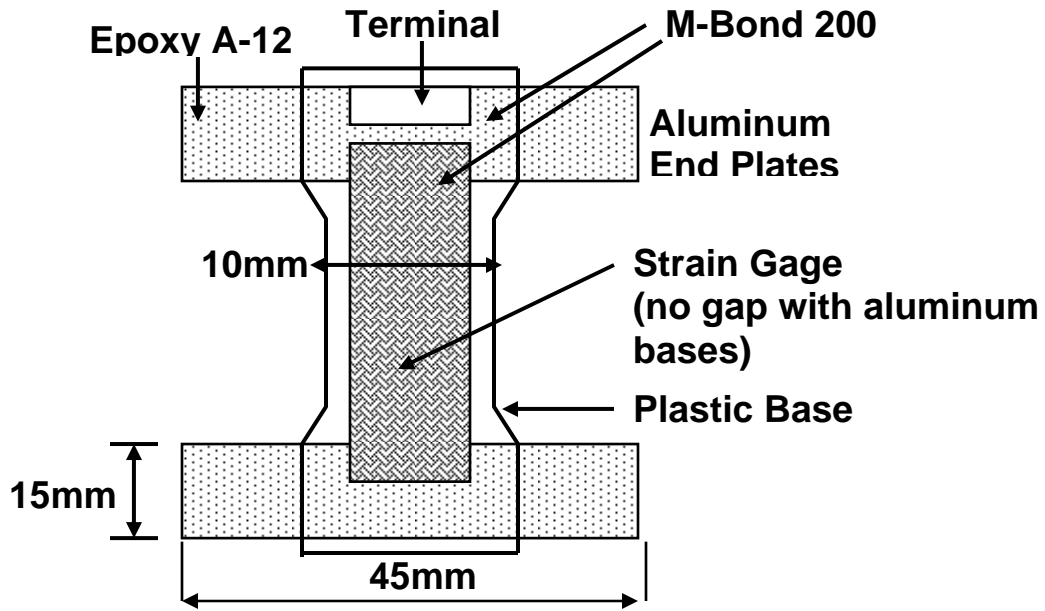
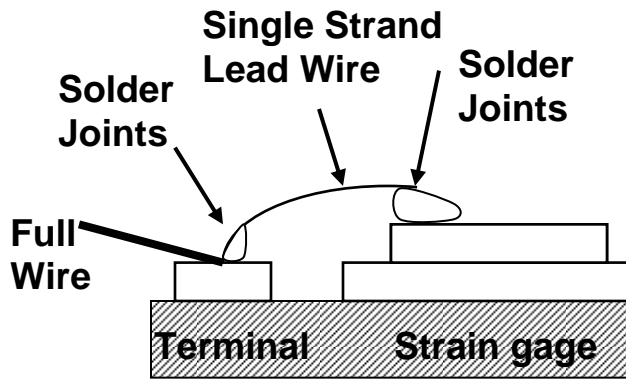


**FIGURE 5** Layout of field monitoring equipments at STH 60.





(a) Gage preparation



(b) Pre-soldering and gage soldering

FIGURE 6 Strain gage installation of geotextile.

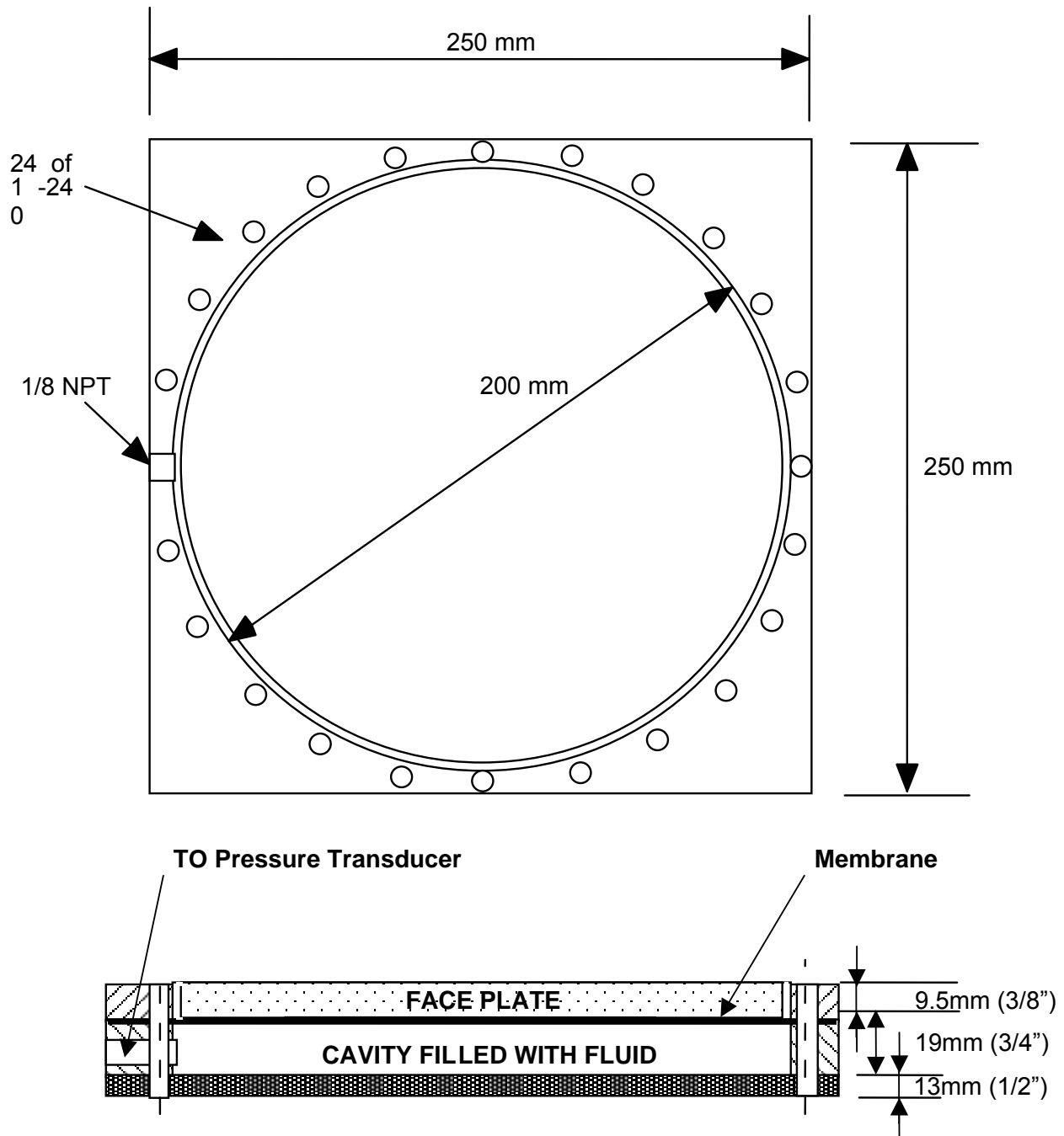


**FIGURE 7 Schematic of earth pressure cell.**

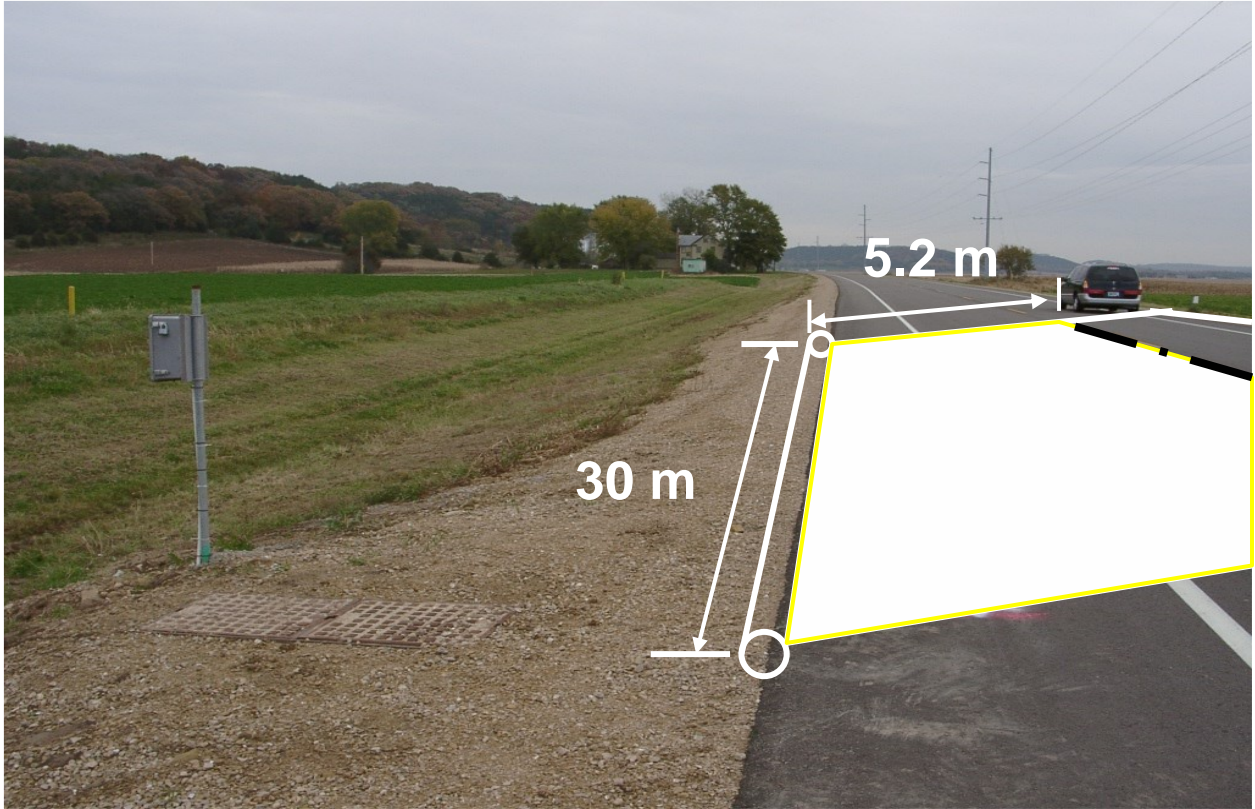


**FIGURE 8** Location of drainage collection pipe.

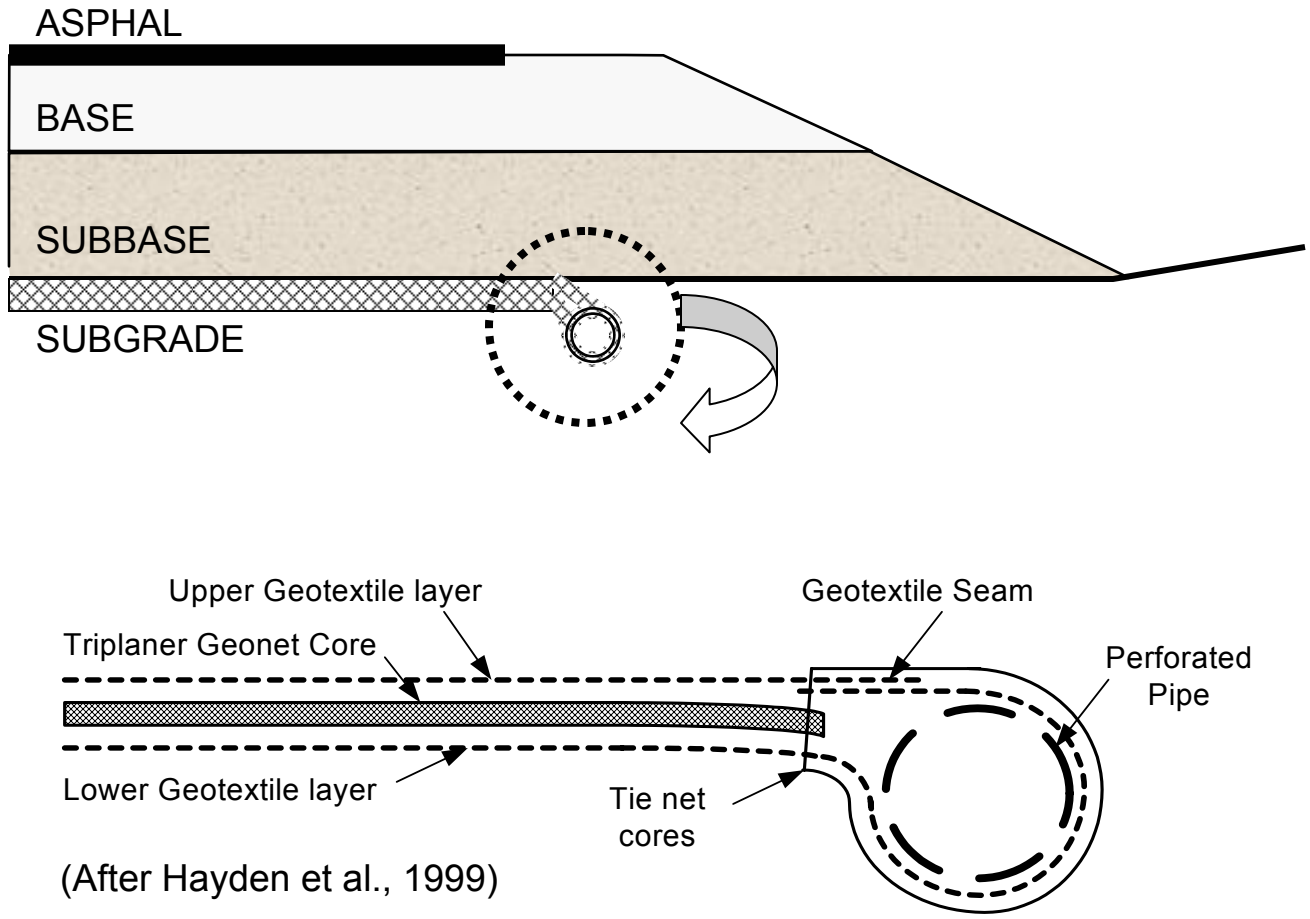


**FIGURE 9 Drainage collection system in geocomposite reinforced section.**

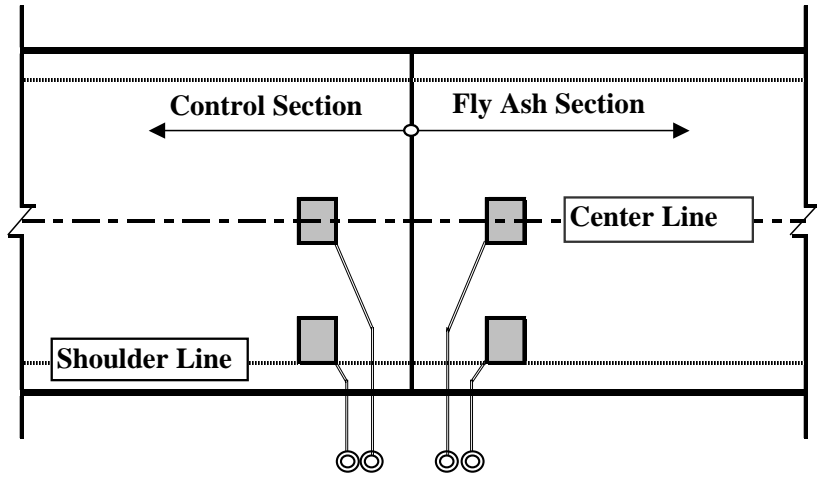


**FIGURE 10** Flowmeter installation and data collection.

**Legend:**

■ Lysimeter

⊙ Collection Tank



(Not to scale)



**FIGURE 11 Typical layout of lysimeters and construction.**



**FIGURE 12 Laydown equipment to spread fly ash on subgrade.**



**FIGURE 13** Placement of foundry slag as subbase.





**FIGURE 14 Placement of foundry sand as subbase.**



**FIGURE 15** Installation of geocell sections infilled with foundry slag.



**FIGURE 16** Installation of geocomposite section.



**FIGURE 17** Installation of geogrid section.



**FIGURE 18** Installation of control section.

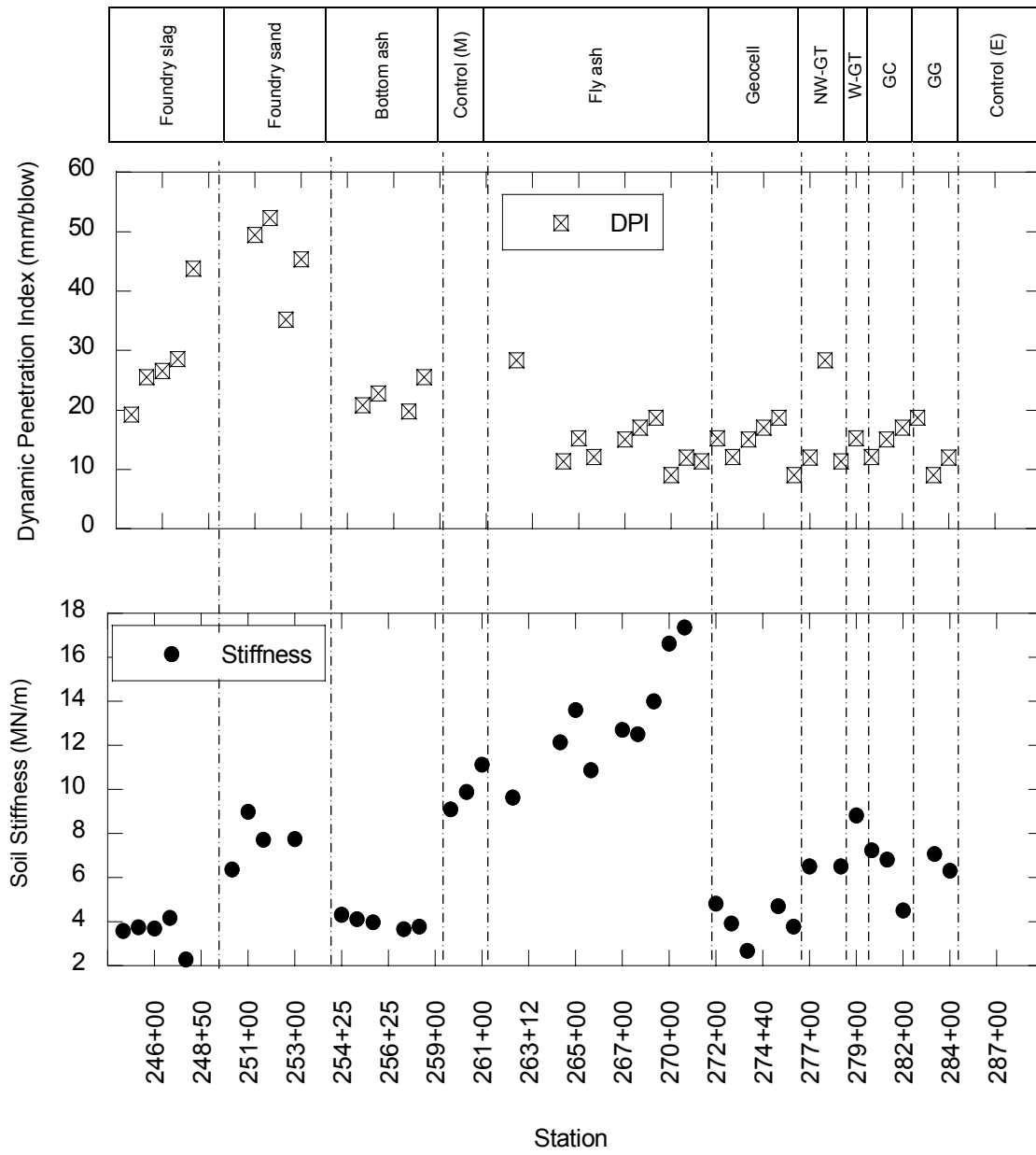


**FIGURE 19 DPI and soil stiffness results of the subbase in STH 60.**

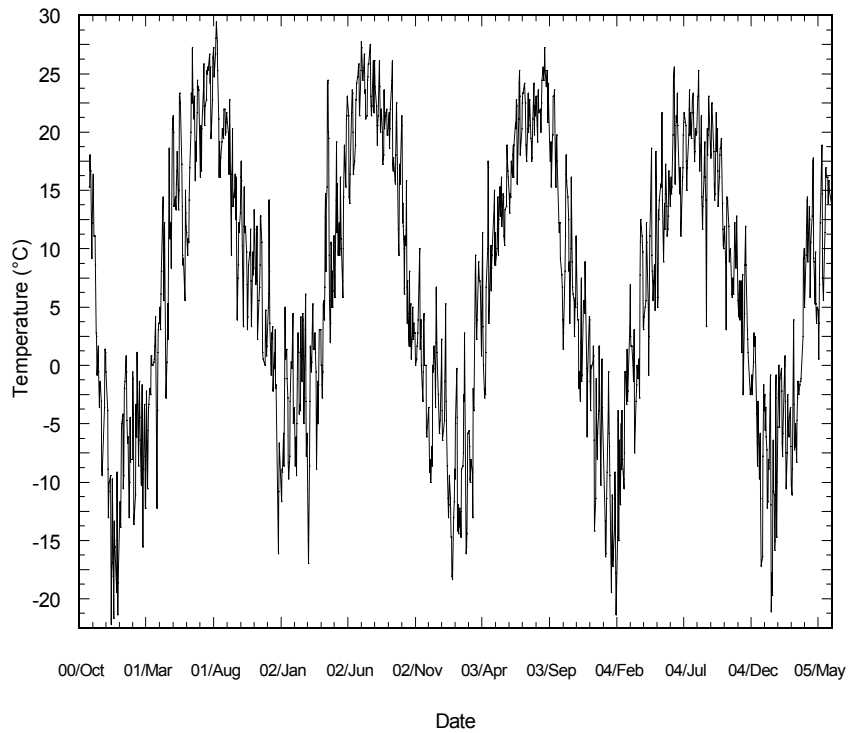
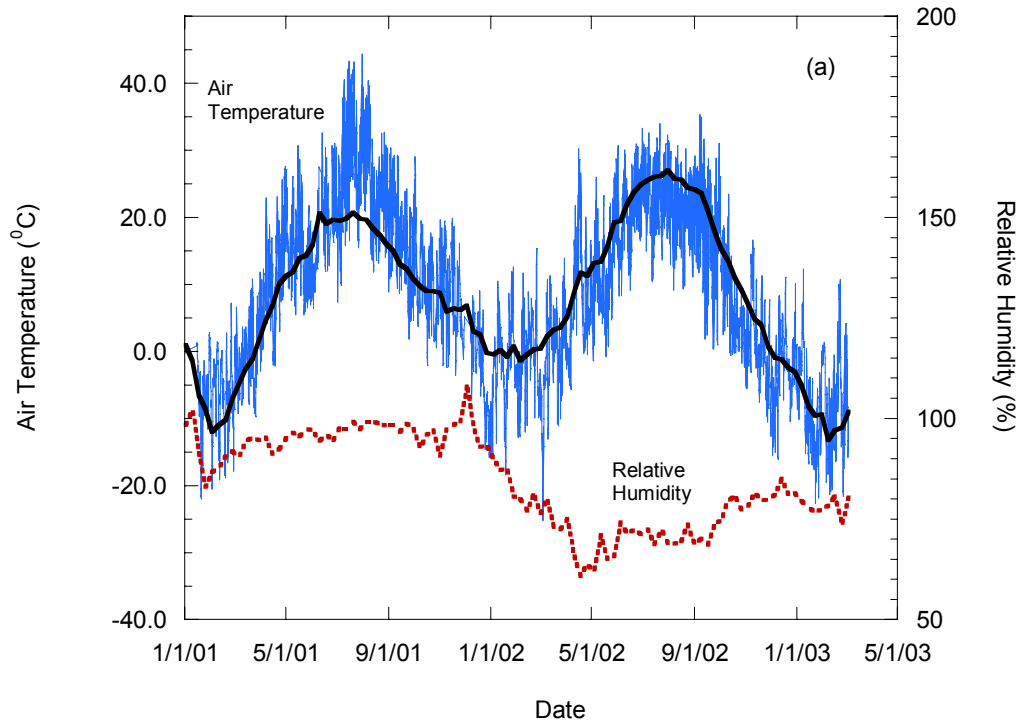


**FIGURE 20 Air temperature and relative humidity data: (a) from site instrumentation and (b) from the NOAA station.**

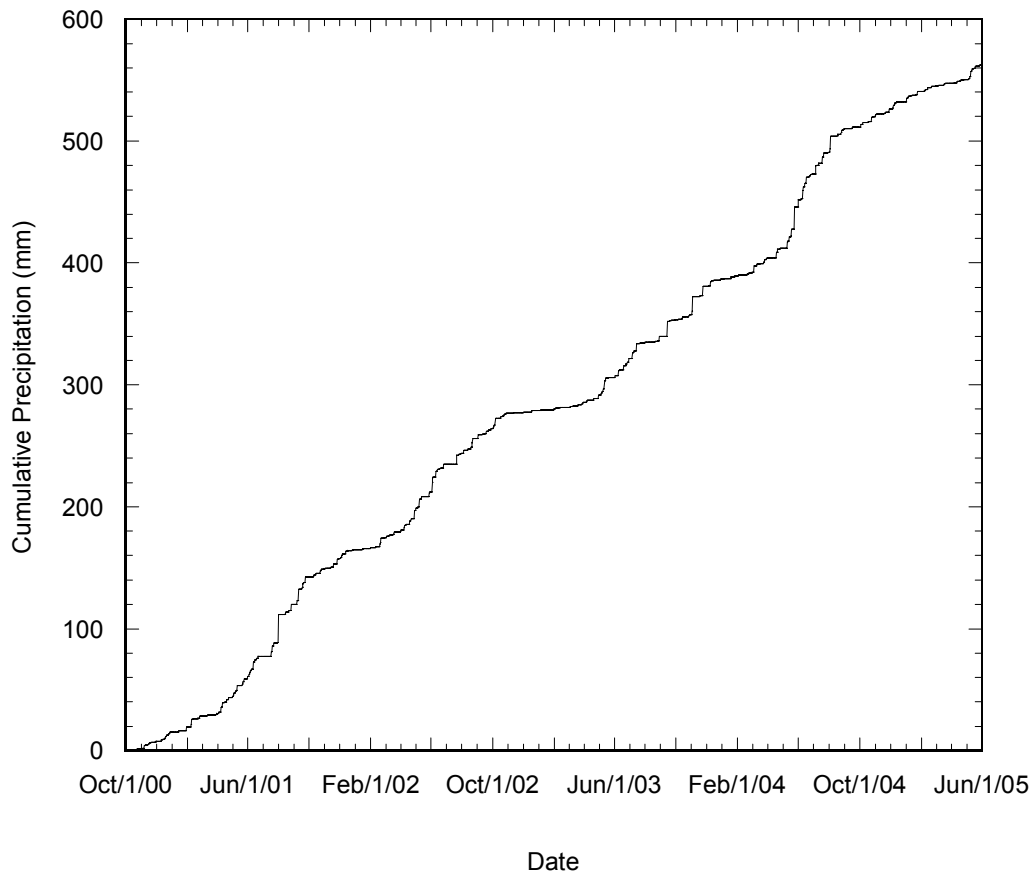


**FIGURE 21 Cumulative precipitation data from the NOAA Weather Station.**



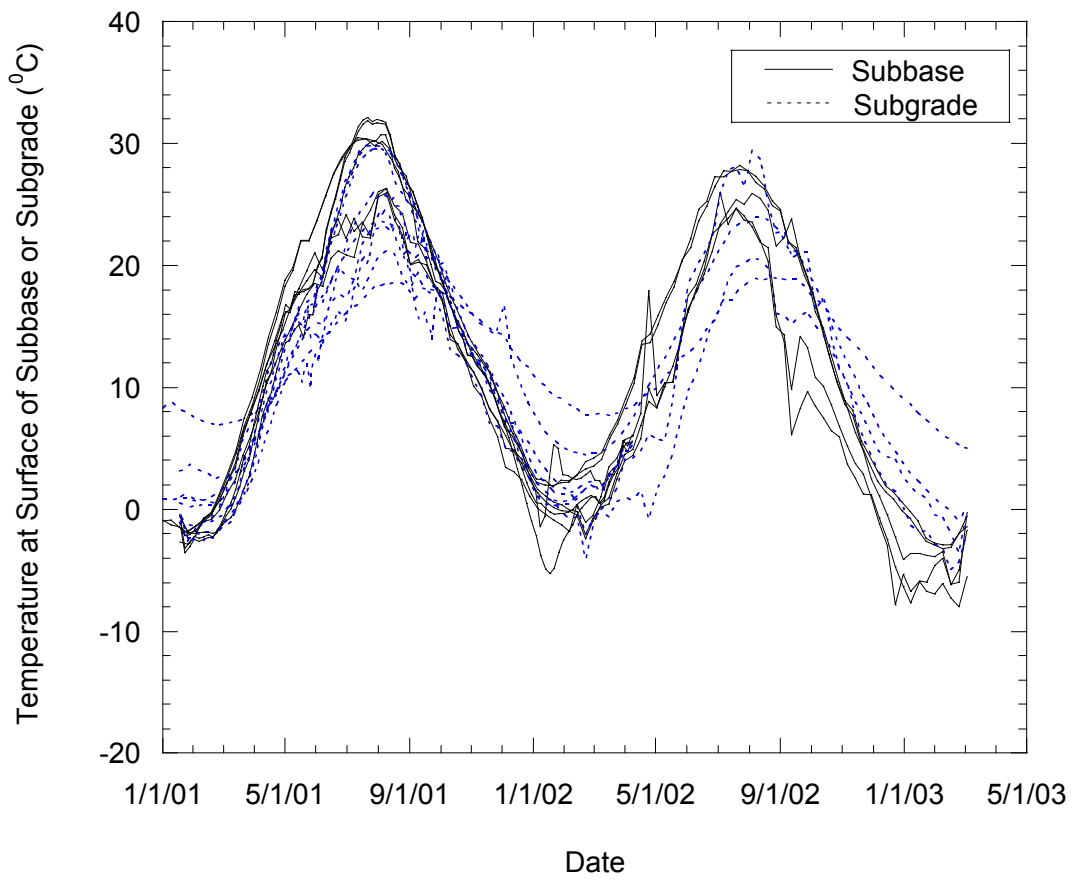


**FIGURE 22** Temperature at surface of the subbase and subgrade at various locations.

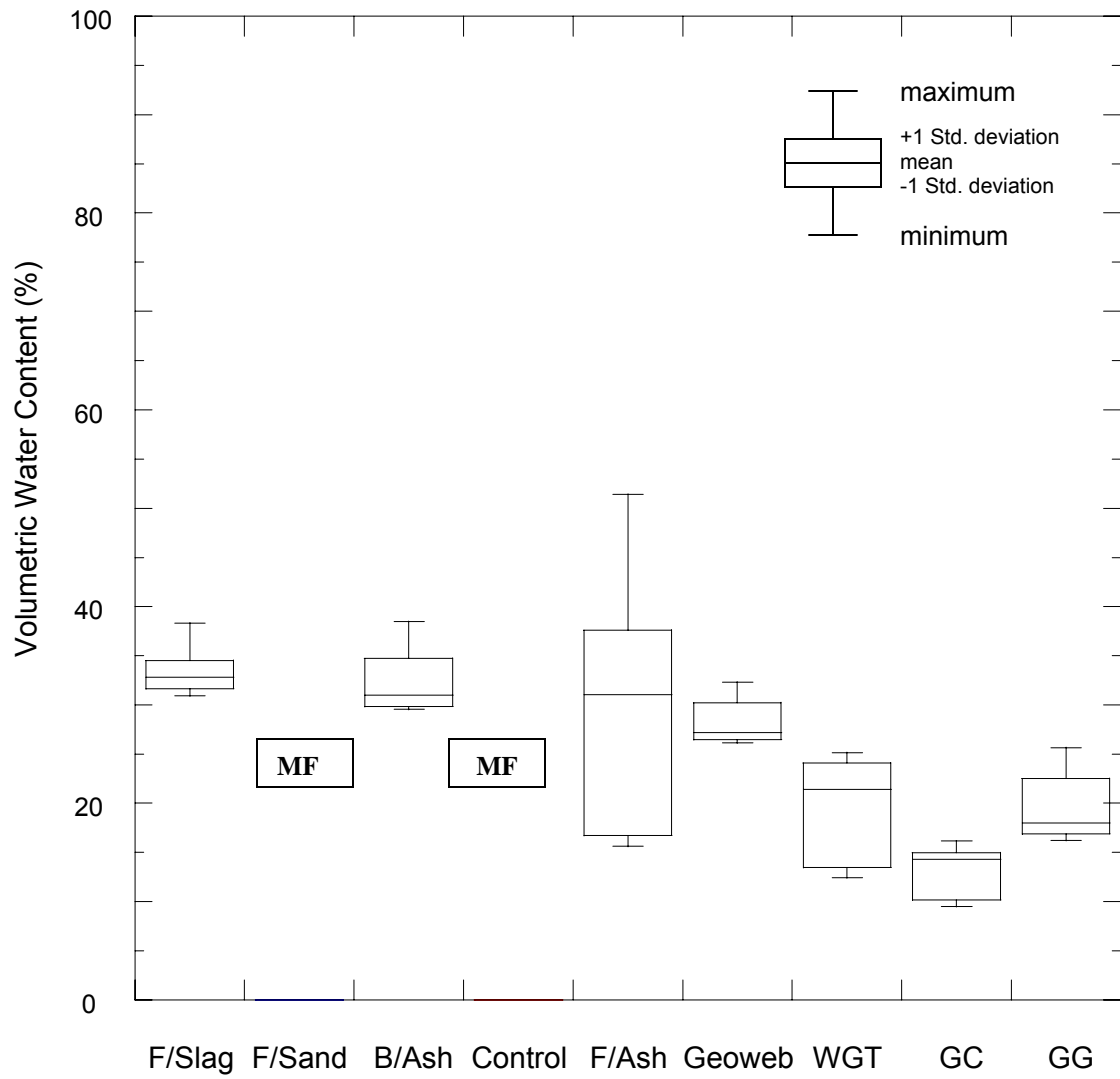


**FIGURE 23** Variation of volumetric water content at the surface of subgrade at different test sections (MF=Instrumentation malfunctioning).

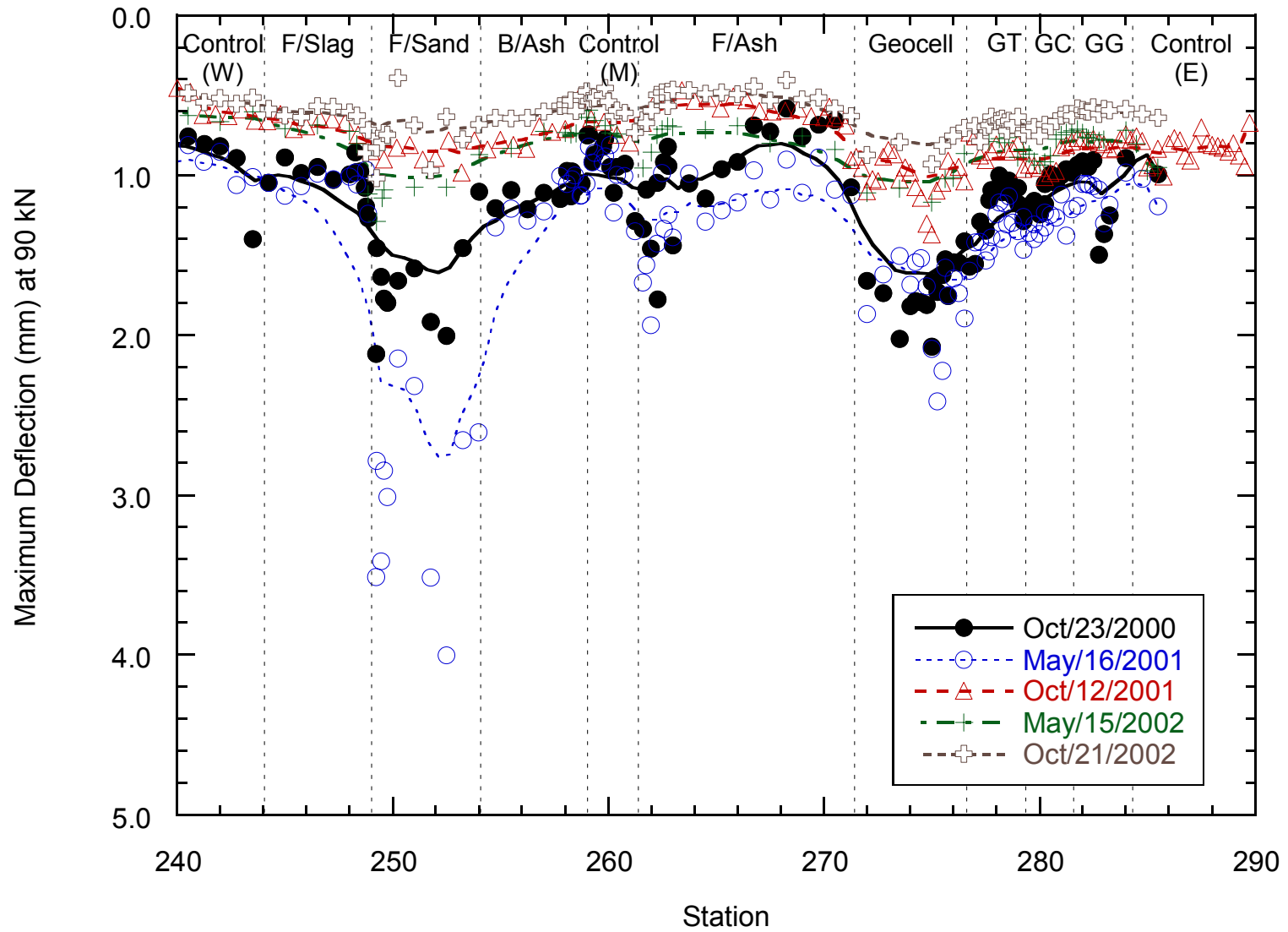


**FIGURE 24** Maximum deflection from falling weight deflectometer tests after construction, following spring, and a year later.

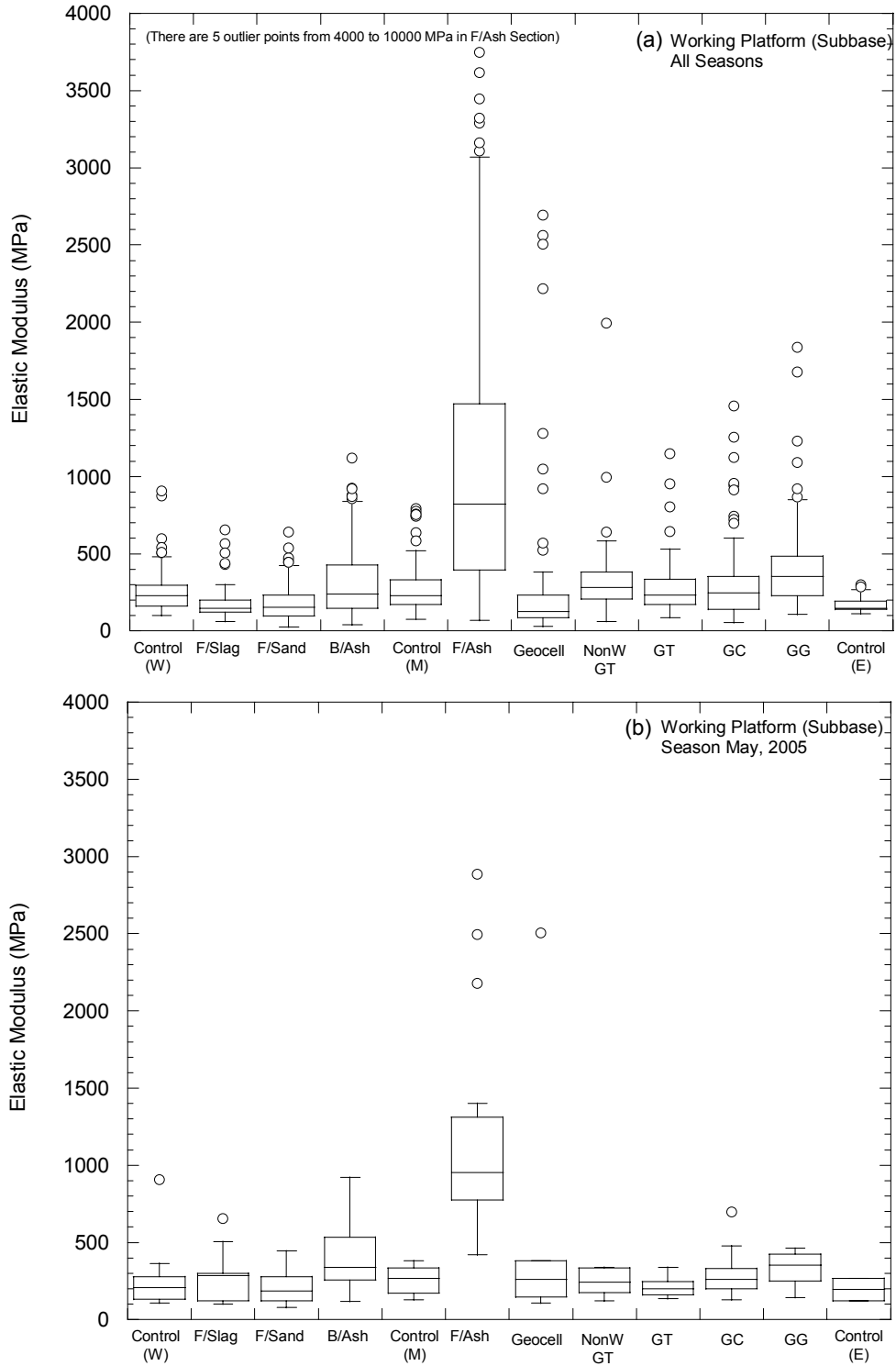


**FIGURE 25 Modulus of Working Platforms (a) October, 2000 to May, 2005, (b) May, 2005**

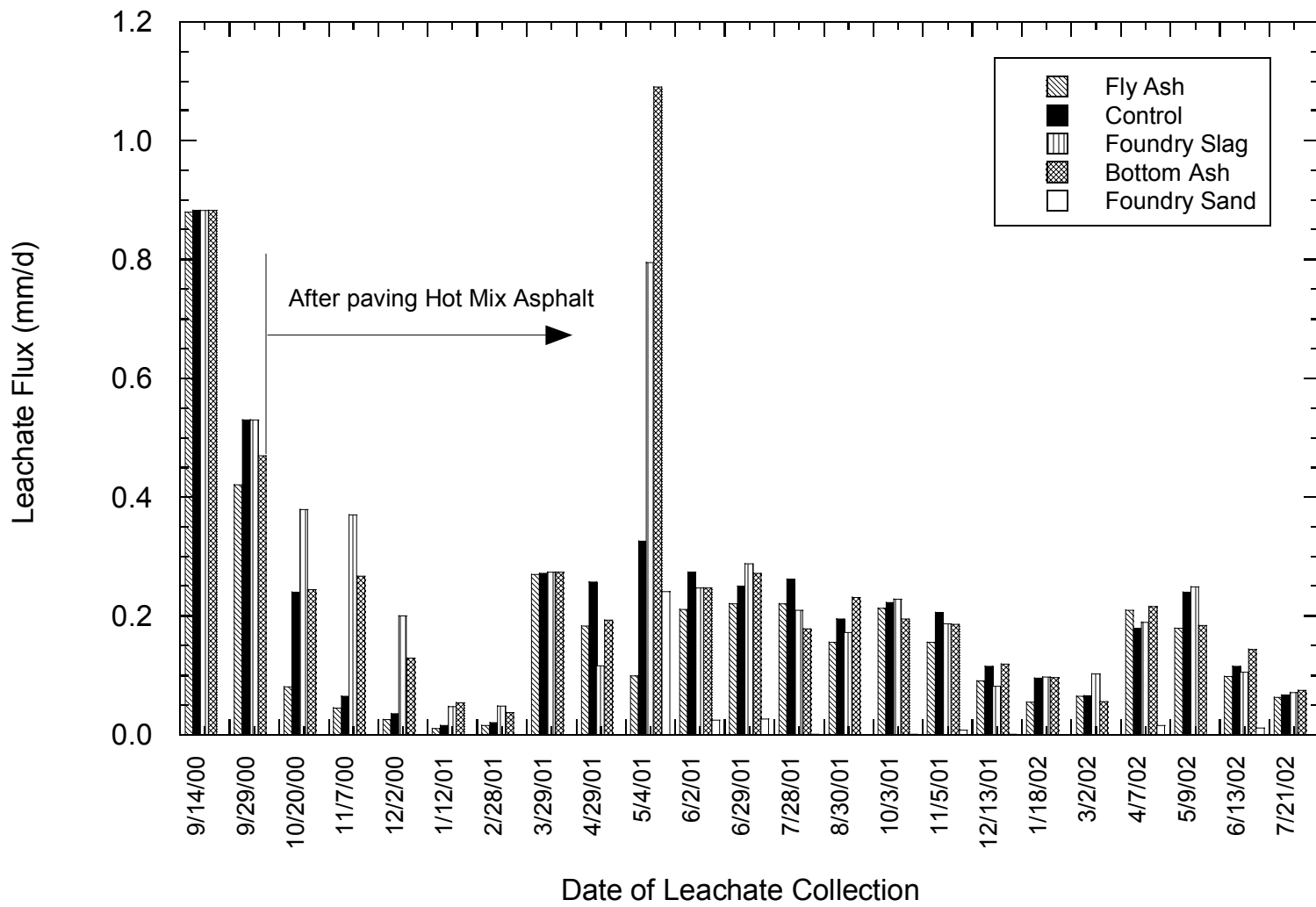


**FIGURE 26 Leachate flux at the bottom of the subbase layer.**

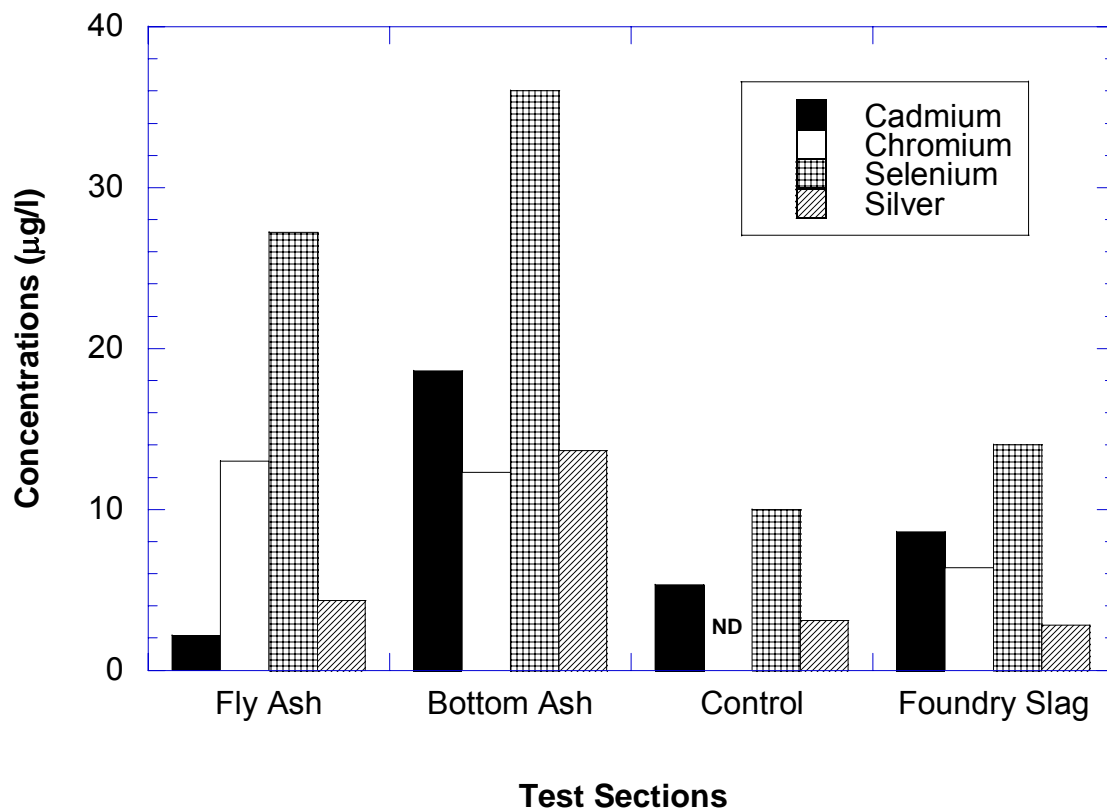


**FIGURE 27 Concentrations of select elements in leachate (ND = Not Detected) on September 14, 2000.**

**APPENDIX A**

**BORING LOGS**





Boring No. 2 Structure \_\_\_\_\_ County Columbia Sheet of 1

Project 5271-08-71 Road S+460

Station 282+50 Offset 21 E of CA Surface Elevation \_\_\_\_\_

GROUND WATER OBSERVATIONS

Streambed Elev. \_\_\_\_\_ Time After Drilling \_\_\_\_\_

Water Elev. \_\_\_\_\_

Top of Well Elev. \_\_\_\_\_ Depth to Water \_\_\_\_\_

MOISTURE

D = Damp  
M = Moist  
W = Wet

HS = Hollowstem  
WA = Wash Ahead  
RB = Rockbit

DRILLING METHOD

ST = Shelby Tube  
SS = Split spoon  
DM = Drilling Mud

A = Auger  
C = Coring  
W = Wash

E = Easy  
M = Medium  
H = Hard

Start 7-24 Unit 1

Finish \_\_\_\_\_ Chief AK

Sample No.	Moisture	Blows on Sampler	Sample and Recovery	Total Blows	VISUAL FIELD CLASSIFICATION AND REMARKS	Unconfined Strength	Boulders	Drilling Method	Probe Blows
					Base				
					1' Black / Br. <u>Silt</u> 1'				
					2' s.t. 2 - 4.5 2'				
					3' Br. <u>SILT</u> 3'				
					4' 4' 1.25				
					5' EOBH 2 5'				
					6' 4.5 6'				
					7' 7'				
					8' 8'				
					9' 9'				
					10' 10'				
					11' 11'				
					12' 12'				

FIELD BORING LOG

Boring No. 3 Structure \_\_\_\_\_ County Columbia Sheet 1 of 1

Project 5271-08-71 Road STH 60

Station 277 + 50 Offset on c/l Surface Elevation \_\_\_\_\_

GROUND WATER OBSERVATIONS

Streambed Elev. \_\_\_\_\_ Time After Drilling \_\_\_\_\_

Water Elev. \_\_\_\_\_

Top of Well Elev. \_\_\_\_\_ Depth to Water \_\_\_\_\_

MOISTURE

D = Damp  
M = Moist  
W = Wet

HS = Hollowstem  
WA = Wash Ahead  
RB = Rockbit

DRILLING METHOD

ST = Shelby Tube  
SS = Splitspoon  
DM = Drilling Mud

A = Auger  
C = Coring  
W = Wash

E = Easy  
M = Medium  
H = Hard

Start 7-21 Unit 1

Finish \_\_\_\_\_ Chief AK

Sample No.	Moisture	Blows on Sampler	Sample and Recovery	Total Blows	VISUAL FIELD CLASSIFICATION AND REMARKS	Unclassified Strength	Boulders	Drilling Method	Probe Blows
	D				Dark Br. Silty				
					1' _____ 1'				
	DM				Br. Silty + or of SAND				
					2' _____ 2'				
					ST, 2-4.5				
					3' _____ 3'				
					4' _____ 4'	25			
					Br. Silty SAND				
					5' _____ 5'				
					EOB #3				
					6' _____ 6'				
					7' _____ 7'				
					4.5				
					8' _____ 8'				
					9' _____ 9'				
					10' _____ 10'				
					11' _____ 11'				
					12' _____ 12'				
					13' _____ 13'				

FIELD BORING LOG

Boring No. 4 Structure \_\_\_\_\_ County Columbia Sheet 1 of 1

Project 5271-08-71 Road SH 60

Station 274+90 Offset on C/C Surface Elevation \_\_\_\_\_

GROUND WATER OBSERVATIONS

Streambed Elev. \_\_\_\_\_ Time After Drilling \_\_\_\_\_

Water Elev. \_\_\_\_\_

Top of Well Elev. \_\_\_\_\_ Depth to Water \_\_\_\_\_

MOISTURE

D = Damp  
M = Moist  
W = Wet

HS = Hollowstem  
WA = Wash Ahead  
RB = Rockbit

DRILLING METHOD

ST = Shelby Tube  
SS = Split spoon  
DM = Drilling Mud

A = Auger  
C = Coring  
W = Wash

E = Easy  
M = Medium  
H = Hard

Start 7-24 Unit 1

Finish \_\_\_\_\_ Chief AL

Sample No.	Moisture	Blows on Sampler	Sample and Recovery	Total Blows	VISUAL FIELD CLASSIFICATION AND REMARKS	Unclassified Strength	Boulders	Drilling Method	Probe	Blows
	D				Dark Br Sil					
					1' Br Sil					
	M				2' S.T. 2.4.5					
					3'					
					4'					
	W				5' EOB# 4				0	
					6'					
					7' 4.5					
					8'					
					9'					
					10'					
					11'					
					12'					

DT1433 96 (Replaces EL3(S))

FIELD BORING LOG

Wisconsin Department of Transportation

Boring No. 5 Structure \_\_\_\_\_ County Columbia Sheet 1 of 1

Project 5271-08-71 Road STH 60

Station 277+25 Offset on C/L Surface Elevation \_\_\_\_\_

GROUND WATER OBSERVATIONS

Streambed Elev. \_\_\_\_\_ Time After Drilling \_\_\_\_\_

Water Elev. \_\_\_\_\_

Top of Well Elev. \_\_\_\_\_ Depth to Water \_\_\_\_\_

MOISTURE

D = Damp  
M = Moist  
W = Wet

HS = Hollowstem  
WA = Wash Ahead  
RB = Rockbit

DRILLING METHOD

ST = Shelby Tube  
SS = Splitepoon  
DM = Drilling Mud

A = Auger  
C = Coring  
W = Wash

E = Easy  
M = Medium  
H = Hard

Start 7:24 Unit 1

Finish \_\_\_\_\_ Chief AK

Sample No.	Moisture	Blows on Sampler	Sample and Recovery	Total Blows	VISUAL FIELD CLASSIFICATION AND REMARKS	Unconfined Strength	Boulders	Drilling Method	Probe Blows
	D				<u>Dark Br. Silt</u>				
	DM				<u>1' Br Silt</u>				
	M				<u>2'</u>				
					<u>3'</u>				
					<u>4'</u>				<u>1.25</u>
					<u>5'</u>				
					<u>6'</u>				
					<u>7'</u>				
					<u>8' Br Silt Seams</u>				
					<u>OT SANDS</u>				
					<u>9'</u>				
					<u>10'</u>				
					<u>FOOT 5</u>				
					<u>11'</u>				
					<u>10'</u>				
					<u>12'</u>				
					<u>13'</u>				

Boring No. 6 Structure \_\_\_\_\_ County Columbia Sheet of \_\_\_\_\_

Project 5271-08-71 Road SH 60

Station 266+25 Offset \_\_\_\_\_ Surface Elevation \_\_\_\_\_

GROUND WATER OBSERVATIONS

Streambed Elev. \_\_\_\_\_ Time After Drilling \_\_\_\_\_

Water Elev. \_\_\_\_\_

Top of Well Elev. \_\_\_\_\_ Depth to Water \_\_\_\_\_

MOISTURE

D = Damp  
M = Moist  
W = Wet

HS = Hollowstem  
WA = Wash Ahead  
RB = Rockbit

DRILLING METHOD

ST = Shelby Tube  
SS = Splitspoon  
DM = Drilling Mud

A = Auger  
C = Coring  
W = Wash

E = Easy  
M = Medium  
H = Hard

Start 7:24 Unit 1

Finish \_\_\_\_\_ Chief AK

Sample No.	Moisture	Blows on Sampler	Sample and Recovery	Total Blows	VISUAL FIELD CLASSIFICATION AND REMARKS	Unconfined Strength	Boulders	Drilling Method	Probe	Blows
					<u>SAND &amp; GRAVEL</u>					
					1'					
					2'	<u>B. Silt</u>				
					3'	<u>+ or of gravel</u>				
					4'	<u>X</u>				<u>2.5</u>
					5'	<u>EO B# 6</u>				
					6'	<u>4.5</u>				
					7'					
					8'					
					9'					
					10'					
					11'					
					12'					

DT1433 96 (Replaces EL3(S))

**FIELD BORING LOG**

Wisconsin Department of Transportation

Boring No. 7 Structure \_\_\_\_\_ County Columbia Sheet 1 of 1

Project 5271-08-71 Road 5+H60

Station 263+12 Offset 20' 0" Surface Elevation \_\_\_\_\_

**GROUND WATER OBSERVATIONS**

Streambed Elev. \_\_\_\_\_ Time After Drilling \_\_\_\_\_

Water Elev. \_\_\_\_\_

Top of Well Elev. \_\_\_\_\_ Depth to Water \_\_\_\_\_

**MOISTURE**

D = Damp  
M = Moist  
W = Wet

HS = Hollowstem  
WA = Wash Ahead  
RB = Rockbit

**DRILLING METHOD**

ST = Shelby Tube  
SS = Splitepoon  
DM = Drilling Mud

A = Auger  
C = Coring  
W = Wash

E = Easy  
M = Medium  
H = Hard

Start 7:24 Unit 1

Finish \_\_\_\_\_ Chief AG

Sample No.	Moisture	Blows on Sampler	Sample and Recovery	Total Blows	VISUAL FIELD CLASSIFICATION AND REMARKS	Unconfined Strength	Boulders	Drilling Method	Probe Blows
	D				SAND & GRAVEL				
					1'				
	DM				2' B. / GRAY SILT ST, 2-4.5				5+
					3' B. SILT				
	M				4' EOBH				1.5
					5'				
					4.5				
					6'				
					7'				
					8'				
					9'				
					10'				
					11'				
					12'				
					13'				

DT1433 96 (Replaces EL3(S))

FIELD BORING LOG

Wisconsin Department of Transportation

Boring No. 8 Structure \_\_\_\_\_ County Columbia Sheet of

Project S271-08-71 Road STH 60

Station 260 +00 Offset on R/L Surface Elevation \_\_\_\_\_

GROUND WATER OBSERVATIONS

Streambed Elev. \_\_\_\_\_ Time After Drilling \_\_\_\_\_

Water Elev. \_\_\_\_\_

Top of Well Elev. \_\_\_\_\_ Depth to Water \_\_\_\_\_

MOISTURE

D = Damp  
M = Moist  
W = Wet

HS = Hollowstem  
WA = Wash Ahead  
RB = Rockbit

DRILLING METHOD

ST = Shelby Tube  
SS = Splitepoon  
DM = Drilling Mud

A = Auger  
C = Coring  
W = Wash

E = Easy  
M = Medium  
H = Hard

Start 7-24 Unit 1

Finish \_\_\_\_\_ Chief R/V

Sample No.	Moisture	Blows on Sampler	Sample and Recovery	Total Blows	VISUAL FIELD CLASSIFICATION AND REMARKS	Unconfined Strength	Boulders	Drilling Method	Probe Blows
	D				B. SAND & GRAVEL				
					1'				
					B. SILT				
					SIT. 2-4.5				
	M				3'				
					4'				
					5' EOBH 8				175
					6' 4.5				
					7'				
					8'				
					9'				
					10'				
					11'				
					12'				
					13'				

DT1433 96 (Replaces EL3(S))

**FIELD BORING LOG**

Wisconsin Department of Transportation

Boring No. 9 Structure \_\_\_\_\_ County Columbia Sheet 4

Project S271-08-71 Road STH 60

Station 256+25 Offset on C/L Surface Elevation \_\_\_\_\_

**GROUND WATER OBSERVATIONS**

Streambed Elev. \_\_\_\_\_ Time After Drilling \_\_\_\_\_

Water Elev. \_\_\_\_\_

Top of Well Elev. \_\_\_\_\_ Depth to Water \_\_\_\_\_

**MOISTURE**

D = Damp  
M = Moist  
W = Wet

HS = Hollowstem  
WA = Wash Ahead  
RB = Rockbit

**DRILLING METHOD**

ST = Shelby Tube  
SS = Splitspoon  
DM = Drilling Mud

A = Auger  
C = Coring  
W = Wash

E = Easy  
M = Medium  
H = Hard

Start 4-24 Unit 1

Finish \_\_\_\_\_ Chief AK

Sample No.	Moisture	Blows on Sampler	Sample and Recovery	Total Blows	VISUAL FIELD CLASSIFICATION AND REMARKS	Unconfined Strength	Boulders	Drilling Method	Probe Blows
	D				B. SAND & gravel				
					1'				
	DM				2' B. SILT				
					3' S.T. 2-4.5				
					4'				
	M				4'			1.0	
					5' EOB# 9				
					6' 4.5				
					7'				
					8'				
					9'				
					10'				
					11'				
					12'				
					13'				



DT1433 96 (Replaces EL3(S))

**FIELD BORING LOG**

Wisconsin Department of Transportation

Boring No. 10 Structure \_\_\_\_\_ County Columbia Sheet of \_\_\_\_\_

Project 5271-08-71 Road SH 60

Station 253+75 Offset on R/L Surface Elevation \_\_\_\_\_

**GROUND WATER OBSERVATIONS**

Streambed Elev. \_\_\_\_\_ Time After Drilling \_\_\_\_\_

Water Elev. \_\_\_\_\_

Top of Well Elev. \_\_\_\_\_ Depth to Water \_\_\_\_\_

**MOISTURE**

D = Damp  
M = Moist  
W = Wet

HS = Hollowstem  
WA = Wash Ahead  
RB = Rockbit

**DRILLING METHOD**

ST = Shelby Tube  
SS = Splitpoon  
DM = Drilling Mud

A = Auger  
C = Coring  
W = Wash

E = Easy  
M = Medium  
H = Hard

Start 4-24 Unit 1

Finish \_\_\_\_\_ Chief R/L

Sample No.	Moisture	Blows on Sampler	Sample and Recovery	Total Blows	VISUAL FIELD CLASSIFICATION AND REMARKS	Unconfined Strength	Boulders	Drilling Method	Probe Blows
	D				BSAND & Gravel				
					1'				
					2' B. Si H St. 2-4.5				
	DM				3'				
					4'				2.25 <del>2.5</del>
					5' EOB# 8				
					6'				
					7'				
					8'				
					9'				
					10'				
					11'				
					12'				

**FIELD BORING LOG**

Boring No. 11 Structure \_\_\_\_\_ County Columbia Sheet of \_\_\_\_\_

Project 5271-0871 Road 57460

Station 251+25 Offset on R/L Surface Elevation \_\_\_\_\_

**GROUND WATER OBSERVATIONS**

Streambed Elev. \_\_\_\_\_ Time After Drilling \_\_\_\_\_

Water Elev. \_\_\_\_\_

Top of Well Elev. \_\_\_\_\_ Depth to Water \_\_\_\_\_

**MOISTURE**

D = Damp  
M = Moist  
W = Wet

HS = Hollowstem  
WA = Wash Ahead  
RB = Rockbit

**DRILLING METHOD**

ST = Shelby Tube  
SS = Split spoon  
DM = Drilling Mud

A = Auger  
C = Coring  
W = Wash

E = Easy  
M = Medium  
H = Hard

Start 4-24 Unit 1

Finish \_\_\_\_\_ Chief DL

Sample No.	Moisture	Blows on Sampler	Sample and Recovery	Total Blows	VISUAL FIELD CLASSIFICATION AND REMARKS	Unclassified Strength	Boulders	Drilling Method	Probe Blows
	<u>D</u>				<u>B. SAND &amp; GRAVEL</u>				
					<u>1'</u>				
					<u>2' B. / GRAY Silt</u>				
	<u>DM</u>				<u>3' S.T. 2-4.5</u>				
					<u>4'</u>				
					<u>5' EOB 11</u>				<u>3.75</u>
					<u>6'</u>				
					<u>7' 4.5</u>				
					<u>8'</u>				
					<u>9'</u>				
					<u>10'</u>				
					<u>11'</u>				
					<u>12'</u>				

**FIELD BORING LOG**

Boring No. 12 Structure \_\_\_\_\_ County Columbia Sheet of 1


Project 5271-08-71 Road SH60

Station 248+50 Offset 0.00 Surface Elevation \_\_\_\_\_

**GROUND WATER OBSERVATIONS**

Streambed Elev. \_\_\_\_\_ Time After Drilling \_\_\_\_\_  
 Water Elev. \_\_\_\_\_  
 Top of Well Elev. \_\_\_\_\_ Depth to Water \_\_\_\_\_

**MOISTURE**  
 D = Damp HS = Hollowstem ST = Shelby Tube A = Auger E = Easy  
 M = Moist WA = Wash Ahead SS = Split spoon C = Coring M = Medium Finish Chief AV  
 W = Wet RB = Rockbit DM = Drilling Mud W = Wash H = Hard

Sample No.	Moisture	Blows on Sampler	Sample and Recovery	Total Blows	VISUAL FIELD CLASSIFICATION AND REMARKS	Unconfined Strength	Boulders	Drilling Method	Probe Blows
	D				1' Br. SAND & GRAVEL				
	M				2' Br./GRAVEL SILT				
					3' ST 2.5 - 5.0'				
					4' 				
					5' EGB #12	1.25			
					6' 5.0'				
					7'				
					8'				
					9'				
					10'				
					11'				
					12'				

**APPENDIX B**

**RWD & FWD DATA AND BACK-CALCULATED  
MODULI  
(2000-2005)**

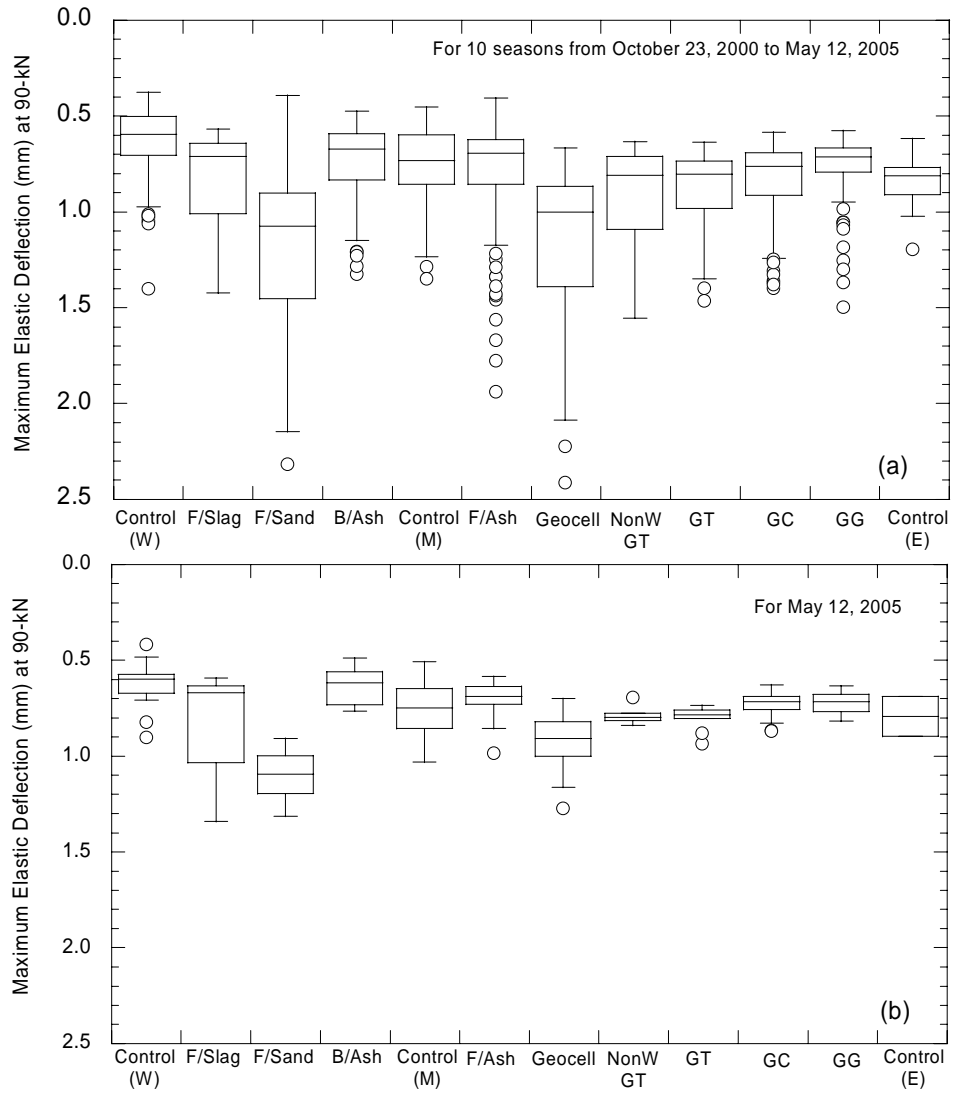


Figure B1 Variation of maximum deflection at 90 kN load (a) for 10 seasons from October 21, 2000 to May 12, 2005, (b) For May 12, 2005

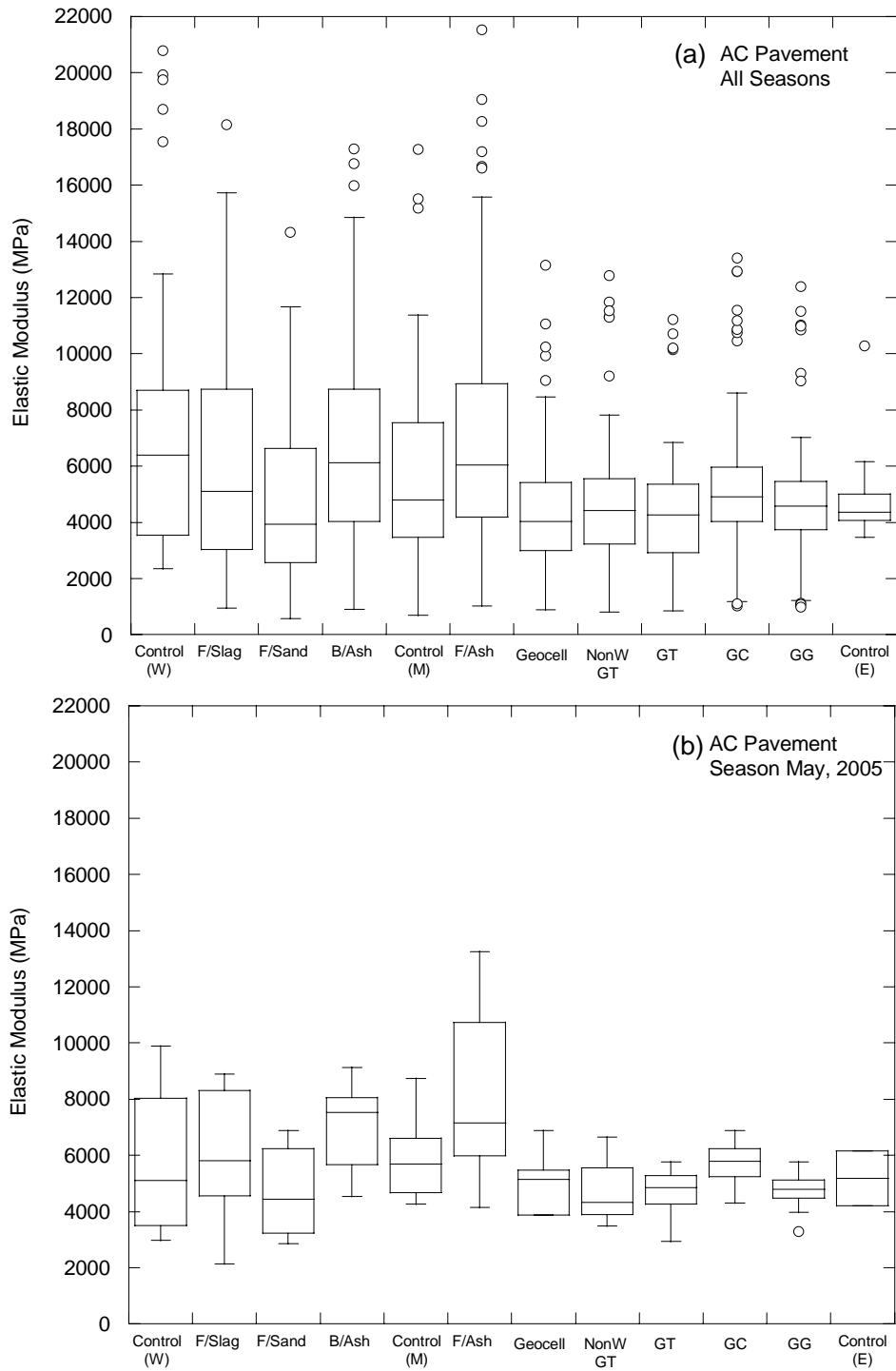


Figure B2 Back calculated Modulus of Asphalt Concrete Pavement (a) seasons from October, 2000 to May, 2005 and (b) for May, 2005

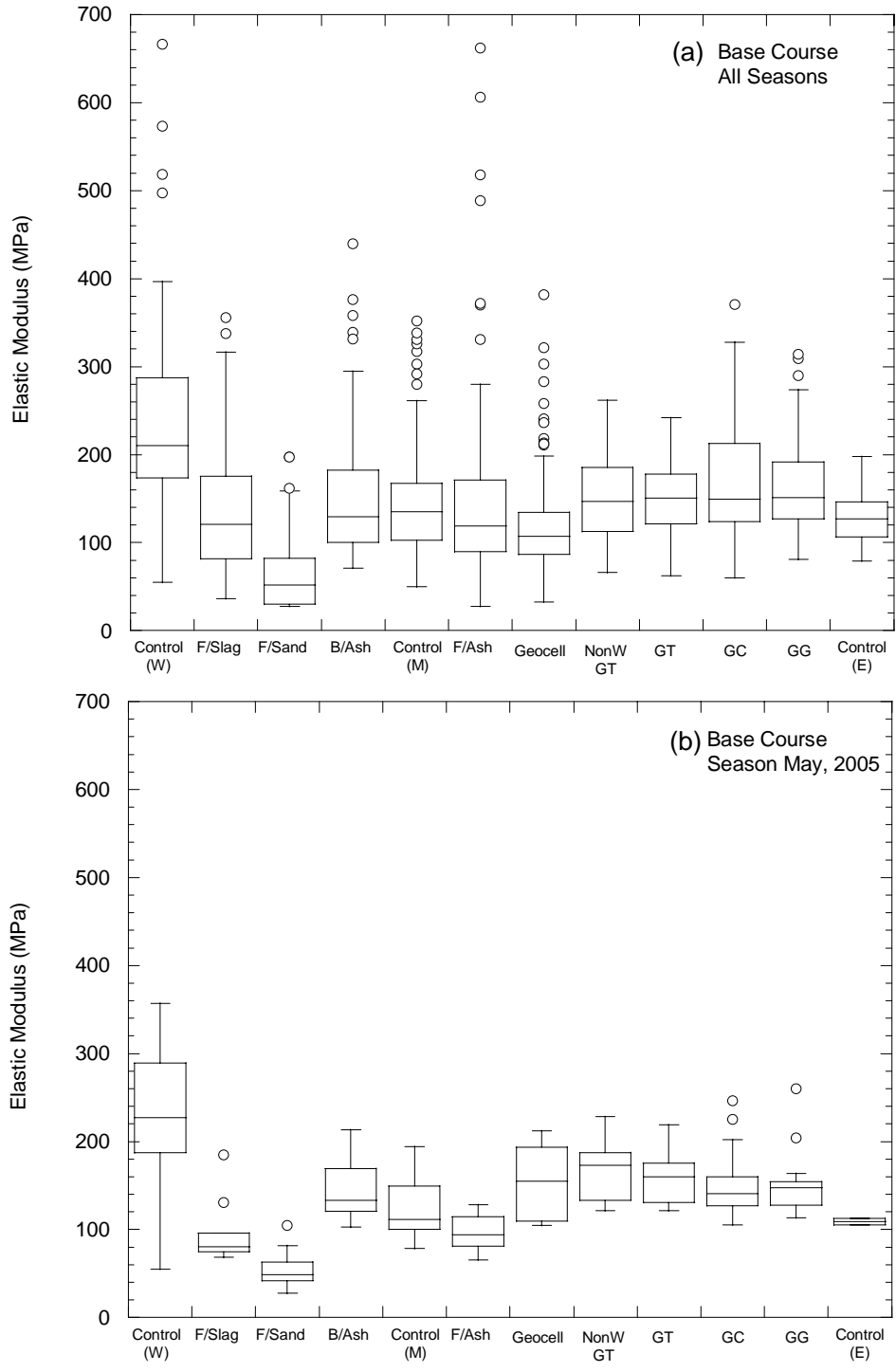


Figure B3 Back calculated Modulus of Base Course (a) Seasons from October 21, 2000 to May 12, 2005, (b) for May 12, 2005

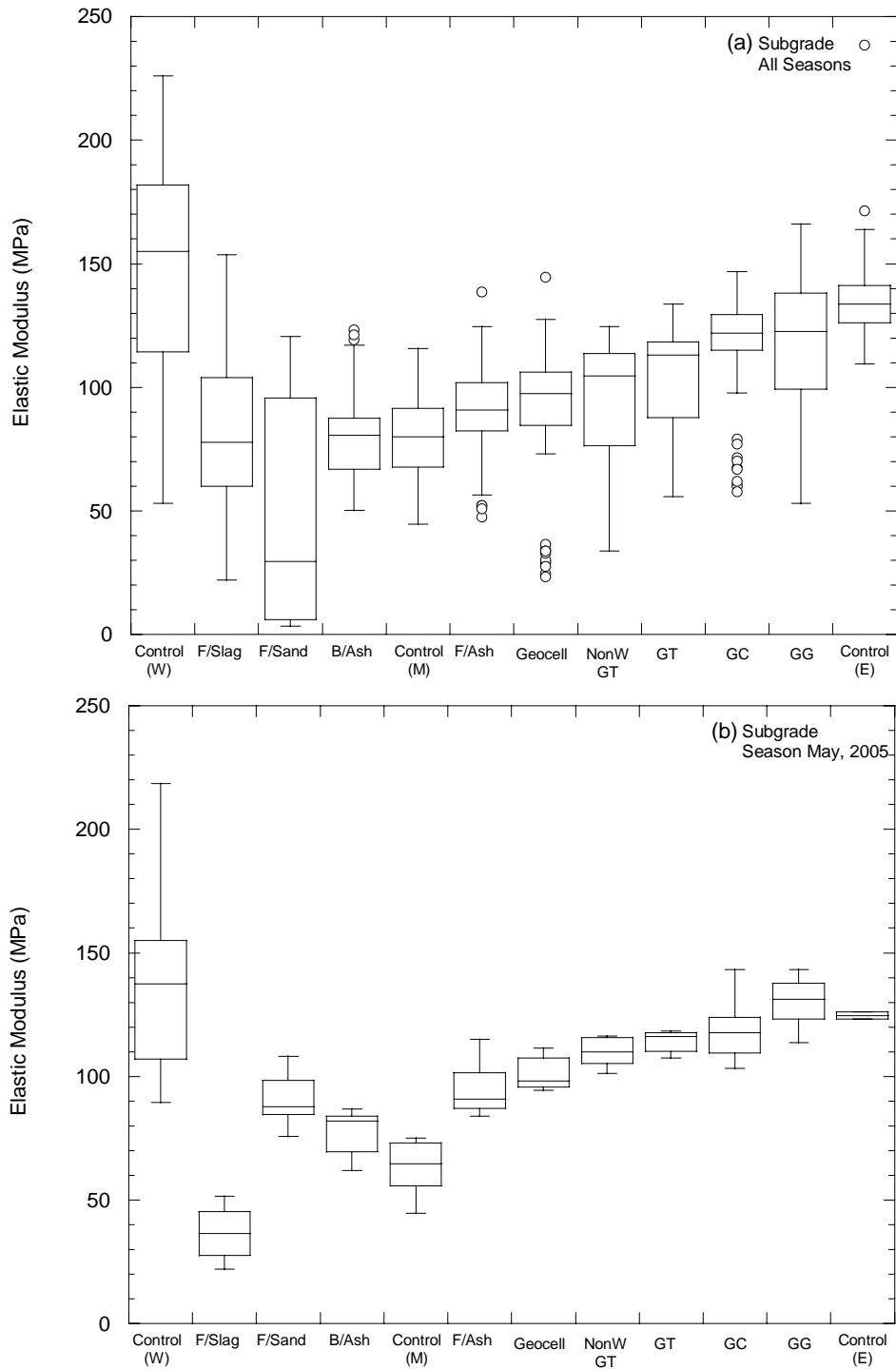


Figure B4 Back calculated Elastic Modulus of Subgrade (a) Seasons from October 21, 2000 to May 12, 2005, (b) for May 12, 2005



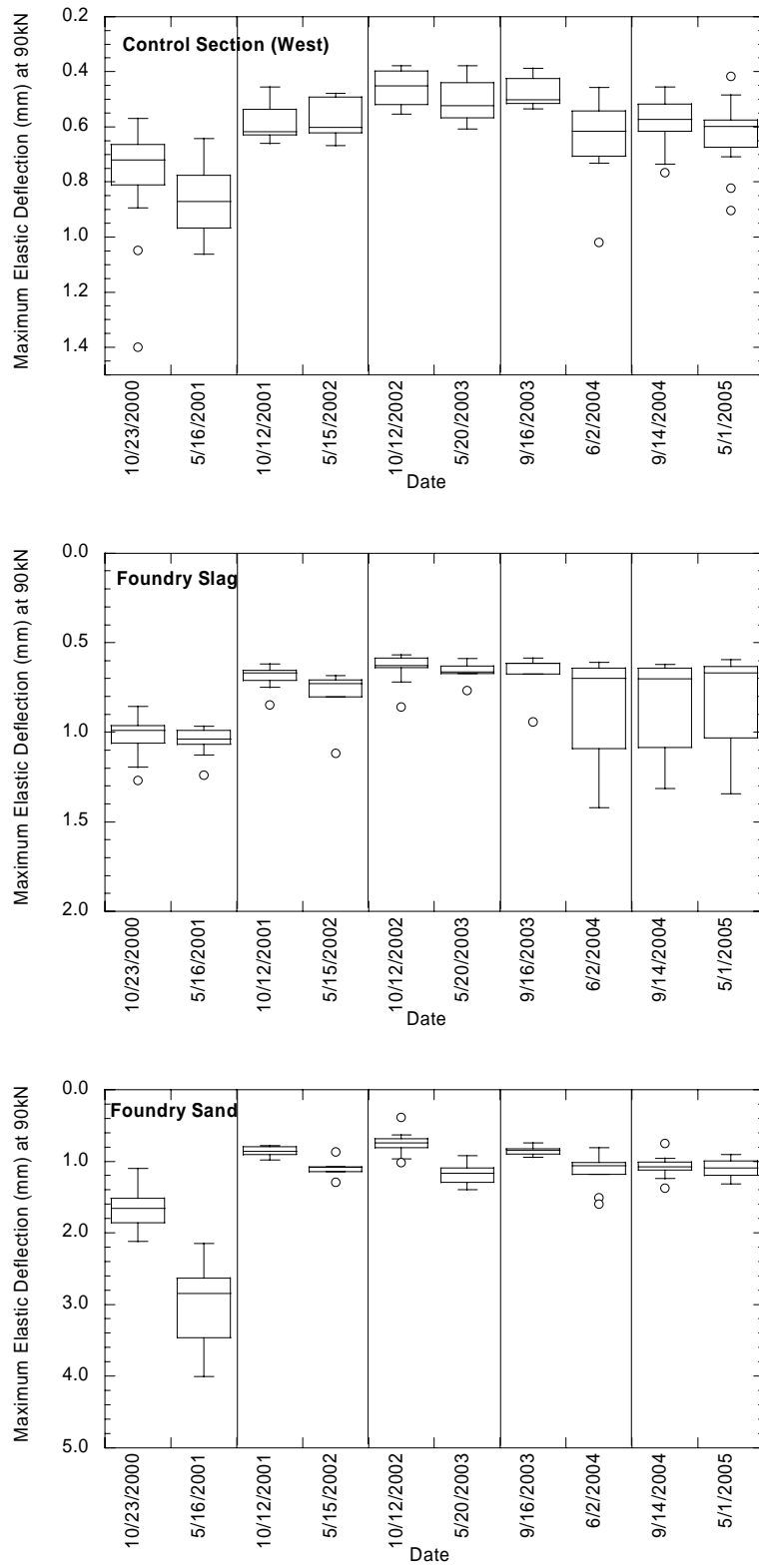


Figure B5 Seasonal Change in Maximum Elastic Deflection at section (a) Control (West) (b) Foundry Slag (c) Foundry Sand

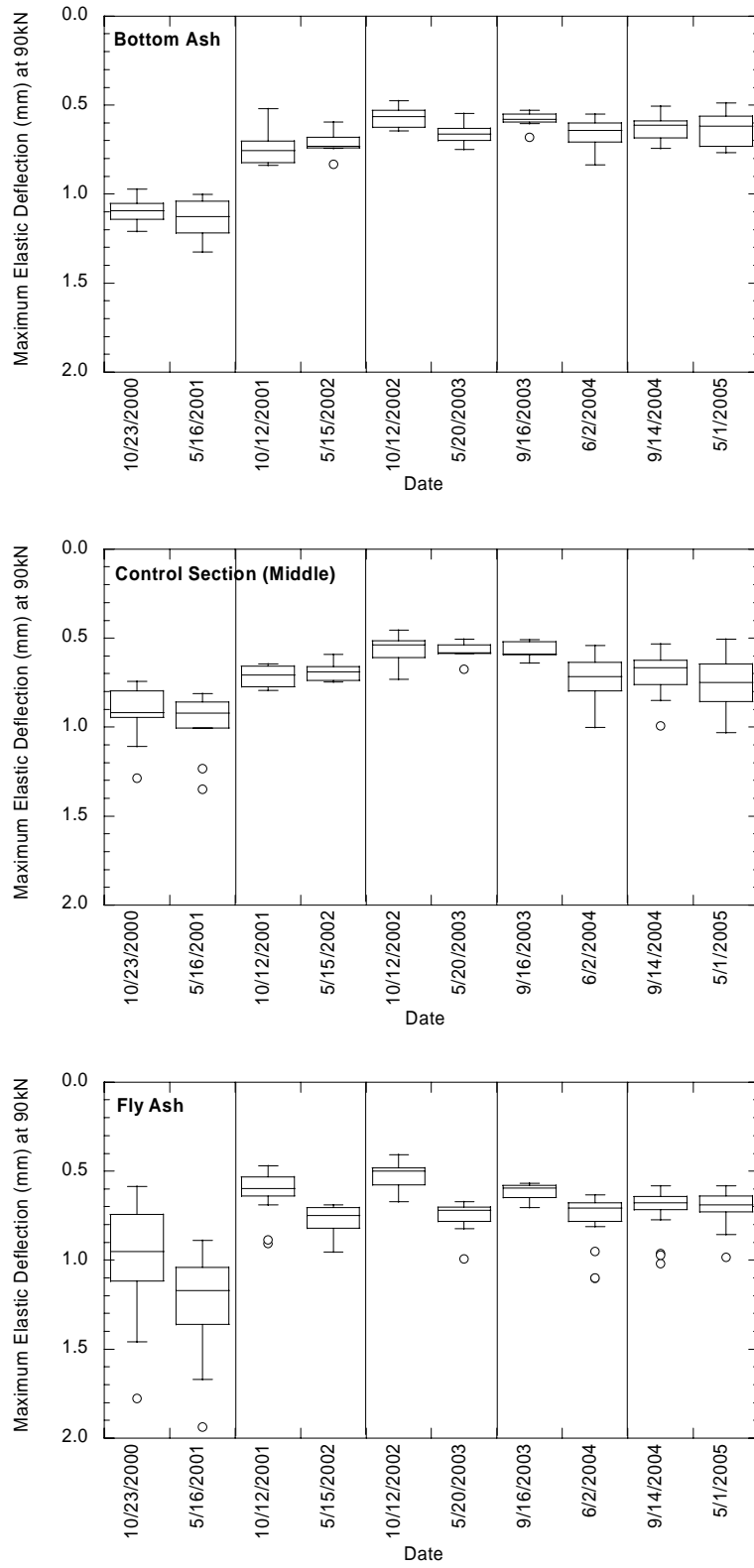


Figure B6 Seasonal Change in Maximum Elastic Deflection at section (a) Bottom Ash (b) Control (Middle) (c) Fly Ash

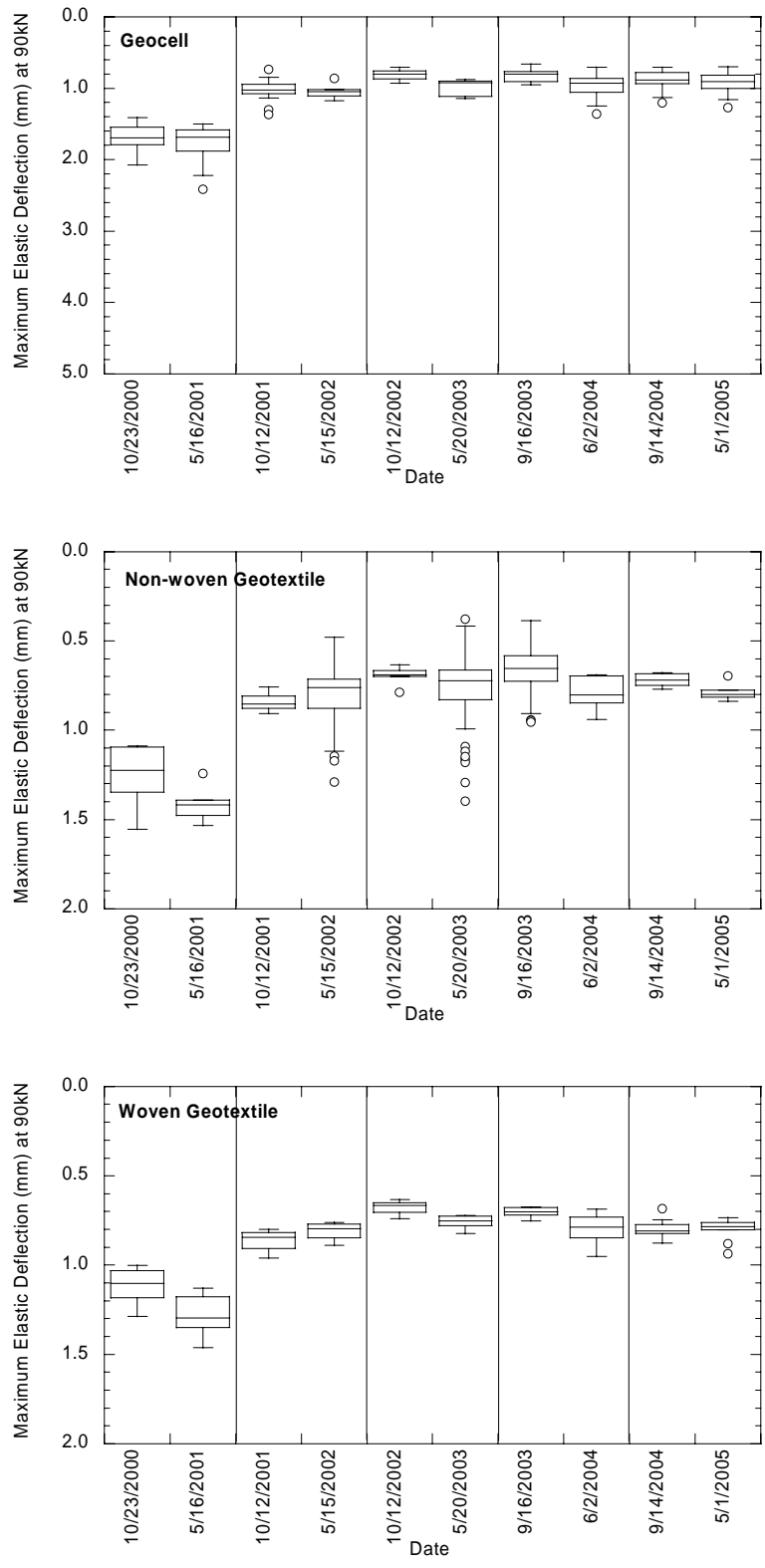


Figure B7 Seasonal Change in Maximum Elastic Deflection at section (a) Geocell (b) Non-woven Geotextile (c) Woven Geotextile

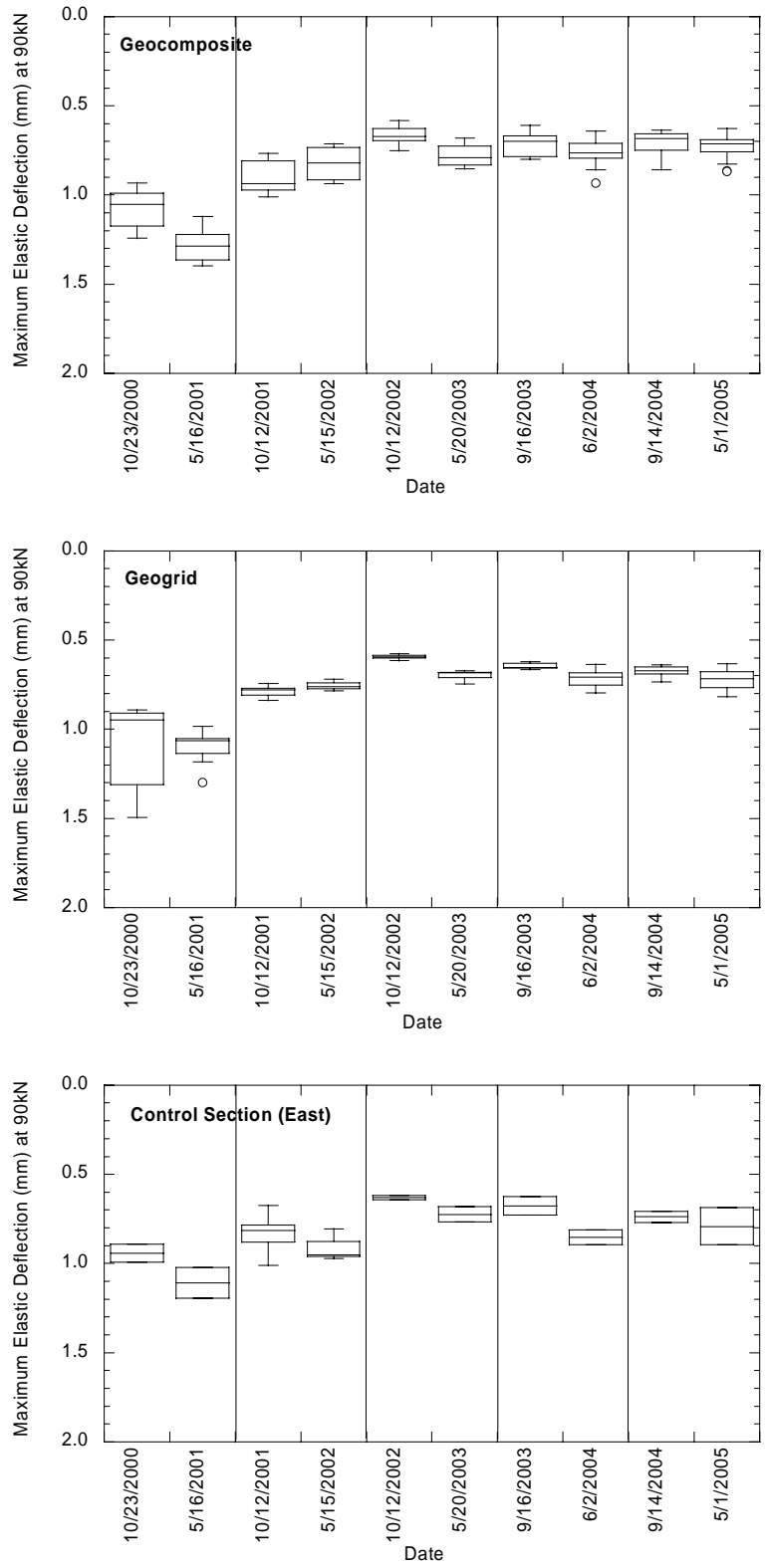


Figure B8 Seasonal Change in Maximum Elastic Deflection at section (a) Geocomposite (b) Geogrid (c) Control (East)

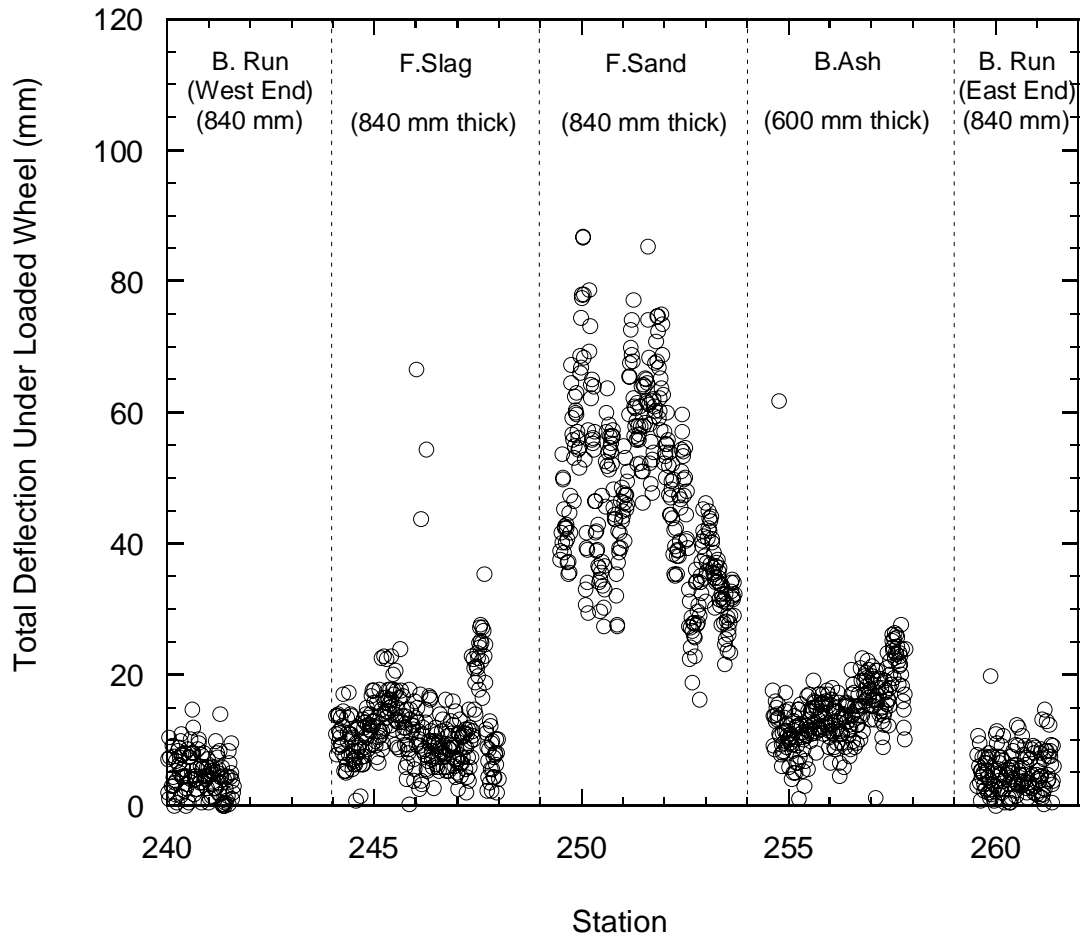


Figure B9. Total deflections at the field site measured using the RWD.

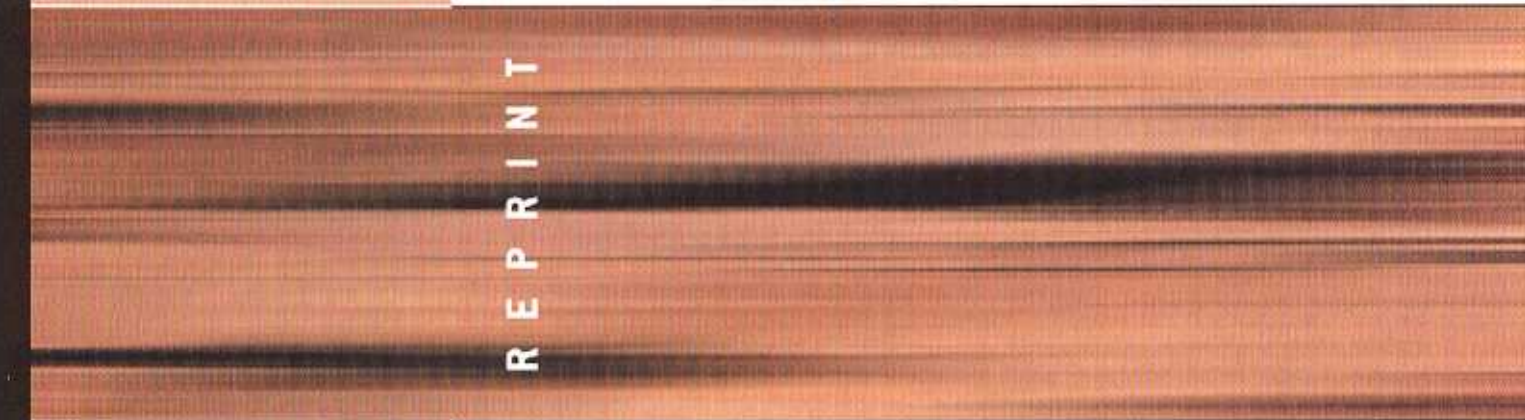
**APPENDIX C**

**INCORPORATING A FLY ASH STABILIZED  
LAYER INTO PAVEMENT DESIGN – CASE STUDY**



ice

Proceedings of the  
Institution of Civil Engineers



REPRINT



Geotechnical  
Engineering



**Sezzad Bin-Shafique**  
Assistant Professor, Department of  
Civil and Environmental  
Engineering, The University of  
Texas at San Antonio, USA



**Tuncer B. Edil**  
Professor, Department of Civil and  
Environmental Engineering,  
University of Wisconsin-Madison,  
USA



**Craig H. Benson**  
Professor, Department of Civil and  
Environmental Engineering,  
University of Wisconsin-Madison,  
USA



**Ayktut Senol**  
Assistant Professor, Civil  
Engineering Faculty, Geotechnical  
Engineering Department, Istanbul  
Technical University, Turkey

## Incorporating a fly-ash stabilised layer into pavement design

S. Bin-Shafique PhD, PE, T. B. Edil PhD, PE, C. H. Benson PhD, PE and A. Senol PhD

This paper describes a case history where the structural support afforded by a fly-ash stabilised layer was accounted for explicitly during the design of two flexible pavements. Pavements were designed and constructed at two sites in southern Wisconsin employing a layer stabilised *in situ* with fly ash. One pavement is for a residential subdivision. The other is a test section located in a secondary highway that was recently reconstructed. A control test section employing a conventional cut-and-fill approach was also constructed in the secondary highway. Fly ash was used to increase the strength and stiffness of the fine-grained subgrade at both sites, which was soft prior to stabilisation. Pavements at both sites were designed using the 1993 American Association of State Highway and Transportation Officials (AASHTO) method for flexible pavements so that their structural number would be equivalent to that of the conventional pavement originally called for in the design. Measurements of California Bearing Ratio (CBR) and resilient modulus ( $M_r$ ) were used with the correlation charts for granular sub-base materials in the AASHTO manual to define layer coefficients for the stabilised layers. Tests were also conducted on specimens collected during construction to verify that the *in situ* mixture had similar properties to those anticipated during design. The pavement at these sites is being monitored seasonally using a falling weight deflectometer and pavement distress surveys. The monitoring programme has indicated that the pavements constructed with fly-ash stabilised layers provide comparable stiffness to conventional pavements employing a cut-and-fill approach. No signs of distress have been observed in the pavements constructed with a stabilised layer. Thus, assigning layer coefficients for fly-ash stabilised soils based on correlations for granular sub-base materials appears reasonable until layer coefficients specific to fly-ash stabilised soils become available.

### 1. INTRODUCTION

Fly ash is an industrial by-product of coal combustion at electric power plants that is generated in large quantities (63 Mg/yr in the US alone) each year.<sup>1</sup> Combustion of sub-bituminous coal produces a fly ash (Class C) that has self-cementing characteristics that can be used for soil stabilisation without activators to improve the mechanical properties of

soil.<sup>2,3</sup> In most subgrade applications, fly ash is used to stabilise a soft soil so that a stable working platform is provided for highway construction equipment.<sup>2,4</sup> Reducing plasticity and shrink-swell potential of fine-grained soils is also a common objective.<sup>4–6</sup>

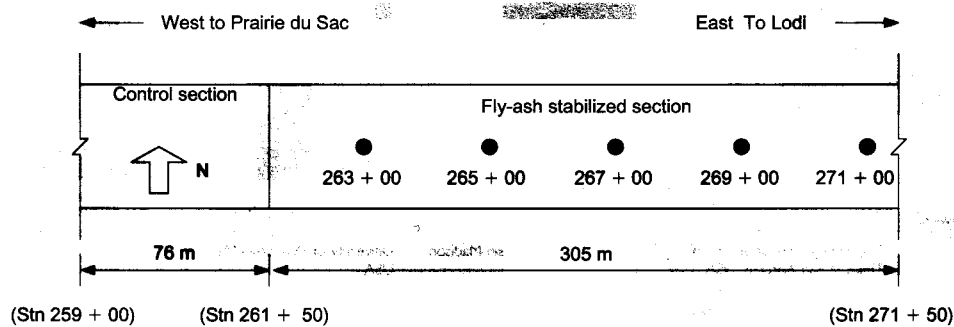
The fly-ash stabilised soil is typically strong and stiff.<sup>7–9</sup> Recent field data show that fly-ash stabilised layers provide a stable working platform for mobilisation of equipment and materials, but also provide appreciable structural support for the overlying pavement.<sup>10</sup> However, there is no standard or accepted method available for designing pavements incorporating fly-ash stabilised soil as a layer in the pavement system.<sup>11</sup> Thus, the structural support provided by the stabilised layer is usually ignored during design, even though accounting for this support provided can result in a less costly pavement through reduction in the thickness of the base and asphalt layers.

This paper describes a case history where the structural support afforded by a fly-ash stabilised layer was accounted for explicitly during the design of two flexible pavements. Procedures described in the 1993 AASHTO (American Association of State Highway and Transportation Officials) method for flexible pavements<sup>12</sup> were followed. Layer coefficients used in the design were estimated from data collected from California Bearing Ratio (CBR) and resilient modulus ( $M_r$ ) tests conducted on fly-ash stabilised soil and charts in the AASHTO manual for granular sub-base materials. Laboratory tests were also conducted on specimens prepared from the *in situ* mixture of soil and fly ash to determine whether the properties anticipated during design were achieved in the field. In addition, the dynamic penetration index (DPI) and stiffness of the stabilised layer were measured at both sites during construction. Falling weight deflectometer (FWD) tests and pavement distress surveys were also conducted after construction to assess the performance of the pavement.

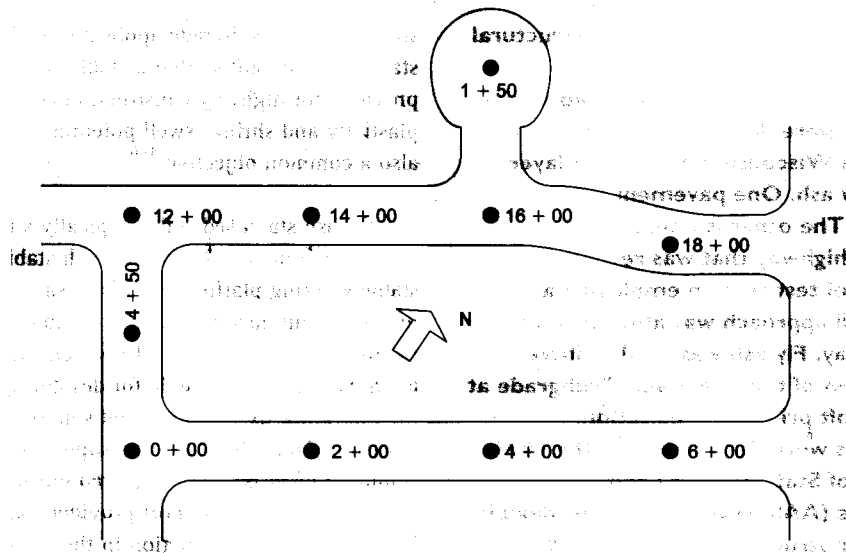
### 2. SITES

The pavements were constructed at two sites in southern Wisconsin in August 2000. Layouts of the field sites are shown in Fig. 1. One pavement is a 0.3 km long test section in a segment of Wisconsin State Trunk Highway (STH) 60 (Fig. 1(a)) that is located between Lodi and Prairie du Sac, WI (Stn 261+50 to 271+50). The other is a 0.7 km city street in the recently constructed Scenic Edge residential subdivision in





(a)



(b)

Fig. 1. (a) Layout of test sections at STH 60; (b) layout of Scenic Edge site (not to scale)

Cross Plains, WI (Fig. 1(b)). Pavement design parameters for both sites are shown in Table 1. These design parameters were selected by the engineers who designed the original pavement, and were used by the authors when designing the pavement for the sections with a stabilised layer.

At the Scenic Edge site, the pavement design originally called for a conventional cut-and-fill approach where the upper 0.75 m of soft subgrade would be replaced with coarse sand prior to placement of base course (175 mm) and asphalt concrete (100 mm). Residents in the area opposed this design because it required trucking large amounts of earthen materials through local neighbourhoods. To alleviate this problem, *in situ* stabilisation of the soft subgrade was selected. However, in contrast to conventional stabilisation projects, the pavement was designed so that it would provide equivalent structural number (SN) to the original design by explicitly accounting for the support provided by the stabilised layer.

The test section at the STH 60 site was constructed as part of a larger project evaluating various methods to stabilise poor subgrades in Wisconsin.<sup>10</sup> The design for STH 60 also included a conventional cut-and-fill approach to address soft subgrade

at the site. The soft subgrade was to be cut and replaced with at least 0.45 m of crushed rock referred to as 'breaker run'. The remainder of the conventional profile consisted of base course (225 mm) and asphalt concrete layer (125 mm). As at the Scenic Edge site, the test section employing a fly-ash stabilised layer at STH 60 was designed to have a structural number equal to that of the conventional pavement profile. At both sites, the thickness of the base course and the asphalt concrete remained unchanged, while the sub-base layer was modified.

### 3. MATERIALS

#### 3.1. Soils

Samples of the subgrade were collected along the centreline of the proposed roadway at Scenic Edge and near the shoulder of the roadway in STH 60. Undisturbed samples were also collected from both sites along the centreline of the proposed roadway using thin-wall sampling tubes. Tests were conducted to determine index properties, soil classification, compaction characteristics, unconfined compressive strength, and CBR of the subgrade. Compaction curves for the subgrade were determined using the Harvard miniature method using standard effort.<sup>13</sup> Unconfined compression tests were conducted

Design parameter	Scenic Edge site		STH 60 site	
	Original design	Modified design	Original design	Modified design
Design period ESALs	76 000	76 000	$2.1 \times 10^6$	$2.1 \times 10^6$
Reliability: %	95	95	95	95
Standard deviation	0.35	0.35	0.30	0.30
Subgrade soil resilient modulus: MPa	10.4	10.4	31	31
Design serviceability loss	2	2	1.8	1.8
SN required	4.0	4.0	4.6	4.6
Surface course material	HMA	HMA	HMA	HMA
Layer coefficient: $\text{mm}^{-1}$	0.0168	0.0168	0.0168	0.0168
Thickness: mm	100	100	125	125
Base course material	Crushed stone	Crushed stone	Crushed stone	Crushed stone
Layer coefficient: $\text{mm}^{-1}$	0.0056	0.0056	0.0056	0.0056
Thickness: mm	175	175	225	225
Sub-base material	Coarse sand	FA stabilised soil	Crushed rock	FA stabilised soil
Layer coefficient: $\text{mm}^{-1}$	0.002	0.0048	0.003	0.0044
Thickness: mm	750	300	450	300
SN provided by pavement	4.15	4.15	4.70	4.70

ESALs = 18 kN equivalent single axle load, SN = structural number, HMA = hot mixed asphalt concrete, FA = fly ash.

Table 1. Pavement design parameters

following ASTM D 2166<sup>14</sup> on undisturbed specimens (50 mm in diameter and 100 mm high) trimmed from the tube samples. CBR tests were conducted on laboratory-compacted specimens prepared at the *in situ* water content and unit weight of the subgrade. A summary of the properties is tabulated in Table 2. Particle size distribution curves for the soils are shown in Fig. 2.

The subgrade classifies as A-7-6 or CL at the Scenic Edge site and A-6 or CL-ML at the STH 60 site. Both subgrade soils contain more than 90% fines (particles finer than 75  $\mu\text{m}$ ) and have a 2  $\mu\text{m}$  clay fraction between 15% and 20%. The *in situ* water content of the subgrades is 6–7% wet of optimum water content based on standard effort.<sup>15</sup> At Scenic Edge, the CBR is 1 and the unconfined compressive strength ranges between 40 and 180 kPa (average = 95 kPa). At STH 60, the CBR is 3 and the unconfined compressive strength ranges between 105 and 136 kPa (average = 124 kPa). Thus, both subgrades are soft to medium stiff soils, which is due largely to their high water content.

The DPI and stiffness of the subgrade were measured at intervals of 30–60 m along the centreline of the roadway after the roadbed was prepared for construction.<sup>16,17</sup> DPI was

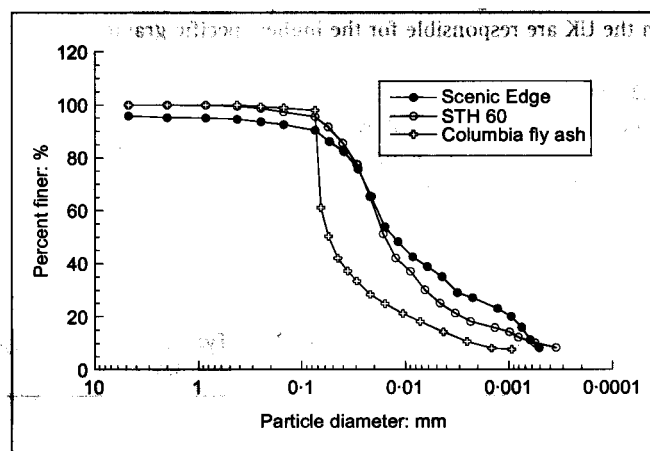


Fig. 2. Particle size distribution curves for the soils and fly ash

measured with a dynamic cone penetrometer (DCP) that measures the depth of penetration of a cone having a 60° apex and diameter of 20 mm that is driven with an 8 kg hammer dropped from a height of 522 mm. The DPI is calculated as the average penetration per blow of the hammer over a depth of 250 mm. Stiffness was measured with a Humboldt soil stiffness gauge (SSG), which measures stiffness of the soil near the

Soil	Liquid limit	Plasticity index	Specific gravity	LOI: %	Classification		Ave. $q_u$ : kPa	CBR	Ave. SSG stiffness: MN/m	$w_N$ : %	$\gamma_{d(\text{CBR})}$ : $\text{kN/m}^3$	$w_{\text{opt}}$ : %	$\gamma_{d\text{max}}$ : $\text{kN/m}^3$
					USCS	AASHTO							
Scenic Edge	44	20	2.71	2	CL	A-7-6 (20)	95	1	5	27	14.6	20	16.2
STH 60	39	15	2.70	1	CL-ML	A-6 (16)	124	3	5	25	15.1	19	16.5

LOI = loss on ignition, USCS = Unified Soil Classification System, AASHTO = Association of American State Highway and Transportation Officials,  $q_u$  = unconfined compressive strength, CBR = California Bearing Ratio, SSG = soil stiffness gauge,  $w_N$  = natural water content,  $\gamma_{d(\text{CBR})}$  = dry unit weight for CBR tests,  $w_{\text{opt}}$  = optimum water content,  $\gamma_{d\text{max}}$  = maximum dry unit weight.

Table 2. Properties of subgrade soils

surface.<sup>18</sup> The DPI ranged between 20 and 120 mm/blow (average = 64 mm/blow), and the stiffness ranged between 4 and 9 MN/m (average = 5 MN/m) for the Scenic Edge site. At the STH 60 site, the DPI ranged between 38 and 112 mm/blow (average = 65 mm/blow) and the stiffness ranged between 4 and 8 MN/m (average = 5 MN/m).

### 3.2. Fly ash

Fly ash from Unit 2 of Alliant Energy's Columbia Power Station in Portage, Wisconsin, was used for stabilisation at both field sites. The chemical composition<sup>19</sup> of the Columbia fly ash is summarised in Table 3. The particle size distribution curve is shown in Fig. 2. The specific gravity of the fly ash is 2.68, the lime (CaO) content is 23%, and the loss on ignition is 0.7%. Accordingly, in accordance with ASTM C 618,<sup>20</sup> this fly ash classifies as Class C fly ash. The fly ash is composed primarily (89%) of silt-size particles.

Columbia fly ash was chosen because of its self-cementing characteristics and high lime content, the latter being higher than typical pulverised fuel ashes (PFA) available in the UK. The higher lime content and small unburned carbon content (i.e. low loss on ignition) of the Columbia ash relative to PFA in the UK are responsible for the higher specific gravity.<sup>19</sup>

### 3.3. Stabilised soil

Mixtures of soil and fly ash were prepared with both soils using fly ash contents of 10%, 14% and 18% (STH 60) or 12%, 16% and 20% (Scenic Edge). Air-dry soil ground to pass a US

No. 10 sieve was first mixed with the fly ash until the mixture appeared uniform. Tap water was then sprayed on the soil-fly ash mixture to achieve a target water content based on total solids (soil mineral and fly ash solids). Mixing continued during moistening to promote uniform water content and hydration.

Two sets of specimens were prepared with the soil-fly ash mixtures. One set was compacted in a mould immediately after mixing with water (referred to herein as 'no delay'). The other set was compacted 2 hours after mixing with water (referred to herein as '2 h delay') to simulate the typical duration between mixing and compaction that occurs in the field.<sup>2,21</sup> All specimens were compacted in a Harvard miniature mould (35 mm in diameter and 70 mm high) using standard effort.<sup>13</sup>

Compaction characteristics of the unstabilised and stabilised soils are summarised in Table 4. For both soils, maximum dry unit weight and optimum water content for the mixture prepared with 'no delay' are comparable to those for the soil alone. However, for the 2 hr delay, the maximum dry unit weight is lower and the optimum water content is slightly (1%) higher than those for the soil alone. Additionally, the maximum dry unit weight decreases and the optimum water content increases as the fly ash content increases. The changes in compaction characteristics of the 2 h delay mixtures reflect the cementing that occurs as the fly ash hydrates during the 2 h delay. Cementing causes the clods of clay to become stronger, and more difficult to remould. As a result, less solid material can be compacted into a unit volume.

Chemical species	Percentage of composition			
	Columbia fly ash*	Typical Class C†	Typical Class F†	Typical Portland cement†
CaO (lime)	23.1	24	9	64
SiO <sub>2</sub>	31.1	40	55	23
Al <sub>2</sub> O <sub>3</sub>	18.3	17	26	4
Fe <sub>2</sub> O <sub>3</sub>	6.1	6	7	2
MgO	3.7	5	2	2
SO <sub>3</sub>	3.7	3	1	2

\*Chemical analysis provided by Alliant Energy

†From reference

Table 3. Chemical composition of Columbia fly ash and typical Class C and F fly ashes

## 4. DESIGN PHASE

### 4.1. Structural requirement

Both pavements (original design and pavement with a fly-ash stabilised layer) were designed using the 1993 AASHTO method for flexible pavements. In this method, the required SN is determined from a nomograph based on the 18 kN equivalent single axle loads (ESALs) from

Soil type	Fly ash content: %	Stabilised soil (no delay)		Stabilised soil (2 h delay)		Soil alone	
		$\gamma_{dmax}$ : kN/m <sup>3</sup>	$w_{opt}$ : %	$\gamma_{dmax}$ : kN/m <sup>3</sup>	$w_{opt}$ : %	$\gamma_{dmax}$ : kN/m <sup>3</sup>	$w_{opt}$ : %
Scenic Edge	12	16.2	21	15.6	21	16.2	20
	16	16.2	21	15.5	21		
	20	16	22	15.5	22		
STH 60	10	16.6	20	16.1	20	16.5	19
	14	16.5	20	15.9	20		
	18	16.4	20	15.8	20		

$\gamma_{dmax}$  = maximum dry unit weight, and  $w_{opt}$  = optimum water content.

Table 4. Compaction characteristics of soils and fly-ash stabilised soils

traffic for the entire life of the pavement, effective subgrade soil  $M_r$ , required reliability (degree of certainty that a given design will perform its intended function over its design life), overall standard deviation (accounts for standard variation in materials and construction, the chance variation in the traffic variation, and a normal variation in pavement performance for a given number of ESAL applications), and allowed loss of serviceability (ability to serve the type of traffic for which it was designed) during the lifetime of the pavement. Layer thicknesses are then calculated using layer coefficients (a layer property defining structural support) in such a way that the total contribution of all layers equals the required SN, i.e.:

$$SN = t_1 a_1 + t_2 a_2 + t_3 a_3$$

where  $t_1$ ,  $t_2$  and  $t_3$  are the thickness of the surface course, base course and sub-base layers, and  $a_1$ ,  $a_2$  and  $a_3$  are the layer coefficients for the surface, base and sub-base layers. The AASHTO layer coefficients are empirically derived. They are based on observations made at the original AASHTO (American Association of State Highway Officials) road test, and have been verified through more recent research and field studies.<sup>22</sup> The layer coefficient also can be obtained from the relationship or chart provided by AASHTO based on the CBR or  $M_r$ .

The stabilised layer replaces the conventional sub-base and performs the same functions. Thus, the stabilised layer effectively is a sub-base layer because the stabilised layer is directly below the base course and directly above the natural subgrade.<sup>22</sup> Thus, in this study, the structural support afforded by the stabilised layer was directly accounted for by treating the stabilised layer as a sub-base. In particular, the pavement was designed so that it would have the same structural number as the conventional cut-and-fill pavement. A key difference in this approach is that  $a_3$  and  $t_3$  characterise the stabilised layer rather than a conventional sub-base layer.

At both sites, the same surface and base layers were used as called for in the conventional design. That is, the only change was replacement of the third layer (i.e. 0.45 m breaker run at STH 60 and 0.75 m coarse sand at Scenic Edge) with a fly-ash stabilised layer that would provide equivalent contribution to the structural number. The thickness of the stabilised layer was also constrained to be 0.3 m (i.e. the depth to which fly ash could be mixed into the *in situ* subgrade). This required that the stabilised soil have an  $a_3$  of at least 0.0048 (1/mm) for Scenic Edge and 0.0044 (1/mm) for STH 60.

California Bearing Ratio and  $M_r$  are the critical parameters affecting  $a_3$ . The AASHTO Guide provides charts relating  $a_3$  to CBR and  $M_r$ , but these charts apply to granular materials typically used as sub-base, not fly-ash stabilised soils that rely on cementing to increase strength and stiffness. No such charts for fly-ash stabilised sub-base are established yet, even though the necessity of such charts was recognised by AASHTO. Thus, in lieu of charts specifically for the fly-ash stabilised layer, the charts for granular sub-base were assumed to apply to fly-ash stabilised sub-base to estimate the layer coefficient. The field testing, described subsequently, was conducted in part to determine whether this assumption is reasonably valid.

## 4.2. Laboratory testing for design

A series of specimens was prepared with different fly ash contents and compacted at different moulding water contents (based on total solids) to define a mix design that would provide equivalent structural support as the conventional sub-base layers used at the Scenic Edge and STH 60 sites. The testing programme for design consisted of two phases. In the first phase, a series of unconfined compression tests was conducted to evaluate the general effects of mix design variables (i.e. fly ash content, moulding water content, and compaction delay) on strength of the fly ash mixture. In the second phase, CBR and  $M_r$  tests were conducted under target conditions identified from the unconfined compression tests. Results of the CBR and  $M_r$  tests were then used to determine the fly ash content needed to achieve the required  $a_3$ .

This two-phase approach was used for pragmatic reasons. Unconfined compression tests were conducted first because specimens prepared for compaction tests could also be used for unconfined compression testing. Thus, no additional effort was required to prepare the specimens. Moreover, unconfined compression tests could be conducted rapidly, which allowed for a quick assessment of the influence of mix design variables on mechanical properties of the mixtures. However, there are significant limitations associated with unconfined compression tests (e.g. lack of confinement). Thus, the unconfined compression strengths were used in a qualitative manner as indices of the degree of stabilisation being achieved. Quantitative design parameters were obtained from the more difficult and time-consuming CBR and  $M_r$  tests. Following this approach resulted in a testing programme for CBR and  $M_r$  that was focused on mixtures most likely to be used in the field.

**4.2.1. Unconfined compression tests.** Specimens prepared for compaction tests were used for unconfined compression testing. Compaction test specimens were wrapped in plastic, allowed to cure for 7 days in a wet room (100% relative humidity), and then tested for unconfined compressive strength following ASTM D 2166.

Unconfined compressive strength is shown as a function of fly ash content and moulding water content in Fig. 3 (Scenic Edge) and Fig. 4 (STH 60). Adding fly ash to both soils increased the compressive strength appreciably (by at least a factor of 2, and as much as a factor of 7). Slightly higher compressive strengths were obtained at higher fly ash contents, owing to greater cementing in the stabilised soil. For both soils, the maximum unconfined compressive strength was obtained approximately at optimum water content for the 'no delay' condition and at a water content 1% wet of optimum for the '2 h delay' condition. Lack of sufficient water for hydration at lower water content, and reduction of contact areas (for bonding) among soil particles at higher water content, are responsible for the reduction in compressive strength as the water content deviates from optimum.<sup>21</sup> Compaction after a 2 h delay caused the strength to decrease by as much as 25%, primarily because compaction breaks down some of the bonds that form during the first 2 h of hydration.

**4.2.2. California Bearing Ratio (CBR) and resilient modulus ( $M_r$ ) tests.** Based on the outcome of the unconfined compression tests, CBR and  $M_r$  tests were conducted at three

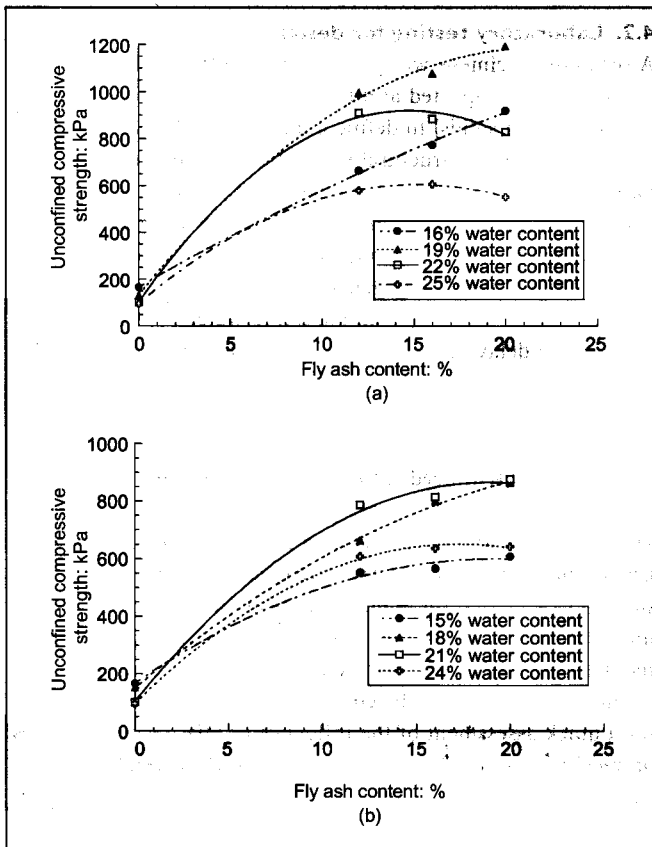


Fig. 3. Unconfined compressive strength of fly-ash stabilised soil from Scenic Edge at various fly ash and moulding water contents: (a) no compaction delay; (b) 2 h delay

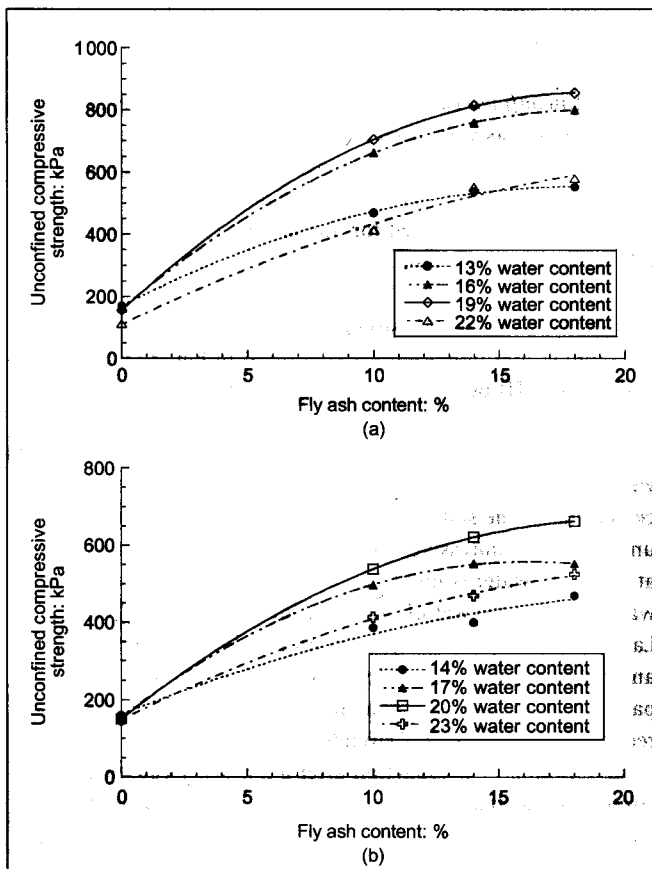


Fig. 4. Unconfined compressive strength of fly-ash stabilised soil from STH 60 at various fly ash and moulding water contents: (a) no compaction delay; (b) 2 h delay

different fly ash contents (12%, 16% and 20% for Plano silt loam, and 10%, 14% and 18% for Joy silt loam). These fly ash contents were selected because the unconfined compression tests indicated that fly ash contents higher than 20% would provide little improvement, and that fly ash contents as low as 10–12% might yield acceptable properties at lower cost. An intermediate fly ash content was tested as well in case the CBR or  $M_r$  achieved at the lowest fly ash content was too small. The tests were conducted at water content corresponding to the water content at which the unconfined compressive strength was maximum.

Specimens for CBR testing were mixed and moistened using the same procedure as used for the compaction tests. The mixture was compacted into a CBR mould using standard effort immediately after mixing, or after a 2 h delay. Specimens for resilient modulus testing were prepared in a split mould using a similar method, except that only 2 h delay specimens were prepared. After compaction, the specimens were sealed in plastic and cured for 7 days in the wet room. The CBR specimens were cured in the mould, whereas the  $M_r$  specimens were extruded prior to curing. After curing, the specimens were tested following ASTM D 1883 (CBR)<sup>23</sup> and AASHTO Standard T 294-91 ( $M_r$ )<sup>24</sup> following the protocol for Type 2 (cohesive) materials. The  $M_r$  test was conducted at a confining pressure of 21 kPa and a seating load of 13.8 kPa.

The CBR of the fly-ash stabilised soils is shown in Fig. 5. As with unconfined compression, adding fly ash increases the CBR significantly. Also, the effect of fly ash addition on CBR is reduced by a 2 h delay in compaction. For Scenic Edge, the CBR is sensitive to fly ash content, whereas for STH 60 the CBR increases only slightly as the fly ash content increases. For both soils, CBRs in excess of 37 (Scenic Edge) and 32 (STH 60) were achieved at the lowest fly ash content, even with a 2 h delay. These CBRs are higher than CBRs generally associated with good sub-base materials, and are more typical of CBRs associated with base materials.<sup>9,25</sup>

The resilient modulus of fly-ash stabilised soil at different fly ash contents is shown in Fig. 6. No  $M_r$  is shown for soil without fly ash because the soil was so soft that the specimens failed during the first loading cycle of the  $M_r$  test. As with the CBR tests, addition of fly ash resulted in relatively large  $M_r$  (at

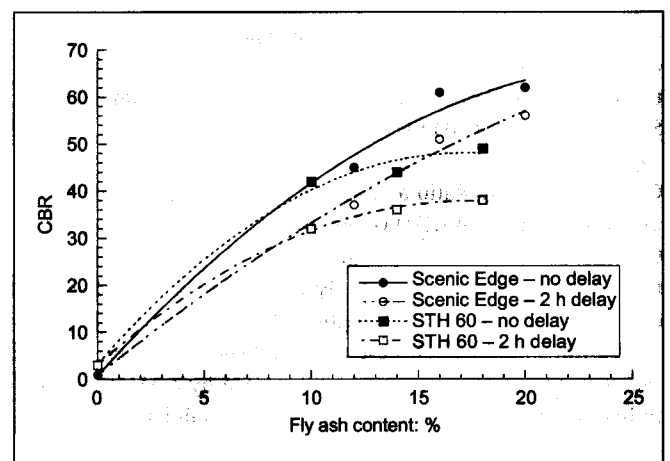


Fig. 5. California Bearing Ratio (CBR) of fly-ash stabilised soils at various fly ash contents

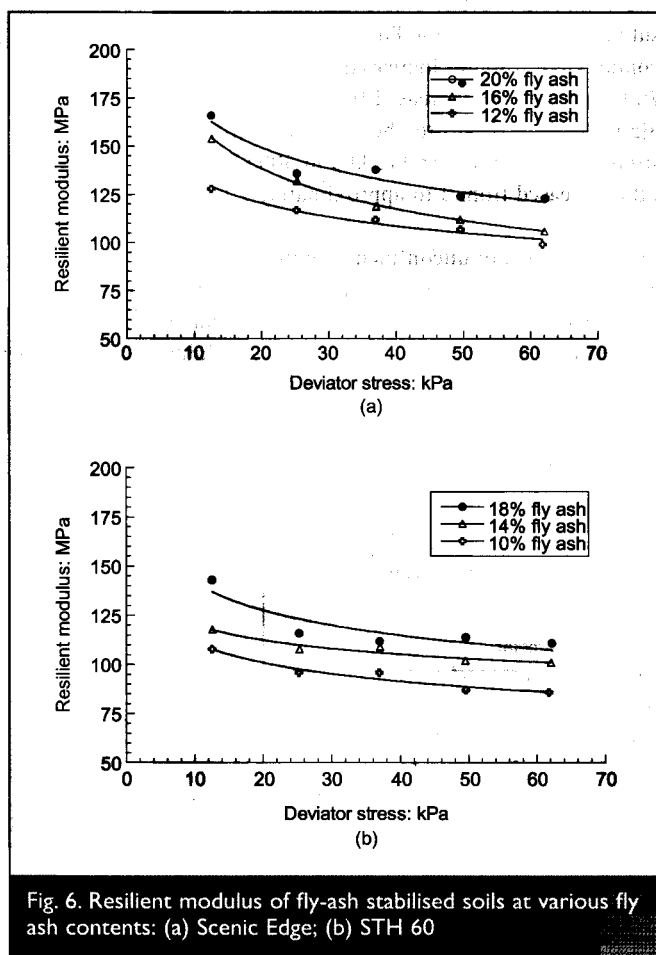


Fig. 6. Resilient modulus of fly-ash stabilised soils at various fly ash contents: (a) Scenic Edge; (b) STH 60

least 90 MPa), and somewhat larger  $M_r$  values were obtained as the fly ash content increased.

#### 4.3. Mixture selection

Results of the CBR and  $M_r$  tests were used to select the fly ash content to be used at each site. For both sites the lowest fly ash content that was tested was selected for field application, because it provided an  $a_3$  exceeding that required for the sub-base layer in the conventional design. Since the strength and stiffness decreases significantly with compaction delay, CBR and  $M_r$  obtained from '2 h delay' specimens were used when estimating  $a_3$ . A summary of the  $a_3$  values that were estimated for the fly-ash stabilised layers is shown in Table 5, along with the  $a_3$  values assigned to the conventional sub-base materials by designers of the original pavement profiles (the conventional pavement profiles were not designed by the authors).

## 5. FIELD CONSTRUCTION

Based on the laboratory mix design, the subgrade was stabilised using a fly ash content of 12% for the Scenic Edge site and 10% for the STH 60 site. The intended mixture water content was 1% wet of optimum (based on total solids) to achieve maximum strength, assuming that a 2 h delay was realistic. Prior to placing the fly ash, the existing water content of the subgrade was measured with a nuclear density gauge. Water was added as needed so that the soil-fly ash mixture would be at the target water content.

The fly ash was spread on to the moist subgrade in a relatively uniform layer using truck-mounted lay-down equipment designed specifically for fly ash application with minimal dust generation.<sup>10</sup> After placing the fly ash over a road segment approximately 200 m long, a road reclaimer was used to mix the fly ash with the subgrade soil to a depth of 0.3 m. Immediately after mixing, the mixture was compacted using three different compactors (tamping foot, steel drum, and rubber tyre) in sequence. Compaction was completed within approximately 1 h after mixing the fly ash and moist subgrade soil at both sites.

A nuclear density gauge was used to measure the dry unit weight and the water content that were achieved. For the Scenic Edge site, the dry unit weight varied between 93% and 106% of the target dry unit weight (16.2 kN/m<sup>3</sup>) and averaged 98% (15.9 kN/m<sup>3</sup>). For the STH 60 site, the dry unit weight varied between 96% and 107% of the target dry unit weight (16.5 kN/m<sup>3</sup>) and averaged 103% (17 kN/m<sup>3</sup>). For both sites, the water content varied within 2% of the target mixture water content.

## 6. POST-CONSTRUCTION TESTING

### 6.1. Laboratory tests

Grab samples were collected from the field sites just prior to compaction. Samples were also collected after compaction using thin-wall (71 mm diameter) sampling tubes. The samples collected in tubes were extruded within 24 h, wrapped with plastic, and cured for 7 days in a wet room. The grab samples were compacted into CBR moulds immediately after sampling to the dry unit weight achieved in the field at the sampling location. After compaction, the CBR specimens were wrapped in plastic, and cured for 7 days in a wet room.

After curing, unconfined compression tests were conducted on

Material	Specimen type	Strength-based $a_3$		Modulus-based $a_3$	
		CBR	$a_3$ : mm <sup>-1</sup>	$M_r$ : MPa	$a_3$ : mm <sup>-1</sup>
Fly-ash stabilised soil (12% FA) Scenic Edge	Laboratory	37	0.0048	115	0.0048
	Field	28	0.0044	NM	NM
Fly-ash stabilised soil (10% FA) STH 60	Laboratory	32	0.0044	99	0.0044
	Field	23	0.10	NM	NM
Coarse sand (Scenic Edge)	NA	NA	0.002	NA	0.002
Breaker run (STH 60)	NA	NA	0.003	NA	0.003

$a_3$  = sub-base layer coefficient, FA = fly ash,  $M_r$  = resilient modulus, NA = not applicable, NM = not measured.

Table 5. Layer coefficients estimated from CBR and resilient modulus

specimens trimmed from the tube samples, and CBR tests were conducted on the specimens compacted in moulds. The specimens for unconfined compression testing were trimmed to a diameter of 50 mm and height of 100 mm. At some locations the tube samples were brittle, and broke into pieces during sampling and extrusion. A pocket penetrometer was used to estimate the unconfined compressive strength at these locations. Resilient modulus tests were not conducted after construction because intact undisturbed samples of sufficient size for  $M_r$  tests could not be retrieved.

Compressive strength and CBR of the stabilised layers are shown in Figs 7 and 8, along with those of the original

subgrades. At the Scenic Edge site, the mean unconfined compressive strength increased from 85 kPa to 370 kPa (Fig. 7(a)), and the CBR increased from 1 to approximately 25 (Fig. 8(a)). At the STH 60 site, the mean unconfined compressive strength increased from 112 kPa to 300 kPa (Fig. 7(b)), and the CBR increased from 3 to approximately 20 (Fig. 8(b)).

These increases in unconfined compressive strength and CBR are smaller than anticipated during design. The unconfined compressive strength in the field is approximately one-half of that measured during design for the Scenic Edge site, and two-thirds of that measured during design for the STH 60 site. Similarly, the CBR of the field mixture at both sites is

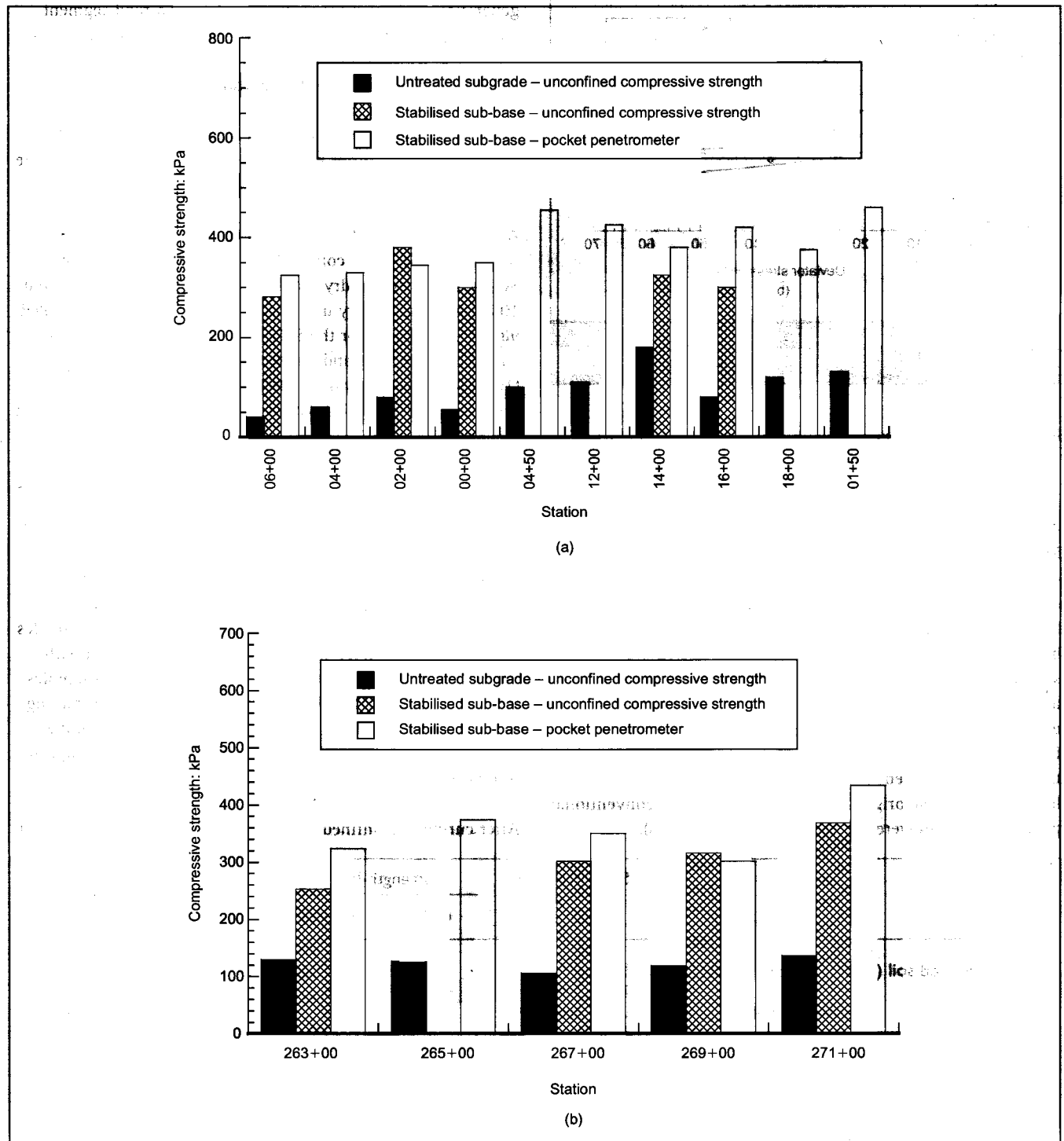


Fig. 7. Compressive strength of untreated subgrade and stabilised layer along centre line of pavement: (a) Scenic Edge; (b) STH 60

$$PDI = \left[ 1 - \frac{A}{B} LTPFESRD_L D_T \right]$$

The parameters on the right-hand side of equation (2) are distress factors for alligator cracking ( $A$ ), block cracking ( $B$ ), longitudinal cracking ( $L$ ), transverse cracking ( $T$ ), patching ( $P$ ), flushing ( $F$ ), edge ravelling ( $E$ ), surface ravelling ( $S$ ), rutting ( $R$ ), longitudinal distortion ( $D_L$ ), and transverse distortion ( $D_T$ ). The PDI can vary between 0 and 100, with 0 corresponding to no distress. WisDOT considers pavements having a PDI between 60 and 75 to be at the end of their service life. To date, WisDOT has reported  $PDI = 0$  for all of the pavements, indicating that there is no evidence of distress. However, the traffic loading to date is well below the design traffic loading. Thus, distress may be observed in the future, and at different times owing to the differences in usage of the two pavements.

The DPI and stiffness measured with the DCP and SSG are shown in Fig. 9 and Fig. 10 for conditions before and after stabilisation. The DPI of the subgrade decreased on average from 64 to 20 mm/blow at the Scenic Edge and from 65 to 16 mm/blow at the STH 60 site as a result of fly ash stabilisation. The stiffness increased from 5 to 12 MN/m, on

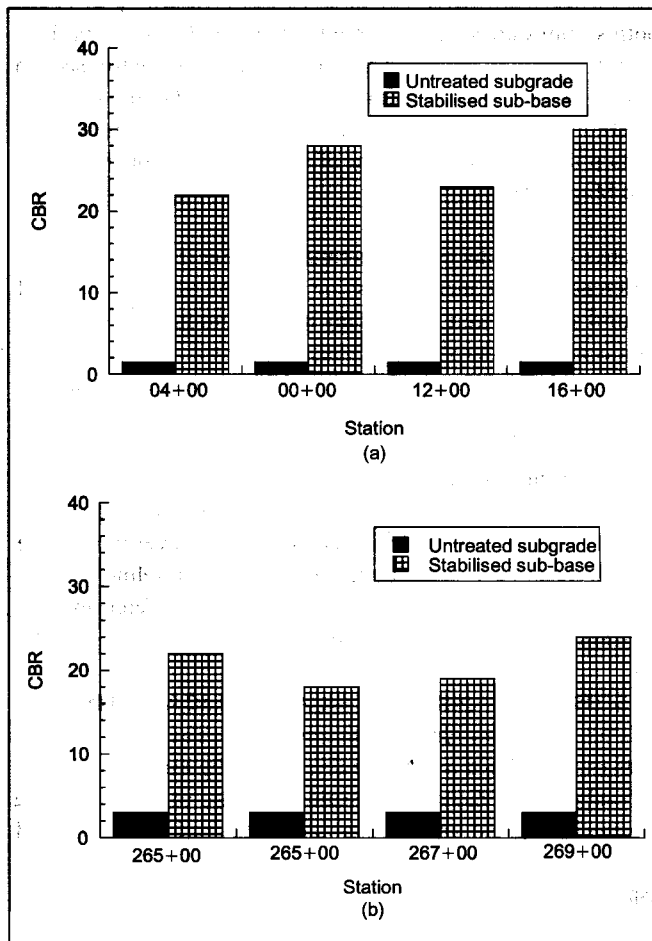


Fig. 8. CBR of untreated subgrade and stabilised layer along centre line of pavement: (a) Scenic Edge; (b) STH 60

approximately two-thirds of that anticipated during design. The reason for these differences has not been determined, but a likely factor is differences in the mixing process that occur in the laboratory and field. In the laboratory, the air-dried soil is ground into small particles and carefully mixed with fly ash, and then water is added to create a uniform material. In the field, the particle sizes are much larger (i.e. moist clods or clumps of clay are mixed with fly ash rather than finely ground soil particles). The larger clod size in the field probably reduces blending of the fly ash and soil particles, and reduces the uniformity of cementing that occurs in the soil.

## 6.2. Field tests

Field testing of the stabilised layer was conducted with the DCP and SSG at both sites. FWD tests and distress surveys are being conducted semi-annually (fall and spring) at the STH 60 site. FWD tests are conducted with a KUAB Model 2m-33 FWD at 24 stations (six in control section, 18 in fly ash section) along the STH 60 alignment using a 90 kN load. More FWD tests are conducted in the fly ash section because it is four times longer than the control section.

The distress survey was conducted by the Wisconsin Department of Transportation (WisDOT). WisDOT uses the survey to calculate the pavement distress index (PDI):

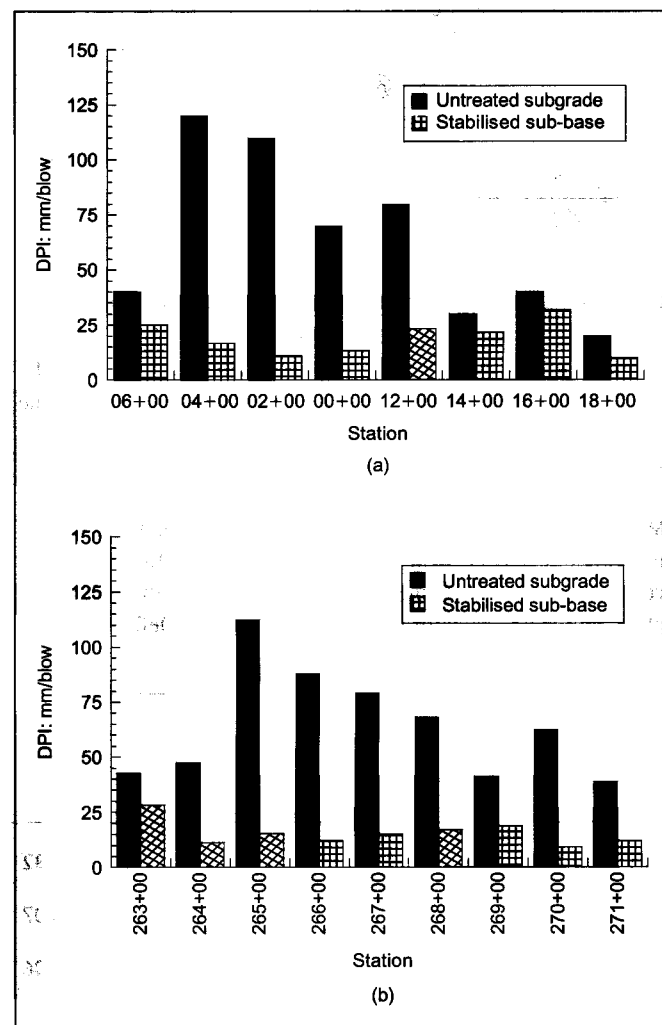


Fig. 9. Dynamic penetration index (DPI) of untreated subgrade and fly-ash stabilised layer measured along centre line of pavement: (a) Scenic Edge; (b) STH 60



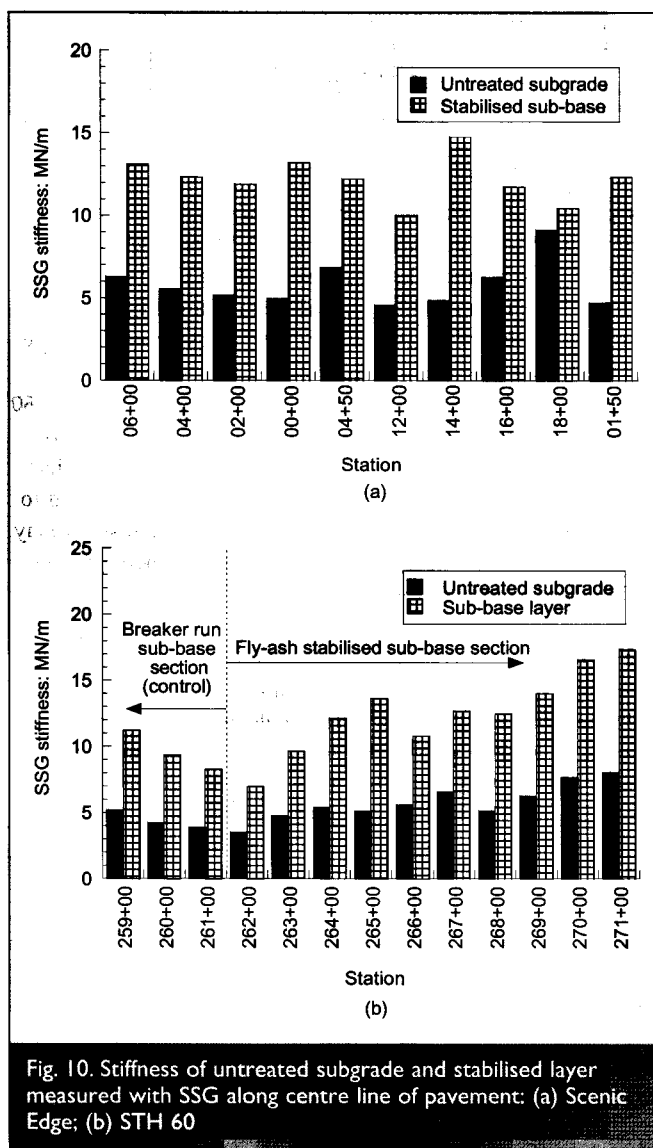


Fig. 10. Stiffness of untreated subgrade and stabilised layer measured with SSG along centre line of pavement: (a) Scenic Edge; (b) STH 60

average, at both sites. Additionally, at STH 60, the stiffness of the fly-ash stabilised layer (12 MN/m) is higher than that of the breaker run sub-base (10 MN/m) in the adjacent control test section.

Means and standard deviations of the centreline deflections measured at STH 60 with the FWD are shown in Table 6. The centreline deflection is measured at the centre of the loading plate, and is an indicator of pavement stiffness. Deflections in

both sections are small (< 2 mm). The mean deflection in the fly ash section is slightly larger than that in the control section during the first year of monitoring (October 2000 and May 2001), but is smaller than or similar to that in the control section during the second year of monitoring (October 2001 and May 2002).

A *t*-test was conducted to determine whether the apparent differences in the mean centreline deflection of the fly ash and control sections were statistically significant. In a *t*-test, the means are considered significantly different if the *p*-value is less than the significance level (i.e. the probability of falsely rejecting the hypothesis that the means are similar). The common significance level of 0.05 was used for the *t*-test. Results of the *t*-test are summarised in Table 6. In all cases the means are not different statistically (*p* > 0.05). The apparent gain in strength and stiffness that is occurring over time in the fly ash section (as shown by the decrease in centreline deflection, Table 6) suggests that the marginal differences between the two sections should diminish over time.

## 7. SUMMARY AND PRACTICAL IMPLICATIONS

This paper has described a case study where pavements at two sites were designed and constructed using fly ash to stabilise a soft subgrade. A control test section was also constructed using a conventional cut-and-fill approach with crushed rock instead of the fly ash stabilisation at one of the sites. The unique aspect of these pavements is that the structural support afforded by the fly-ash stabilised soil was incorporated into the pavement design. The design followed the 1993 AASHTO method for flexible pavements, and was based primarily on laboratory measurements of CBR and resilient modulus of the fly-ash stabilised soil. The relationship between CBR and layer coefficient for granular sub-base in the 1993 AASHTO Guide was assumed to apply to the fly-ash stabilised soil. Field tests were conducted after construction to evaluate the effectiveness of the design methodology.

At both field sites, stabilisation with fly ash improved the strength and stiffness of the subgrade significantly. However, the CBR of the field mixture at both sites was approximately two-thirds of the CBR measured during design. Nevertheless, the increase in strength was more than adequate to provide a strong working platform for construction equipment, and the increase in stiffness resulted in small pavement deflections during testing with a falling weight deflectometer (< 2 mm

using a 90 kN load). FWD testing at the STH 60 site showed that similar centreline deflections and stiffness (as measured with an SSG) were achieved in the fly ash and control sections, indicating that the two pavements are comparable structurally. In addition, no distress has been observed in either section since construction. Thus, assigning layer coefficients for fly-ash stabilised soils based on correlations for granular sub-

Date	Mean deflection: mm (standard deviation)		<i>p</i> -value	Significant difference?
	Control section	Fly ash section		
21 Oct. 2000	0.95 (0.17)	1.00 (0.31)	0.32	No
16 May 2001	1.04 (0.27)	1.23 (0.28)	0.07	No
12 Oct. 2001	0.72 (0.07)	0.61 (0.11)	0.06	No
15 May 2002	0.73 (0.12)	0.74 (0.06)	0.70	No

Table 6. Statistical analysis of maximum deflection obtained from FWD at STH 60

base materials appear reasonable until layer coefficients specific to fly-ash stabilised soils become available.

## 8. ACKNOWLEDGEMENTS

Financial support for this study was provided by the US Department of Energy through the Combustion By-products Recycling Consortium, the University of Wisconsin-Madison Consortium for Fly Ash Use in Geotechnical Applications (funded by Mineral Solutions, Inc., Alliant Energy Corporation, and Excel Energy Services, Inc.), and the Wisconsin Department of Transportation (WisDOT). The opinions and conclusions described in the paper are those of the authors and do not necessarily reflect the opinions or policies of the sponsors. Auckpath Sawangsuriya collected the SSG data and Robert Albright collected the DCP data. Dr Tarek Abichou assisted with construction. The authors also acknowledge the many contributions made by the contractors for both projects, as well as WisDOT personnel who provided assistance. Mr Fred Gustin is acknowledged for his efforts in initiating this research effort.

## REFERENCES

1. ACAA. ACAA's CCPs Production and Use Survey. American Coal Ash Association, Alexandria, VA, 2000.
2. FERGUSON G. Use of self-cementing fly ash as a soil stabilizing agent. In *Fly Ash for Soil Improvement*. ASCE, Reston, VA, 1993, GSP No. 36, pp. 1–14.
3. MISRA A. Stabilization characteristics of clays using Class C fly ash. *Transportation Research Record 1611*, TRB, National Research Council, Washington, D.C., 1998, 46–54.
4. NICHOLSON P. G. and KASHYAP V. Fly ash stabilization of tropical Hawaiian soils. In *Fly Ash for Soil Improvement*. ASCE, Reston, VA, 1993, GSP No. 36, pp. 15–29.
5. COKCA E. Use of Class C fly ashes for the stabilization of an expansive soil. *Journal of Geotechnical and Geoenvironmental Engineering*, 2001, 127, No. 7, 568–573.
6. ZHANG J. Stabilization of expansive soil by lime and fly ash. *Journal of Wuhan University of Technology*, Materials Science Edition, 2002, 17, No. 4, 73–77.
7. KANIRAJ S. R. and HAVANAGI V. G. Compressive strength of cement stabilized fly ash–soil mixtures. *Cement and Concrete Research*, 1999, 29, No. 5, 673–677.
8. KANIRAJ S. R. and HAVANAGI V. G. Behavior of cement-stabilized fiber-reinforced fly ash–soil mixtures. *Journal of Geotechnical and Geoenvironmental Engineering*, 2001, 127, No. 7, 574–584.
9. PANDIAN N. S. and KRISHNA K. C. The pozzolanic effect of fly ash on the California Bearing Ratio behavior of Black Cotton Soil. *Journal of Testing and Evaluation*, 2003, 31, No. 6, 479–485.
10. EDIL T. B., BENSON C. H., BIN-SHAFIQUE S., TANYU B. F., KIM W. and SENOL A. Field evaluation of construction alternatives for roadway over soft subgrade. *Transportation Research Record 1786*, TRB, National Research Council, Washington, D.C., 2002, pp. 36–48.
11. TURNER, J. P. Evaluation of Western Coal fly ashes for stabilization of low-volume roads. In *Testing Soil Mixed with Waste or Recycled Materials*. American Society for Testing and Materials, West Conshohocken, PA, 1997, STP 1275, pp. 157–171.
12. AASHTO. *Guide for Design of Pavement Structures*. American Association of State Highway and Transportation Officials, Washington, D.C., 1993.
13. ASTM D 4609. *Standard Guide for Evaluating Effectiveness of Chemicals for Soil Stabilization (D 4609-01)*, American Society for Testing and Materials, West Conshohocken, PA, USA, 2001.
14. ASTM D 2166. *Standard Test Method for Unconfined Compressive Strength of Cohesive Soil (D 2166-00)*, American Society for Testing and Materials, West Conshohocken, PA, USA, 2000.
15. ASTM D 698. *Standard Test Methods for Laboratory Compaction Characteristics of Soil Using Standard Effort (D 698-00)*, American Society for Testing and Materials, West Conshohocken, PA, USA 2000.
16. SAWANGSURIYA A. *Evaluation of the Soil Stiffness Gauge*. MS thesis, Department of Civil and Environmental Engineering, University of Wisconsin–Madison, Madison, WI, 2001.
17. ALBRIGHT, R. *Evaluation of Dynamic Cone Penetrometer and its Correlation with Other Field Instruments*. MS thesis, Department of Civil and Environmental Engineering, University of Wisconsin–Madison, Madison, WI, 2002.
18. HUMBOLDT. *Soil Stiffness Gauge (GeoGauge) User Guide: Version 3.3*. Humboldt Mfg Co., Norridge, IL, 1999.
19. FHWA. *Fly Ash Facts for Highway Engineers*. Federal Highway Administration, US Department of Transportation, 1995, Report No. FHWA–SA–94–081.
20. ASTM C 618. *Standard Specification for Coal Fly Ash and Raw or Calcined Natural Pozzolan for Use as a Mineral Admixture in Concrete (C 618-03)*, American Society for Testing and Materials, West Conshohocken, PA, USA, 2003.
21. ACAA. *Soil and Pavement Base Stabilization with Self-Cementing Coal Fly Ash*. American Coal Ash Association, Alexandria, VA, 1999.
22. HUANG W. H. *Pavement Analysis and Design*. Prentice-Hall, Englewood Cliffs, NJ, 1993.
23. ASTM D 1883. *Standard Test Method for CBR (California Bearing Ratio) of Laboratory-Compacted Soils (D 1883-98)*, American Society for Testing and Materials, West Conshohocken, PA, USA 1998.
24. AASHTO T-294-91. *Resilient Modulus of Unbounded Granular Base/Subbase Materials and Subgrade Soils-SHRP Protocol P46*, American Association of State Highway and Transportation Officials, Washington DC, USA, 1991.
25. BOWLES J. E. *Engineering Properties of Soils and their Measurement*. McGraw-Hill, New York, NY, 1992.

Please email, fax or post your discussion contributions to the secretary by 1 April 2005: email: mary.henderson@ice.org.uk; fax: +44 (0)20 665 2294; or post to Mary Henderson, Journals Department, Institution of Civil Engineers, 1–7 Great George Street, London SW1P 3AA.

---

Wisconsin Highway Research Program  
University of Wisconsin-Madison  
1415 Engineering Drive  
Madison, WI 53706  
608/262-2013  
[www.whrp.org](http://www.whrp.org)